



Faculty of Science and Technology

MASTER'S THESIS

Study program/ Specialization: Petroleum Engineering/Drilling	Spring semester, 2011 Restricted access
Writer: Margodt Marie Larsen (Writer's signature)
Faculty supervisor: Professor Udo Zimmermann External supervisor: Alberto Caycedo, Smith Bits	
Title of thesis: "A Comparative Study on PDC Drill Bit Performance With A 4D Dynamic Model On Samples Of Late Cretaceous Chalk For North Sea Applications"	
Credits (ECTS):30	
Key words: - Chalk - Vibrations - Drill bits	Pages: 120 + enclosure: 27 Stavanger,30 June /2011 Date/year

Abstract

The overall goal of this work has been to select the most suitable PDC bit for 8 ½" Chalk-sections located in the North Sea. The Ekofisk field is the largest field in the North Sea and has long sections with Chalk of late cretaceous age. This Chalk is considered to be soft, homogenous and relatively easy to drill. However, stick slip, poor hole cleaning and limited penetration rates have been observed. The main goal was therefore to optimize Chalk drilling by reducing stick slip and increasing penetration rates.

Using sophisticated and advanced simulation software, several bits were simulated in order to determine the best recommendation for Chalk applications in the Ekofisk Field. In order to simulate a formation as close to the reservoir characteristics as possible, offshore Chalk was sampled from cores at NPD and studied in detail. At the same time several samples from offshore and onshore Chalk were collected and analyzed. Based on geological data as a whole and not only porosity, the Kansas Chalk (for medium porosity) and Ulster Chalk (for lower porosity) were the most similar ones to North Sea Chalk. These observations are valuable for future work.

Based on the rock study, two different simulations were performed. #5 bits were first simulated in hard, compressive Lueders Limestone followed up by simulating #2 bits in medium-soft Austin Chalk. Through these extensive simulations, an MDi619LBPX PDC bit generated the lowest amount of vibrations with highest penetration rates, and was selected for chalk drilling applications.

Table of Contents

Abstract	2
Abbreviations	6
Preface	7
1. Introduction	8
2. Shock and Vibration	10
2.1 Shock and Vibration definitions	10
2.2 Vibration Mechanisms	11
2.2.1 Axial Vibrations	12
2.2.2 Lateral Vibrations	13
2.2.3 Torsional vibrations	16
3. Basic Petroleum Geology	18
3.1 Geological Terms and Nomenclature	18
3.1.1 Classification of Carbonate Sedimentary Rocks	18
3.1.2 Carbonate Rocks	18
3.1.3 Chalks	19
3.2 Fundamentals of Rock Mechanics	22
3.2.1 Stress	22
3.2.2 Strain	22
3.2.3 Porosity	22
3.2.4 Unconfined Compressive Strength (UCS)	24
3.2.5 Mohr-Coulomb Failure Criterion	24
3.2.6 X-Ray Diffraction Analysis	25
3.3 Depositional Environments	26
3.3.1 Deep Marine/ Transition Zone	26
3.4 Petroleum Geology of the Norwegian North Sea	27
3.4.1 Cretaceous (144- 65 Ma)	28
3.4.2 The Ekofisk Field	30
3.5 Geological setting	31
3.5.1 Depositional Environment of Chalk in the Ekofisk field	31

4.	Sample testing.....	33
4.1	Sample description and results.....	34
4.1.1	Offshore Chalk: North Sea	35
4.1.2	Onshore Chalk.....	44
4.1.3	Northern Ireland Chalk	47
4.1.4	Final considerations: Resemblances of Chalk	51
4.2	Kansas outcrop description	52
4.2.1	Mineralogical description	53
4.2.2	Hardness	54
5	The Drilling Assembly.....	57
5.1	Drill pipe	58
5.2	Bottomhole Assemblies.....	59
5.2.1	Stabilizers.....	60
5.2.2	Jars.....	61
5.2.3	Rotary Steerable Systems	62
5.3	Drill Bit.....	65
5.3.1	Bit Terminology and Features	67
6	PDC bit.....	68
6.1	Introduction.....	68
6.2	PDC Applications	69
6.3	PDC Cutter Technology	70
6.3.1	PDC cutter manufacturing process.....	72
6.3.2	Thermally Stable Polycrystalline cutters.....	73
6.3.3	Leached cutters	73
6.3.4	ONYX cutters	74
6.3.5	PDC cutter design	75
6.4	PDC bit design	77
6.4.1	Blade count	77
6.4.2	Blade Layout.....	78
6.4.3	PDC Materials.....	79
6.4.4	Bit Profile	80
6.4.5	Bit Profile shapes.....	83

6.5	PDC cutting structure characteristics.....	85
6.5.1	Mechanical Specific Energy (MSE).....	85
6.5.2	PDC Cutting structure	86
6.5.3	PDC cutter orientation.....	89
6.5.4	Cutter Density	91
6.5.5	Cutter exposure.....	92
7	IDEAS [Integrated Dynamic Engineering Analysis System]	94
7.1	The system Approach Applied to Drilling.....	95
7.2	FEA Mesh Model Contents	96
7.3	Simulation Approach for Chalk Drilling Challenge	99
8.	Applied Lab results to Virtual Drilling Environments.....	101
8.1	IAP Method.....	101
8.2	IDEAS Program Description	101
8.2.1	BHA Input.....	102
8.2.2	Drilling Parameters.....	102
8.2.3	Bit Selection	103
8.2.4	Well Profile.....	104
8.2.5	Request Summary Report.....	105
9.	Report on Virtual Results	106
9.1	Lueders Limestone & Pierre Shale II	106
9.1.1	Primary results	111
9.2	Austin Chalk	111
9.2.1	Final Results	116
10.	Conclusion	118
11.	Future Work	119
12.	Acknowledgements.....	120
13.	References.....	121
	APPENDIX A.....	126
	APPENDIX B.....	145

Abbreviations

ROP	-	Rate of Penetration
WOB	-	Weight on Bit
RPM	-	Revolutions per Minute
PDC	-	Poly Crystalline Diamond Compact
TCI	-	Tungsten Carbide Insert
IDEAS	-	Integrated Dynamic Engineering Analysis System
BHA	-	Bottom-hole Assembly
API	-	American Petroleum Institute
NPD	-	Norwegian Petroleum Department
OD	-	Outer Diameter
ID	-	Inner Diameter
RSS	-	Rotary Steerable System
TSP	-	Thermally Stable Polycrystalline
MSE	-	Mechanical Specific Energy
DOC	-	Depth Of Cut
MDOC	-	Managed Depth Of Cut
FEA	-	Finite Element Analysis
DC	-	Drill Collar
DP	-	Drillpipe
HWDP	-	Heavy Weight Drillpipe
IAP	-	IDEAS Analysis Project
RC	-	Roller Cone
UCS	-	Unconfined Compressive Strength
MWD	-	Measurements While Drilling
LWD	-	Logging While Drilling

Preface

This master thesis is a result of the study during my graduation at the University of Stavanger, conducted at Smith Bits, A Schlumberger Company (Forus) in Stavanger. I have been employed by Smith Bits, A Schlumberger Company for 2 years now, working part time during my studies. Through this part time work, I have been included in operations and field engineering projects. I have been working closely with Senior Field Engineer, Alberto Caycedo, and the rest of the team located at our facilities at Forus, Stavanger. I have also participated in the tests performed on the onshore and offshore samples in close cooperation with Udo Zimmermann, professor at the University of Stavanger.

Alberto Caycedo involved me in this project in November 2010 to give me experience and the opportunity to learn the work of a Field Engineer. Since a lot of research was necessary to make the project complete, we decided together with the team in Smith Bits to make it my topic for my master thesis work. The objective was to study offshore Chalk, find a comparable onshore Chalk and use our state of art IDEAS software, to simulate drilling in the comparable sample and to select the best PDC bit approach for Chalk applications.

Since the samples from the exact North Sea formations are too small for rock library implementation in IDEAS, we are quite confident that this approach will provide reliable results.

This has been an interesting experience for me and I have learned a lot in the process. In addition to the lab work at the University, I also got to visit the rock library in Houston, Texas for two weeks in February 2011. Through my years in the company, I have gotten to know many knowledgeable and interesting people. Even though my future is in the Drilling and Measurement department in Schlumberger, I hope to see and work with the Smith Bits team again.

1. Introduction

The demand for energy and oil has never been higher and neither has the complexity and difficulty of extracting desirable amounts in a cost-effective manner. Reservoirs are getting smaller, deeper and more difficult to reach, continually increasing drilling costs and pressuring manufactures to develop bits that can drill through almost any formation in one effective run.

True to what was predicted a couple of years ago, bits are being custom-designed to fit particular applications. Customers don't want a bit with multiple features that can be used in majority of formations, they want a bit with excellent performance in the desired formation to be drilled. Providing the bit to get the job done safely and efficiently is what customers expect nowadays.

The Ekofisk Field is known for having long sections with high, porous Chalk that can be a challenge for the bit downhole. Carbonate settings are characterized by fractures and faults that can cause differential sticking of the bit, poor hole-cleaning, vibrations and limited penetrations rates. The main focus will be to find a suitable bit that will drill efficiently and stable in chalk applications. An extensive study on offshore and onshore Chalks will also be included.

Offshore Chalk will be sampled from cores stored at NPD according to the need of the study. Onshore Chalk will be collected in different locations. Offshore samples from Kansas, Belgium (Mons, Liege), Denmark (Aalborg, Stevns Klint) and Northern Ireland will be analyzed and studied to find a Chalk comparable with North Sea Chalk (for low and medium porous Chalk).

The main tool in this project will be IDEAS [Integrated dynamic Engineering Analysis System]. IDEAS is a 4D dynamic simulation software used to design, test and analyze bit performance in specific applications. The software provides an expert bit selection tool as it accurately predicts how different bit designs will perform in particular formation types, with a specific drive type, under various operating parameters and with a specific BHA configuration.

Most of the 8 ½" Chalk sections in the North Sea today are drilled horizontally. A horizontal well path will therefore be used in the simulations. The rotary steerable tool of choice will be Schlumberger's PowerDrive, which is a push-the-bit system designed for full directional control while rotating the drillstring.

Several bit design and drilling parameters will also be used in the simulations to find best suitable bit with corresponding, optimal drilling parameters. The formation input will be based on the results from the Chalk studies.

The main challenge that will be discussed in this project will be to find the optimal drill bit for 8 ½" Chalk sections in the Ekofisk Field. Through discussions with Alberto Caycedo and engineers in Smith Bits, the focus will be on the following through the work:

- Chalk formation characteristics
- Comparative studies of onshore and offshore Chalks
- Vibrations
- PDC bit design selection (with optimized drilling parameters)
- Cutter design (cutter size, manufacturing)

Through this master thesis work, IDEAS was used to simulate #6 PDC bits. The simulation process predicts the vibrations and behavior of the entire drilling assembly including the drill bit. The most important aspect in this thesis is finding the optimized and best bit selection for this particular formation.

Two onshore Chalks (#1 for medium porosity and #1 for lower porosity) were considered as comparable North Sea Chalks. The characteristics of the medium porosity Chalk were used as a basis when selecting formation input in the simulations.

The simulation process was conducted in two sessions. The first step was to simulate drilling action through a hard, compressive Chalk to analyze bit performance in what was considered a worst-case-scenario for the bit in Chalk applications. The final and last step was an extended simulation of two bits in an Ekofisk-comparable formation with variable drilling parameters.

2. Shock and Vibration

2.1 Shock and Vibration definitions

Vibration can be defined as a repeated motion after an interval of time. It is aggregated when the energy of a particle or elastic solid are transferred from kinetic to potential energy, and from potential to kinetic energy alternately. A system that vibrates is dynamic and will be naturally dampened if there is no input of external energy. The response of a vibrating system generally depends on both initial conditions and external excitations.

Drillstring vibrations are extremely complex due to the multitude of random factors such as bit-formation interaction, drillstring-wellbore interaction and hydraulics.

However, the motions can be simplified into three basic vibrations modes:

1. Lateral (transverse):
 - Side to side motion generating flexing and bending (two degrees of freedom).
2. Axial (longitudinal):
 - Motion along drill string axes changing the axial tension in the string (One degree of freedom).
3. Torsional (stick-slip):
 - Motion causing twist-off and torque. Created due to varying levels of torque in the drill string (one degree of freedom).

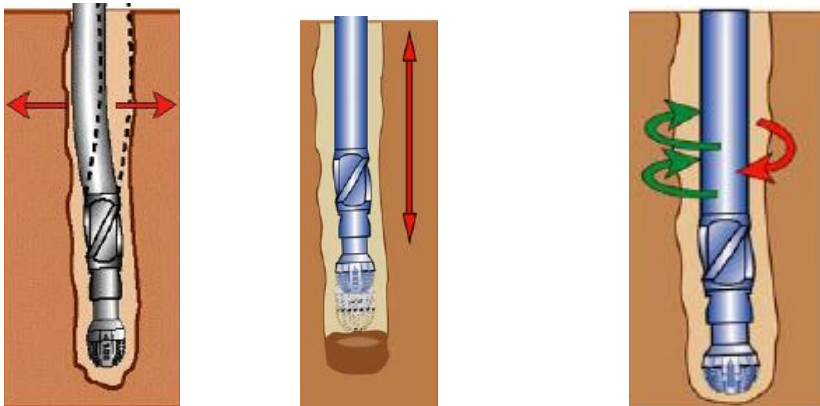


Figure 2.1 -Illustration of the basic vibration modes; lateral, axial and torsional respectively [5].

Shock can be defined as a sudden input of energy. This can be aggregated when the bit, BHA or drill string interacts with the borehole wall. The responses of the bit, BHA and drill string after the shock loading are vibrations. It will gradually decrease if the interaction doesn't repeat itself. If it does, the shocks generated may be considered part of the vibration [1, 2, 5].

2.2 Vibration Mechanisms

A vibrating system is not fully understood in terms of mathematics due to its complexity. However, it is known that the three different vibration modes can initiate several different vibration mechanisms. A typical vibration mechanism can be stick-slip, bit whirl, bit bounce etc.

All of the mechanisms are initiated by a primary mode over a range of frequencies. A secondary mode can also be associated with the vibration mechanism. As the table below illustrates, it is possible to go from one distinct vibration mechanism to another. If the primary mode is torsional vibration (stick-slip), a secondary mode of axial vibration can occur, which again can lead to bit bounce [4, 5].

Vibration Mechanism	Vibration mode (Primary)	Vibration Mode (Secondary)	Frequency (Hz)
Stick-slip	Torsional	Axial	0-5
Torsional resonance	Torsional	Lateral	20-350
Bit whirl	Lateral	Torsional	5-100
Bit chatter	Lateral	Torsional	20-350
Bit bounce	Axial	Torsional	1-10
Parametric Resonance	Axial, Lateral		1-10

Table 2.1 - *Vibration chart- describing the most common mechanisms and corresponding frequencies [4]*

Shock and vibrations can have a major negative impact on reliability. In a significant percentage of failures or damage to the BHA (collars, stabilizers, connections, downhole tools) and drill bit, shock and vibrations are contributing factors. If not monitored, understood and mitigated, excessive shock and vibrations may cause [1]:

- Damaged BHA's and Drill Bits
- Increase work hazards (twist off, fishing, mud invaded tools etc)
- Non Productive Time (NPT) and damaged tool charges, increasing the cost of operation

2.2.1 Axial Vibrations

Axial vibration is defined as a motion along the drill string axes changing the axial tension in the string. More easily it can be described as an up and down motion of the drillstring where the bit doesn't actually leave the bottom of the hole. The axial motion has a characteristic frequency which depends primarily on the type of bit, mass of BHA, drillstring stiffness and formation hardness.

Axial vibrations are most often experienced when drilling low inclination wells in hard, competent rocks. This vibration mechanism is related to roller cone bits since they tend to create patterns that may result in large amplitude-longitudinal vibrations on the BHA, which in turn initiate axial vibrations [1, 5].

2.2.1.1 Bit Bounce

Kelly bounce is sometimes observed when drilling large, shallow holes in hard formations with a roller cone bit. This motion is a result of large longitudinal motions of the drillstring that originate at the bit, hence the name "Bit bounce". The effects of bit bounce are reduction in ROP, premature wear of the bit and dynamics loading on drill-pipe and surface equipment.

The root cause of bit bounce is the roller cones interaction with the bottom hole. Under specific conditions, a three-lobed pattern can develop on the bottom of the hole, complementing the three cones of the bit, see Figure. This leads to an accelerated BHA in axial direction at a frequency three times the rotary speed. Whether the initial vibration will grow or damp out depends on the interaction of the bit with the bottomhole pattern and the dynamics of the suspended BHA [4, 5].

Axial vibrations/Bit whirl			
Observation	Typical environment	Short term corrective action	Long term counter measure
Top drive or Kelly bouncing at 3* RPM. Premature bit failure	Roller cone bit in hard competent rocks Low inclination wells	Change RPM Increase WOB	Run drillstring vibration software to find critical speeds for axial vibrations Change bit type to fixed cutter bit

Table 2.2: Observation and counter measures chart for axial vibrations [6].

2.2.2 Lateral Vibrations

Lateral vibrations are induced by side impacts to the bit, BHA and drill pipe sections of the drillstring. Lateral vibration of the BHA is the single type of vibration which is responsible for most of the downhole tool and drillstring failures. Impacts of the BHA against the borehole wall generate high shock loads, which can cause failure of measurement-while drilling (MWD) tools. Additionally BHA whirl generates high cyclic bending stresses leading to fatigue failures in threaded connections [4, 5].

2.2.2.1 Bit Whirl

In extreme conditions, lateral vibrations can generate a vibration mechanism referred to as “Bit whirl”. It is a condition where friction between the rotating bit and rock causes the bit and lower portion of the drill-string to precess around the borehole in a direction opposite that of the drill-string rotation. Whirls is self sustaining because centrifugal force pushes the whirling bit into the borehole wall or tapered portion of the bottom hole pattern, creating more friction. When the whirl is initiated it may continue as long as the bit rotation continues or until something interrupts bit rock contact [4, 5].

There are five main types of whirl:

1. Forward whirl
2. Snaking motion
3. Backward whirl
4. Partial Backward whirl
5. Chaotic whirl

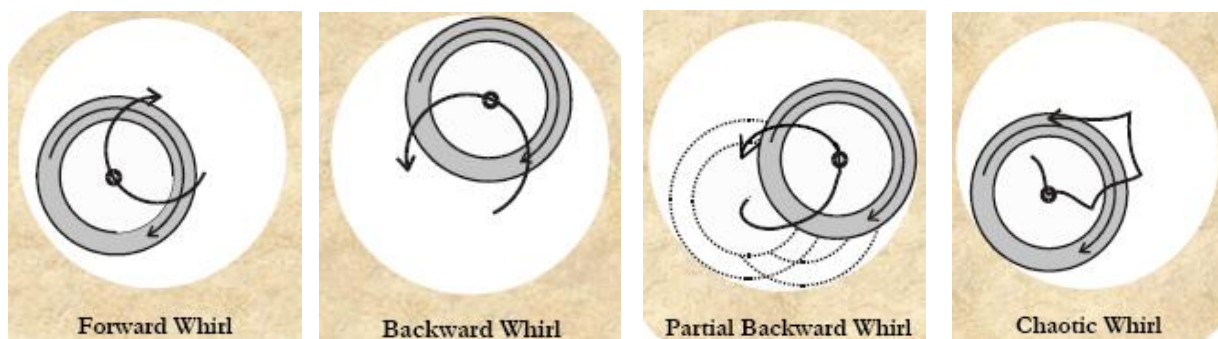


Figure 2.2: *Types of whirl in cross sectional view from above [5]*

1] During forward whirl, the centre of rotation is moving in the same direction as the drillstring rotation. This mode typically creates flat spots on the BHA components because the same side of the BHA component is always on the outside. Forward whirling amplitudes are maximal when the rotary speed equals the speed of the assembly. However, forward whirl generally does not create excessive cyclic bending stresses. The mode is most widely experienced in drill collar sections in between stabilizers (see Figure 3).

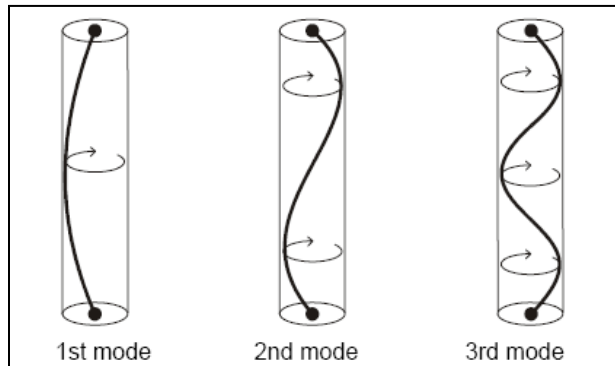


Figure 2.3: *Forward whirling of the drillstring between stabilizers. This illustrates the ideal situation when the drill collar is suspended between the stabilizers without contacting the borehole wall. The 1st, 2nd and 3rd mode of forward whirling vibration relate to the 1st, 2nd and 3rd critical speed [42].*

2] The snaking motion is a vibration mode that occurs in long non-stabilized sections of drill pipe that are lying on the side of the hole in high angle extended reach wells. When the rotary speed exceeds a certain threshold the drillstring starts to snake, thereby sliding up and down the borehole wall. Well beyond this speed, the drillstring will eventually start to backward whirl which can cause severe damage to string components after only a short period of time.

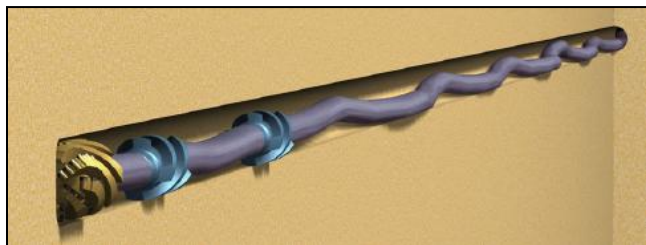


Figure 2.4: *Snaking motion of BHA [5].*

3] Backward whirl is one of the predominant types of vibration that damages PDC bits. It is a condition where the centre of rotation is moving in the opposite direction as the drilling rotation. In fact the BHA is rolling over the borehole wall. The vibration is driven by the frictional interaction of the BHA and the borehole wall.

It generally starts at the stabilizer but can, under certain conditions, propagate further into the BHA. The backward whirl is fully developed when large parts of the BHA are whirling backwards. During this stage, the BHA takes form of a helix (see Figure). Backward whirl causes frequency cyclic bending stresses leading to drill collar connection failures.

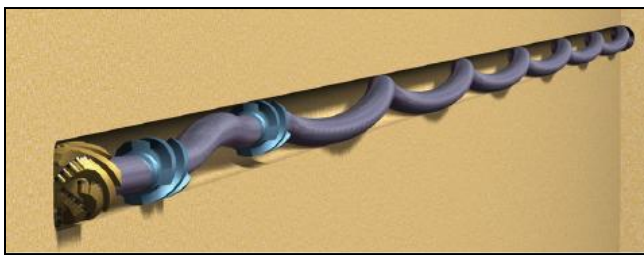


Figure 2.5: During fully developed backward whirl the BHA takes the form of a helix [5].

4] Partial backward whirl is a special type of backward whirl that exists in inclined holes. The BHA, from its neutral position at the bottom of the hole, rolls up against the borehole wall. Once it has rolled up to above 90°, it will lose contact with the wall and fall back to a low position. The impact on the lower side of the hole can be quite violent and damage MWD equipment and motors.

5] The chaotic whirl is a chaotic mixture of forward and backward whirl. The drillstring slams on to the borehole wall several times per string revolution, leading to very high loading on drillstring components. This type of whirling can occur for (near) vertical wells.

Lateral vibrations/BHA whirl			
Observation	Typical environment	Short term corrective action	Long term counter measure
<u>On site:</u> Frequent wash-outs and twist-offs. Many cracks found on inspection Poor ROP High torque	Hard rock Unstabilized BHA's Vertical Wells Over gauge holes	<u>Step 1:</u> Stay on bottom, decrease RPM <u>Step 2:</u> If no effect the pick off bottom and restart with lower RPM	Optimize BHA with critical speed analysis Use a downhole motor Use anti-whirl or stabilized bit

Table 2.3: Observation and counter measures chart for lateral vibrations [6].

2.2.3 Torsional vibrations

Torsional vibration is a non-uniform bit rotation in which the bit stops rotating momentarily at regular intervals. This causes the drillstring to periodically torque and spin free (i.e., stick-slip). Because the top of the drillstring keeps rotating, the string is wound up, the torque increases, and energy is stored in the string, which acts as a torsional spring. When the bit can no longer withstand the increasing torque, the energy is suddenly released and the bit starts spinning. The bit spins so fast that the drillstring unwinds and torque drops. As a result, the bit slows down again until it finally comes to a complete standstill, after the whole process of winding and unwinding repeats itself.

Torsional vibration modes can be classified in two categories:

1. Transient
2. Steady state

1] Transient vibrations are typically localized vibrations of a drilling condition such as change in lithology.

2] Steady state vibrations are vibrations that develop and last for an extended time duration.

Torsional vibrations are an important cause of reduced ROP, overtorqued drill pipe connections, twist-offs and premature bit wear. Torsional vibration, commonly referred to as stick/slip is heavily related to drillstring characteristics. The bit can often be responsible for initiating stick slip, but the phenomenon is primarily a torsional oscillation of the drill string [2, 7, 8].

2.2.3.1 *Stick Slip*

Stick slip is defined as the variation in acceleration of the BHA components and is a typical vibration mechanism related to torsional vibrations. Stick slip is caused by irregular or cyclic torque variations acting on the BHA/drill-pipe and formation interaction. This is due to friction along the lower end of the drillstring or due the friction from the borehole wall. To simply determine the cause of stick slip, the bit can be lifted from bottom with continuous rotation. If the drill string still oscillates, the stick slip is initiated due to friction between the drillstring and the borehole wall.

Stick slip is often experienced when drilling with a PDC bit in high angle wells and with high WOB, where downhole friction torque exceeds the rotary torque. Stick slip can produce ten times the initial rotation speed, as well as total standstill or reverse motion of the bit. This can lead to cutter breakage since no PDC bits are designed for this movement.

Stick slip is more common when drilling with a PDC bit compared to a rock bit. This is due to the negative correlation between bit rotation speed and bit torque. When the RPM (rotation per minute) increases, the torque decreases and provides feedback that initiates the stick slip torsional oscillation of the bit [3-5, 9]



Figure 2.6: Bit damage caused by stick slip [1].

Torsional Vibration/Stick slip			
Observation	Typical environment	Short term corrective action	Long term counter measure
On site: Large surface torque oscillations (<1Hz) Decrease in ROP	High Angle wells Aggressive PDC bits Percussion drilling High friction formations	Increase RPD, reduce WOB Feed soft torque	Use less aggressive bits Use roller reamers Use oil based muds

Table 2.4: Observation and counter measures chart for torsional vibrations [6].

3. Basic Petroleum Geology

3.1 Geological Terms and Nomenclature

3.1.1 Classification of Carbonate Sedimentary Rocks

Sedimentary rocks are one of the three main rock groups in the rock cycle, with the other two being igneous and metamorphic rocks. When rocks undergo weathering, materials that result will be transported by erosional agents, such as water, wind or gravity. Eventually the results of these processes are called clastic *sediment*. Furthermore, sediments can be produced by precipitation from fluids, mostly water. These groups of sediments include carbonates, evaporites, inorganic cherts and banded iron formations as their largest and most important groups. The nature of sediment, or after the lithification, a sedimentary rock therefore not only depends on the sediment supply, but also on the sedimentary depositional environment in which it formed. The latter includes a variety of parameters including climate, transporting agent, morphology etc. Rocks and especially sedimentary rocks have the characteristic of being porous and permeable to a certain degree and can therefore store fluids and gases. The most important rock type with regards to the oil and gas industry is sedimentary rocks.

3.1.2 Carbonate Rocks

Carbonate sedimentary rocks constitutes 10 to 25 percent of all sedimentary rocks on earth and may be parted in two main mineralogy groups; limestone and dolomite. Limestone consists for the most of calcite (CaCO_3), while dolomite consist of calcium magnesium carbonate ($\text{CaMg}(\text{CO}_3)_2$). Limestone is formed by organisms which precipitate calcite. When the organisms die, they dissolve on the seabed and become buried on a later stage by new layers. During sedimentation, the layers of calcite form Chalk, while layers of sand and clay-rich sediments form sandstone. Limestone is normally discovered in areas that earlier were under water. [9, 10]

3.1.2.1 Calcareous Biogenic Sediments

There are three basic sedimentary types: clastic sediments, siliceous biogenic sediments, and calcareous biogenic sediments. All sedimentary types are defined on the basis of variations in the relative proportions of clastic, siliceous biogenic and calcareous biogenic grains. Chalk is categorized as a biochemical limestone. A brief description of calcareous biogenic sediments will be presented in this chapter in order to fully understand the composition of Chalk.

Calcareous biogenic sediments are composed of less than 30% clastic grains, less than 30% siliceous-biogenic grains, and greater than 30% biogenic carbonate grains. The main name of calcareous biogenic sediment describes its degree of consolidation and/or its composition, using the following terms:

1. Ooze: Soft, unconsolidated biogenic carbonate
2. Chalk: Partially to firmly consolidated biogenic carbonate
3. Limestone: cemented biogenic carbonate

The work of Matter (1974), Schlanger and Douglas (1974), and Scholle (1975) have shown that all nannofossil deposits undergo progressive lithification as a function of burial depth and other factors. Thus, any distinction between soft, intermediate, and hard deposits are completely arbitrary and of no major significance; it simply gives three different names to the same deposits as it passes through a continuous spectrum of diagenetic stages. In this thesis, the term “Chalk” will be used broadly to cover the whole range of nannofossil deposits, with modifiers to describe the degree of lithification. [10, 11]

3.1.3 Chalks

Chalks are fine-grained limestones composed largely of microscopic calcite plates called coccoliths. The coccoliths are derived from a group of planktonic algae, the coccolithophores. When the coccolithophores die, the coccoliths get detached from the membrane, and sink to the sea floor. In areas with little supply of other types of sediment such as clays and sands, thick layers of calcareous ooze (“rain”) is formed. Figure 3.1 shows a scanning-electron microscope (SEM) photograph of a typical porous Chalk. Generally, Chalks are considered to be soft, friable deposits.

Examination of outcrop Chalks indicates that Chalks undergo significant diagenetic changes during their post-depositional history. The major factors that control the patterns of Chalk alteration are scanning-electron microscopy, light microscopy, oxygen-isotopic analysis, and trace- element analysis.

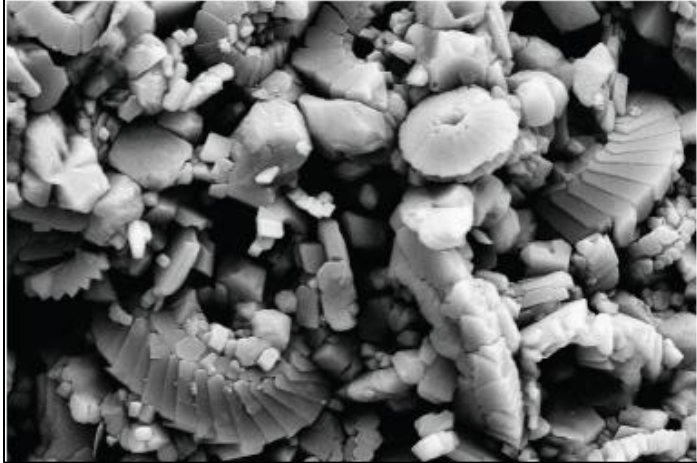


Figure 3.1: *Typical biogenetic structure of Chalk, Kansas Chalk magnified 14050X [12].*

The major mechanism of Chalk cementation is pressure solution and local re-precipitation. Although small variations in grain size, clay content, or faunal deposition can lead to significant bed-to-bed variations in cementation, overall patterns of Chalk diagenesis appear to be related to two main factors:

1. Maximum depth of burial, and
2. Pore-water chemistry

Under normal circumstances, a typical nannofossil Chalk (ooze) will have 70 % porosity at the sediment water interface. As burial depth increases, the porosity should decrease. At 1 km of burial depth, the porosity should be reduced to half of its initial porosity (35%).

With an even deeper burial depth of 2 km, the porosity should be decreased to 15%, and at 3 km, to essentially 0%. With a few notable exceptions, the porosity and permeability of Chalks decreases as a direct function of burial depth.

The exceptions include cases where:

1. Oil entered the rock, reducing or terminating carbonate reactions.
2. Chalks are over-pressured and therefore not subject to the normal grain-to grain stresses expected at those depths
3. Tectonic stresses increase solution and cementation in areas where fresh water entered the pores before major burial, Chalks show a much steeper gradient of porosity loss versus burial depth as compared with regions where marine pore fluids were retained.

In areas, such as the Ekofisk field in the southern North Sea, major quantities of oil is produced from Chalks having as much as 50% porosity at depths greater than 3 km. Scholle (1977) described this abnormal high porosity as a result of constraints on both physical and chemical compaction processes. Firstly, that the effect of overpressured reservoirs physically maintained the porosity as the overburden is supported by the fluid itself, and secondly, that early oil invasion and high oil saturation inhibited chemical induration of the Chalk. [12-15]



Figure 3.2: Coccoliths “raining down” onto the Cretaceous sea floor. The coccolith plates are normally 1-10 microns in diameter. [14]

3.2 Fundamentals of Rock Mechanics

3.2.1 Stress

Stress is symbolized by the creek letter sigma, σ , and represent the axial force applied vertically down on the cross sectional area, A, of the Chalk.

— —

3.2.2 Strain

Strain is defined as the change in shape, or deformation of a rock under pressure. The strain is calculated from the change in length (ΔL) or diameter (Δd) of the core, divided by the original Length (L_0), or diameter (d_0).

Strain in x-direction:

Strain in y-direction:

3.2.3 Porosity

Majority of rocks contain a certain volume of voids. This is distributed within the solid rock in the form of pores, cavities and cracks of various shapes and sizes. The total sum of these empty spaces is called porosity, a fundamental characteristic of rock material that affects its physical properties (durability, mechanical strength, etc.).

The total porosity (ϕ) is defined as the ratio between the volume of the pores (V_p) and the bulk volume expressed as a percentage.

—

Where:

- (Pore volume) is the fraction of the total volume of a solid occupied by the pores (i.e. the empty space of a solid).
- (Bulk Volume) is the volume of a solid including the space occupied by pores.

Porosity can further be divided into two different sub- definitions: effective and total porosity. The pore throats in a rock can either be closed or open. When pores are closed, they are completely isolated from the external surface and do not allow access of fluids. When pores are open, they are connected with the external surface and permit the passage of fluids. Total porosity represents the total void space in the rock whether or not it contributes to fluid flow. I.e. it includes both closed and open pore throats. The effective porosity is the interconnected pore volume in a rock that contributes to fluid flow in a reservoir. I.e. it excludes isolated pores. Thus, effective porosity is typically less than total porosity. [9, 11, 16, 17]

The calculation for the total porosity is represented above. Calculation for the effective porosity excludes isolated pores, and ϕ_e is therefore obtained from the following formula:

—————

Where:

- W_s is the saturated weight,
- W_d is the dry weight
- ρ_f is the density of the saturation fluids.

3.2.4 Unconfined Compressive Strength (UCS)

One way to estimate the hardness of a rock sample is to measure its unconfined compressive strength (UCS). The UCS test is performed in a triaxial cell where the rock sample is subjected to axial load and confining pressure. The first step is to apply axial load with zero confining pressure until the rock fails. This is the initial UCS of the rock sample. Then confining pressure is applied in steps (500, 1000, 1500 psi) in order to extend the UCS potential. When confining pressure is applied, the rock sample can withstand higher axial loads before failure. For each step, axial load is applied until breakage occurs. If breakage occurs at a confining pressure of 2000 psi and no axial loading is applied, the absolute maximum compressive strength of the rock is at the point of breakage, in this case at 1500 psi. This value gives an indication of the hardness of the rock sample.

Figure 3.3 illustrates an idealized stress-strain curve for an elastic-plastic material. As the load is applied, the material first deforms elastically then plastic deformation occurs after the stress exceeds the yield point. Point B in the figure is when breakage occurs and the UCS is determined for each step [18, 19].

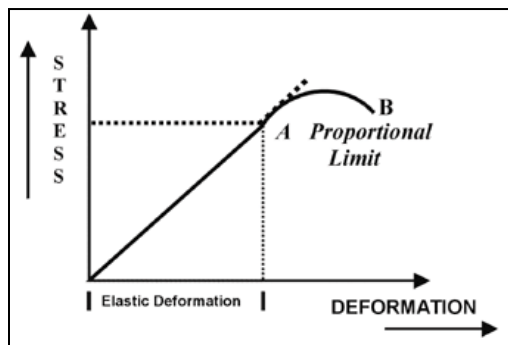


Figure 3.3: *Idealized stress-strain curve. The highest stress-point equals the UCS of the rock sample [19].*

3.2.5 Mohr-Coulomb Failure Criterion

Another way to estimate the hardness and abrasiveness of a rock sample is to conduct the tests in a triaxial cell. A positive displacement pump is used to generate the confining pressure while a testing machine is used for applying the axial load. In addition, the rock sample is jacketed in a plastic tube to apply side forces. The unconfined pressure (stress) is increased in steps as for the UCS test.

For each step, the shear stress applied naturally increases as well as the normal stress experienced by the rock sample. Each step represent a half circle (new envelopes will be formed as the material strain hardens) referred to as Mohr's circles, see Figure 3.4.

Failure occurs when the state of stress is such that the Mohr stress circle becomes tangent to an experimentally determined envelope. The fit of the line, plotted tangent to the Mohr's circles, is used to define the failure envelope. The straight line reflects the friction angle. The friction angle tells something about the abrasiveness of a rock. A high friction angle, above 42 deg, indicates an abrasive rock (neglecting RCB as a valid bit type), while a low friction angle indicates a non-abrasive, soft rock (PDC and RCB usable). If the rock is under sufficient pressure to be ductile, the linear envelope can be used as a yield criterion [18, 19].

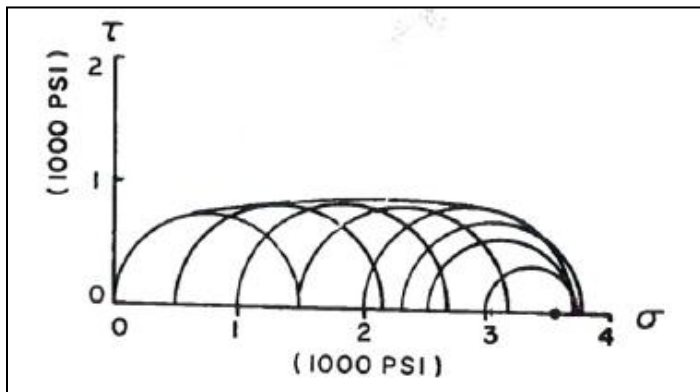


Figure 3.4: Illustration of a typical Mohr failure envelope [19].

3.2.6 X-Ray Diffraction Analysis

An X-Ray diffraction analysis investigates crystalline material structure, including atomic arrangement, crystallite size and imperfections. This is an exact measure of the mineralogy of a material. The sample to be identified is first crushed into powder, than X-Rays of known wavelength are passed through the sample in order to identify the crustal structure [15].

X-ray diffraction analysis were performed for different Chalk samples available at the University of Stavanger and compared with each other. Results are presented in Chapter 5.

3.3 Depositional Environments

The environment, in which sediments are deposited, is an important factor in sediment distribution, type, structures and other aspects important to formation evaluation. This chapter will briefly address the depositional environment encountered in the geological record of the Ekofisk field, namely the deep marine/transition zone.

A depositional environment is defined as a particular (geomorphic) setting in which a particular set of physical, chemical and biological processes operate. Deposition within a particular sedimentary environment, generate a certain kind of sedimentary deposit. These certain kinds of sedimentary deposits may enable geologists to recognize the particular sedimentary depositional environment. And when knowing the environment, one is able to predict and/or explain other sediment-logical aspects related to the same or adjacent rocks. The physical environment is shaped by factors such as basin geometry, grain size population available, water depth, temperature, wind regime, tides and essentially all other physical processes that occurs in the given environment. To recognize ancient environments, geologists use criteria such as lithology and mineralogy, geometry of litho-logical units, sedimentary structures and textures, sedimentary textures, fossils and chemical properties [20, 21].

3.3.1 Deep Marine/ Transition Zone

The seas of the deeper marine environments produce their own sediments. Or, more correctly, small animals that live in the water column produce sediments. Some animals produce siliceous sediments of clay and silt sizes, that rain down to the sea floor. Other animals, like foraminifera and coccoliths make up the sediments themselves. When the animal dies, it gradually sinks to the sea floor and such deposits of small shells may accumulate enormous successions. In the North Sea, the Shetland Chalk group of Cretaceous age is an example of this type of sediment. The sediments, produced at sea, are called pelagic sediments [20, 21].

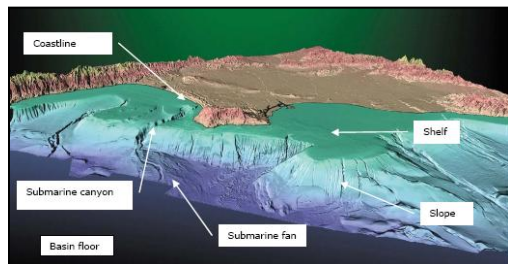


Figure 3.5: *Illustration of a deep marine/ transition zone. (The Los Angeles margin, California [22])*

3.4 Petroleum Geology of the Norwegian North Sea.

The North Sea is a fairly large area, and consequently, several depositional environments have existed laterally at the same time, or overlapping the same timeframe. Some formations are widespread throughout large parts of the area, while others are local deposits existing in a limited amount of space and time. This means that the order of groups and formations cannot be expected as exact as the overview presented in the figure below for any given well. Notice that the Tor and Hod Formations are of Cretaceous age, while the Ekofisk formation is in the Paleocene/Cretaceous transition [20, 21].

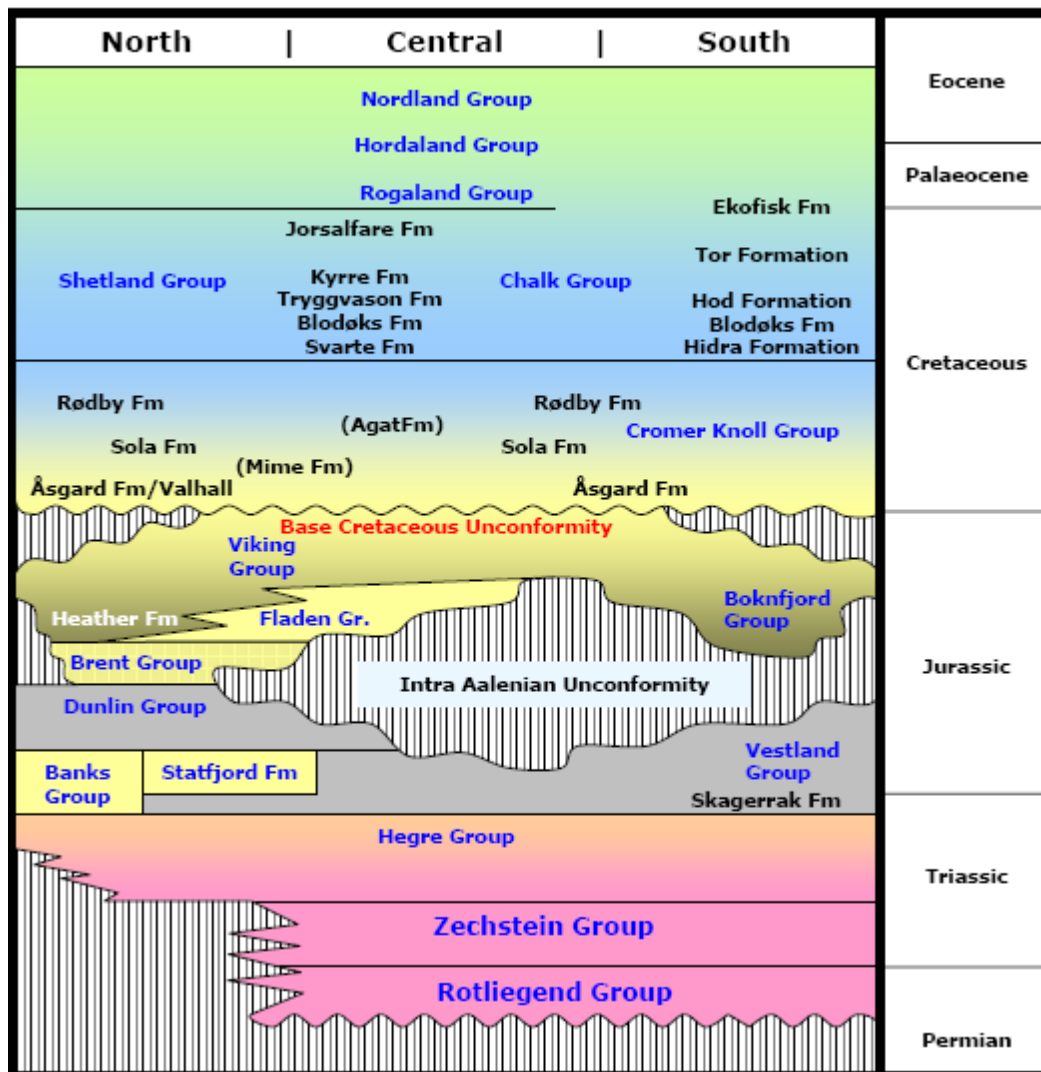


Figure 3.6: Very schematic overview of the stratigraphy of the North Sea. Modified after several authors, including Millennium Atlas and Brennand et.al (1998) [20].

3.4.1 Cretaceous (144- 65 Ma)

Since the Tor and Hod Formations are of Cretaceous age, this geological time period is the only one presented here. The word “Cretaceous” is derived from the Latin “creta”, which is a term for the fine-grained, white limestone called Chalk.

The Cretaceous age was a period of warm climatic conditions and with a global high sea level. The sea level was 350 m higher than at the present day, and over half the continental landmasses were submerged. The combination of high sea levels and low topographic relief resulted in large and shallow shelf seas. This pattern was completely different from our-present day oceans. Great amounts of Chalk were deposited in these shallow seas where plant and animal life was abundant.

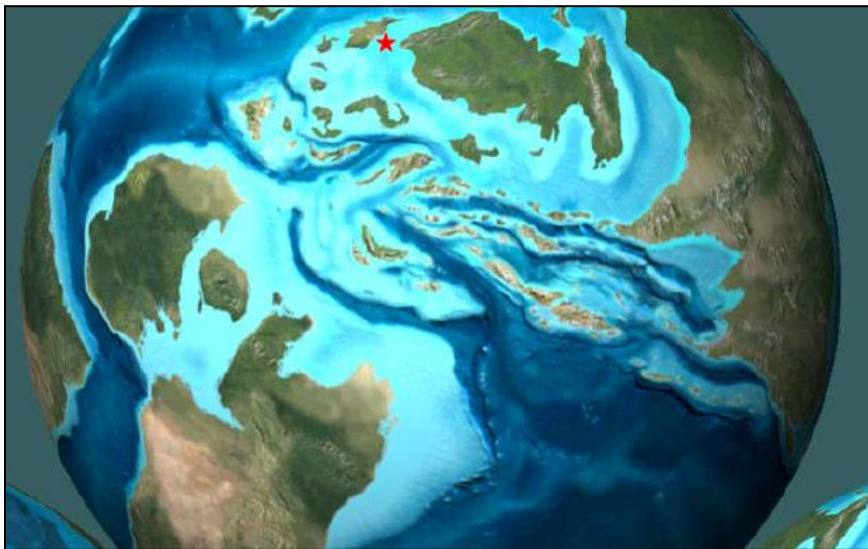


Figure 3.7: Late Cretaceous (60Ma) N. Hemisphere. North Sea area marked by red star. [22]

The upper Cretaceous of the southern part of the North Sea (location of the Ekofisk field) is dominated by Chalk with little or no siliclastic deposits, whereas in the northern part of the North Sea (location of the Sleipner field) more siliclastic clay-dominated sediments are present.

Despite a vast amount of literature addressing Chalk problems and challenges, this type of deposit is still poorly understood. The needs for more knowledge include aspects of deposition, re-deposition, diagenesis and reservoir characteristics [20, 21, 23].

3.4.1.1 Cretaceous Stratigraphy

The Tor and Hod Formations belong to the Chalk group and are located in the central North Sea, as the table below illustrates. The Chalk group was deposited in an open marine environment during a general rise in sea level. The Chalk facies formations were deposited as coccolith debris and other carbonate grains and sequences often show a cyclic pelagic sedimentation pattern termed periodites. In the central Trough, extensive subsidence resulted in the Chalk facies being dominated by re-deposited Chalks which were transported down-slope as major slide, slumps and debris flows, and proximal and distal turbidites [20].

NORTHERN NORTH SEA		CENTRAL NORTH SEA		
North Viking Graben	South Viking Graben			
Rogaland Group				
		Ekofisk Formation		
Shetland Group	Jorsalfare Fm	Tor Formation		
	Kyrre Fm			Hod Formation
	Tryggvason Fm	Blodøks Formation		
	Blodøks Formation			Hidra Formation
	Svarte Fm			
Cromer Knoll Group				
Cromer Knoll Group	Rødby Formation	Agat Fm	Rødby Formation	
	Sola Formation	Ran SST Unit	Sola Formation	
	Munk Marl Bed	Åsgard Sands	Ran Sandstone Unit	
	Åsgard Fm	Mime Fm	Tuxen Fm	
	Kimmeridge Clay Formation		Mandal Formation	

Table 3.8: Illustration of the Cretaceous stratigraphy [20].

3.4.2 The Ekofisk Field

The Ekofisk field is Norway's largest oil field with an area extent of 56 . It is located at 70-75 meters below sea level in the southern North Sea. The field was discovered in 1969 by Phillips Petroleum Company. The field was originally produced to tankers until a concrete storage tank was installed in 1973. Since then, the field has been further developed with many facilities, including riser facilities for associated fields and export pipelines.

The Ekofisk field produces from naturally fractured Chalk of the Ekofisk and Tor Formations of Early Paleocene and Late Cretaceous ages. The reservoir rocks have high porosity, but low permeability.

In 1984 Phillips Petroleum Company identified a severe seabed subsidence. The reservoir management during early Ekofisk production involved pore pressure depletion from 7000 psi towards 3500-4000psi. The high porosity Chalk reservoir was experiencing significant porosity reduction due to this primary depletion, which resulted in reservoir compaction that propagated and caused subsidence of the seabed. Two actions were taken; One to secure the platforms, and one to prevent further seabed subsidence. First the platforms were elevated by an enormous jacking operation. This compensated for the subsidence that had already occurred. Secondly, seawater was injected to compensate for the subsidence problem. The pore pressure was still declining for some years after 1988, before it stabilized in 1994 and then slowly started to increase [12, 13, 24].

Ekofisk Field

Discovery year	1969	
Development approval	01.03.1972	
On stream	15.06.1971	
Operator	Conoco Phillips Scandinavia AS	
Licensees	Conoco Phillips Scandinavia AS	35.11%
	Total E&P Norge AS	39.90%
	Eni Norge AS	12.39%
	Petero AS	5.00%
	Statoil Petroleum AS	6.60%
Recoverable resources	Original	Remaining as of 31.12.2009
	532.6 million oil	118.5 million oil
	156.5 billion gas	18.8 billion gas
	14.6 million tons NGL	2.0 million tons NGL

Table 3.1: Schematic overview, Ekofisk facts [24].

3.5 Geological setting

Chalk has played a decisive role in the Norwegian oil industry since the first discovery of the Ekofisk field. Chalks are present in a wide variety of environments largely because coccoliths, as a group, have a wide salinity tolerance (Bukry, 1974). Coccoliths are pelagic organisms which have an extremely wide environmental and latitudinal distribution. However, their rate of production is slow causing coccolith-rich sediments or Chalks only to be present in settings that have low rates of input of other materials. Examples can be found in shallow- water areas where other clastic terrigenous and other carbonate inputs are low. In general though, modern Chalks are found in water depths between 400 and 4000 m [20, 21, 23].

3.5.1 Depositional Environment of Chalk in the Ekofisk field

This chapter will briefly address the depositional environment encountered in the geological record of the Ekofisk Field (Tor and Hod Formation) in the southern North Sea.

The Chalk reservoir in the Ekofisk field was created during Late Cretaceous. The sea level continued to rise through this period and large areas of Norway and Sweden were submerged. In the northern part of the North Sea, the muds and Chalk were contaminated by particles and sand, creating sandstones and clays in the reservoir sections.

The southern North Sea was cut off from any terrestrial sediment supply during the late Cretaceous. At the same time plankton flourished in the warm upper layers, which promoted the exceptional depositional conditions required to produce the pure, calcareous coccolith muds [15] (so-called ooze). The Tor and Hod Formations were deposited with nearly no contamination of clastic particles, creating Chalk deposits with little or no siliclastic content. The Hod Formation shows partly intercalations of shale horizons (well 15/12-05). However, onshore age equivalent deposits are characterized by varying amounts of intercalated chert bands or chert nodules. This is difficult to evaluate for the North Sea deposits as only wells are drilled. Nevertheless, in certain areas chert is abundant (ex. Well 2/04-4X), while in others no chert was found so far (well 7/01-01). Moreover, the origin of the chert is often only poorly understood and not in detail studied [15, 20, 21, 23].

3.5.1.1 *The Tor Formation*

The Tor Formation consists of white to light grey, tan to pink, hard, Chalky limestones. The succession is generally homogenous, or consists of alternating white, grey or beige, moderately hard to very hard, rarely soft, mudstones or wackestones, rarely packstones, Chalks, Chalky limestones or limestones. Occasional fine layers of soft grey-green or brown marl occur and also rare stringers of grey to green calcareous shales.

In the Norwegian sector, seismic interpretation indicates that the thickness of the formation may exceed 600 m in the northwestern part of the Central Through.

Distribution: The formation is present throughout the central North Sea (fig). In the Norwegian sector it is very thin or absent on the Lindesnes Ridge and the Utsira High.

Depositional environment: Open marine with deposition of calcareous debris flows, turbidities and autochthonous periodites.

Age: Late Campanian to Maastrichtian.

3.5.1.2 *The Hod Formation*

The Hod Formation consists of hard, white to light grey, crypto- to microcrystalline limestones which may become argillaceous or Chalky in places. White, light grey to light brown, soft to hard Chalk facies may dominate the formation or alternate with limestones. The limestones may be pink or pale orange. Thin, silty, white, light grey to green or brown, and soft, grey to black, calcareous clay/shale laminae are occasionally present. Pyrite and glauconite may occur throughout the succession with the latter more common in the lower part.

In the Norwegian sector, seismic interpretation indicates that the thickness of the formation may exceed 700 m in the northwestern part of the Central Through.

Distribution: The Hod Formation is widely distributed in central and eastern parts of the central North Sea, passing laterally into sediments of the Herring and Flounder Formations to the west and the Tryggvason and Kyrre formations to the northwest.

Depositional environment: Open marine with deposition of cyclic pelagic carbonate-rich (turbidity currents) and distal turbidities (Skovbro 1983; an d'Heur 1986).

Age: Turonian to Campanian [24].

4. Sample testing

Several samples from offshore and onshore Chalk were collected. Offshore Chalk was sampled from cores stored at NPD according to the needs of the study with sample size not exceeding 50 g at best. This small sample size is by far from ideal but no other source for samples is available. Following wells were sampled:

- North Sea (Central Graben):
 - Well: 2/4-8 AX (existing porosity data)
 - Well: 25/11-17
 - Well: 15/12-4 (existing porosity data)
 - Well: 16/2-3
 - Well: 7-1-1 (existing porosity data)
 - Well: 2-4-4X (existing porosity data)

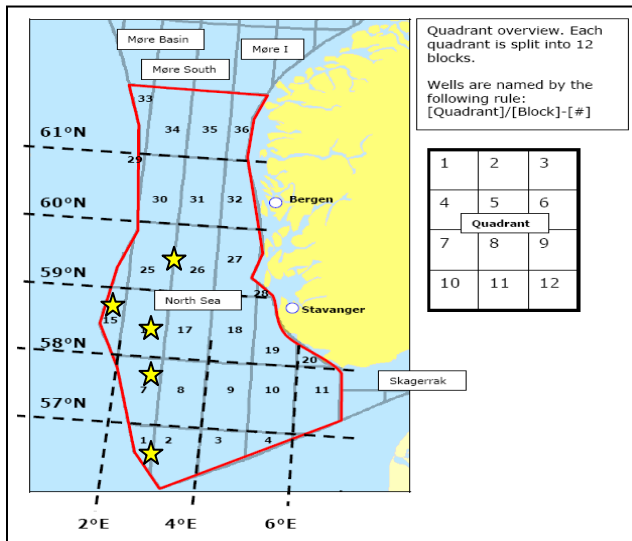


Figure 4.1: Modified map from NPD showing location of core samples from the selected wells. The yellow stars show the location of the core samples from selected quadrants [20].

Onshore Chalk was collected in different localities. Samples from Kansas, Belgium (Mons, Liege), Denmark (Aalborg, Stevns Klint) were stored at UiS and taken from large rock slabs without a definite stratigraphic control. This Chalk is claimed to be high porosity Chalk (< 30%) and often studied as so-called 'reservoir equivalent' (e.g. Hjuler (2007), Omdal (2010) and references therein). Chalk with a variety of porosities but mainly below 20% is exposed in Northern Ireland and at the same time the most complete stratigraphic section of Late Cretaceous carbonates in Europe (Mitchell, 2004) was collected.

4.1 Sample description and results

To reach the given objective different geological methods were applied:

1. Petrography
2. X-ray diffraction
3. Geochemistry
4. Isotope geochemistry (C-O stable isotope measurements)

1] Petrographic analyses include studies with binoculars and white light microscopes as well as scanning electron microscope analyses on polished thin sections.

2] X-ray diffraction (XRD) were executed with a Philips X'Pert PRO PW 3040/60 diffractometer, with Cu K α X-ray radiation, Si monochromator, at 40kV y 30mA, step scan at $\sim 1^\circ$ /minute and step size of 0.02 $^\circ$ 2 θ . Whole rock powders were prepared in random mounts.

3] Geochemical analyses are based on milled samples and ICP-MS analysis under highest standards performed at ACEM labs in Canada.

4] Isotope geochemistry includes C-O stable isotope analyses carried out at the University of Edinburgh with a Thermo Electron Delta⁺ Advantage with Windows (XP professional) OS and controlled by Isodat 2 software and VG Isogas Prism III, wherefore 0.5-1.0 mg of sample material was loaded after careful drilling.

The sample preparations for the mentioned methods have been executed according to highest scientific standards and are routine therefore elsewhere in detail described. These methods together with porosity measurements were applied to gain sufficient geological information for the understanding of the different Chalk samples.

[This extensive rock study is conducted and written by Udo Zimmermann, professor at the University of Stavanger].

4.1.1 Offshore Chalk: North Sea

4.1.1.1 *Sampling and stratigraphy:*

Different wells were sampled with representative samples for the different mentioned methods. The sample number cannot be used to describe the entire formation or the drill core, as more detailed sampling would have been necessary. However, key samples were taken at the top of the formations or from samples with different porosities when these data were available.

The sampled sections are mainly the Tor and Hod Formations, while in some cores the Ekofisk Formation was collected. All are successions of the Chalk Group deposited in the Central North Sea, where the Tor Formation has a Maastrichtian age and the Hod Formation is older from Upper Turonian to Campanian and the Ekofisk Formation often reaches the Lower Paleocene (Surlyk et al., 2003). In the north of the sampling area the Hod Formation has been affected by clastic input and thin clay and silt horizons are developed.

4.1.1.2 *General observations*

In wells 2/04-8 and 2/04-4X porosity variation oscillates between 0 and 45 % and is not dependent on depth, while porosity in well 15/12-04 varies only between 3 and 22 % (Table 4.1). However, it is nothing known about the quality of the data and the process of developing this database (NPD open source).

It is expected that Chalk porosity decreased during lithification while overpressure affected or hampered this process, as such that Chalk might retain higher porosities as it happened in the North Sea basin during the Late Cretaceous. The formation of overpressure may be related to the abundance of fluids and clays in rocks, although no agreements upon this topic exist in the research community. However, off-shore Chalk is characterized by different porosities at different depth related to the depositional environment, basin position and post-depositional fluid flow and sedimentation rates (Surlyk et al., 2003).

All these factors vary from area to area in the North Sea basin and are difficult to quantify and to predict. Related to the varying porosity the Chalk of the two sampled formations (Tor and the older Hod

Formation) have slightly different colors and hardness easy to identify in the handsample. The Tor Formation is generally more porous and whiter, while the Hod Formation is generally harder with a slight orange stain. However, this may change when the Tor Formation is affected by hydrocarbon flow.

4.1.1.3 Petrography

Similar in all cores the samples do show recrystallization and cement of new growth after bury. The new growth is very fine grained and is abundant in pore spaces and along crystal surfaces. The main phase, which could be identified despite the small grain-sizes, is calcite. Small chert grains and few clay minerals are visible. Some samples show styloliths and here a larger amount of clay minerals are detectable. The samples are mostly composed of coccolith debris, while other fossil fragments are very rare.

In few cores chert was drilled and in one well a Chalk conglomerate observed. Chalk in wells 7/01-01 and 25/11-17 is extremely white and seems to be very pure. These results match those by earlier studies on off-shore Chalk (e.g. Hjuler (2007), Omdal (2010) and references therein).

4.1.1.4 Mineralogy

There are no significant qualitative differences in between the different wells. Most of the limestone samples are dominated by calcite with only few traces of clay minerals. The following clay minerals could be identified: smectite, illite and kaolinite. In some samples quartz was recognized as well as chlorite. The amounts vary slightly from sample to sample but not in a significant amount. Dolomite and Fe-oxides were not identified. Small variations of clastic material might have influence of wettability and hydrocarbon fluid flow and will affect fluid injection but are not significant on a microscopic scale for drilling exercises. However, the different abundances are triggered by geological conditions as described above. In only two cores chert pebbles were hit by the drill, which can be explained by slight diversions of the drill bit when hitting the ultra-hard chert or the low abundance of chert.

4.1.1.5 Porosity

Porosity was measured for nearly all sampled wells. Well 2/04-4X shows for the Tor Formation porosities between 5 and 32 % for the sampled Chalk (Table 4.1). This covers more or less the entire variation of porosities in the drilled section. The samples from well 2/04-8AX show the same range for the Ekofisk and Tor Formations. In well 7/01-01 the Tor Formation shows definitely higher porosities than the Hod Formation Chalk. In well 15/12-04 the porosities are lower (between 15 and 9%) than in all other wells.

locality	North Sea	Formation	depth (ft, m)	ROCK TYPE	POROSITY (%)
Well: 2-4-4X	VE 44	EKOFISK	10171	chert	24
	VE 45	EKOFISK	10186	chalk	15
	VE 46	EKOFISK	10222	chalk	29
	VE 47	EKOFISK	10299	chalk	32
	VE 48	TOR	10444	chalk	17
	VE 49	TOR	10450	chalk	15
	VE 50	TOR	10595	chalk	19
	VE 51	TOR	10625	chalk	5
	VE 52 A	TOR	10634	chalk	9
	VE 52 B	TOR	10634	chalk	9
Well: 2/4-8 AX	VE 31	EKOFISK	10089	chalk	22
	VE 57	EKOFISK	10095	chalk	11
	VE 33	EKOFISK	10124	chalk	6
	VE 32	EKOFISK	10130	chalk	11
	VE 34	TOR	10131	chalk	13
	VE 35	TOR	10151	chalk	25
	VE 36	TOR	10184	chalk	11
	VE 37	TOR	10198	chalk	31
	VE 58	TOR	10283.5	chalk	33
	VE 38	TOR	10284	chalk	33
	VE 39	TOR	10362	chalk	8
	VE 40	TOR	10366.5	chalk	9
	VE 41	TOR	10466	chalk	12
	VE 42	TOR	10502	chalk	27
	VE 43	TOR	10516	chalk	3
Well: 7-1-1	VE 6	TOR	7360	chalk	24
	VE 7	TOR	7371	chalk	23
	VE 9	TOR	7372	chalk	23
	VE 8	TOR	7384	chalk	24
	VE 11	HOD	8066	chalk	c. 10
	VE 12	HOD	8075	chalk	c. 15
	VE 13 A	HOD	8087	chalk	c. 13-15
	VE 13 B	HOD	8087	chalk	c. 13-15
	VE 14	HOD	8100	chalk	8

Well: 15/12-4	VE 26	MAUREEN	2446.5	shale	27
	VE 27	TOR	2494.5	chalk	13
	VE 28	TOR	2503.65	shale/chalk?	13
	VE 29 A	TOR	2506.35	chalk	9
	VE 30	TOR	2513.35	chalk	15
Well: 16/2-3	VE 15	LISTA	1715.8	shale	
	VE 16	LISTA	1715.8	Shale/chalk	
	VE 17	TOR	1716.9	chalk	
	VE 18	TOR	1720.9	oil rich chalk	
	VE 53	TOR	1721	oil rich chalk	
	VE 19	TOR	1762.8	chalk	
	VE 54	TOR	1766.5	chalk	
				chalk containing	
	VE 21	TOR	1775.2	chert	
	VE 20	TOR	1788.1	chalk	
	VE 22	HOD	1814.1	chalk	
	VE 23	HOD	1833.7	chalk	
				shale laminae in	
	VE 24	HOD	1832.1	chalk	
	VE 55	HOD	1836.8	chalk	
VE 25	HOD	1852	chalk		
Well: 25/11-17	VE 1	VÅLE	1733.7	shale	
	VE 2	VÅLE	1740.5	shale	
	VE 3	TOR	1742.8	chalk	
	VE 4	TOR	1748.7	chalk	
	VE 56	TOR	1752.6	chalk	
	VE 5	TOR	1756.5	chalk	

Table 4.1: Porosity and sampling of core samples from the North Sea.

4.1.1.6 Geochemistry

Generally, the major element geochemistry is addressed to clarify the content of non-carbonate phases. Descriptions of the trace element geochemistry are made to reveal the influence of clastic material, which can be monitored by Zr, Rb and Y. Rare earth elements (REE) are sensitive to slightest changes in the water composition and the influence of detrital material in a carbonate. This is based on the fact that the REE budget in a carbonate reflects the water composition from which the carbonate precipitated. Influence of clastic material would rise the REE concentrations significantly and visible as water is strongly depleted in REE in comparison to rocks, like sandstones or shales. Values below 8 ppm for Zr, 3 ppm for Rb and 2 ppm for Y would exclude significant clastic input (below 2 %), which affected REE pattern. Characteristic seawater pattern of REE show a negative Ce anomaly, a positive Eu and Y anomaly. Influence of meteoric water would lower the Y/Ho ratio below 40

Well 2-4-4-X:

The Tor Formation shows lower SiO₂ concentrations than the Ekofisk Formation while key trace elements are relatively similar. Hence, the latter has higher amounts of chert but not of other clastic material. Sums of REE are low and Y/Ho ratios point to a secondary fluid flow, which might have originated in a continental area. Clastic input is negligible as Rb and Zr concentrations are extremely low (Table 4.2).

Sample	Formation	well	SiO ₂ %	Al ₂ O ₃ %	CaO %	Rb PPM	Zr PPM	Y PPM	ΣREE PPM	Y/Ho	Porosity %
VE47	Ekofisk	2-4-4X	4.1	0.2	51.3	1.3	7.8	7.9	22.5	36	32
VE49	Tor	2-4-4X	1.4	0.2	54.1	1.1	4.4	10.2	27.5	41	15
VE52A	Tor	2-4-4X	1.4	0.3	54.3	1.4	3.9	8.4	25.0	38	9
VE32	Ekofisk	2-4-8XA	9.7	0.6	48.7	2.8	5.7	11	39.5	38	11
VE36	Tor	2-4-8XA	3.4	0.3	52.7	1.1	9.6	11.3	31.6	38	25
VE37	Tor	2-4-8XA	3.1	0.2	52.3	1	6	12.7	34.5	41	31
VE39	Tor	2-4-8XA	1.8	0.5	54.1	2.5	5.5	11.8	37.0	36	8
VE42	Tor	2-4-8XA	2.6	0.2	52.5	1.6	6.3	7.3	21.3	37	27
VE43	Tor	2-4-8XA	2.9	0.6	53.2	3.6	5	10.9	40.6	34	3
VE7	Tor	7-1-1	0.9	0.2	54.6	0.8	13.4	6.6	19.5	39	23
VE13A	Hod	7-1-1	4.0	0.6	51.6	4.2	8.7	11.9	50.4	33	14
VE29B	Tor	15-12-4	5.5	0.7	50.5	3.2	7.2	15.3	65.9	32	9
VE18	Tor with oil	16-2-3	1.3	0.2	51.6	0.8	4.5	10.6	23.1	44	
VE20	Tor	16-2-3	1.1	0.2	54.0	1	8.1	5.1	15.7	43	
VE25	Hod	16-2-3	2.2	0.3	53.2	1.9	6.8	9.1	33.9	34	
VE5	Tor	25-11-17	0.9	0.1	53.8	0.7	4.4	5.2	15.7	35	
VE4	Tor	25-11-17	1.6	0.2	52.9	1	5	6.9	19.5	43	

Table 4.2: Main geochemical values for the collected samples (from Lie, 2011).

Well 2-4-8XA:

The same can be observed in this well but the Chalk shows definitely higher clastic input with increased concentrations for Y and Rb and slightly enriched Sum REE (ΣREE). Y/Ho ratios seem to decrease with depth, which might point to circulating intra-formational fluids. Silica is in all samples higher than in the well 2-4-4-X and might be a result of diagenesis.

Well 7-1-1:

Although the sample of the Tor Formation shows ultra-clean Chalk, Zr concentrations are high which might be explainable by the influence of wind-transported grains. Y/Ho ratios are not high, hence the Chalk was affected similarly by fluids as the others. The sample of the Hod Formation is very different and is clearly enriched in clastic material and has higher REE normalized to shales (Fig. 4.2) and was possibly affected by a different fluid flow regime.

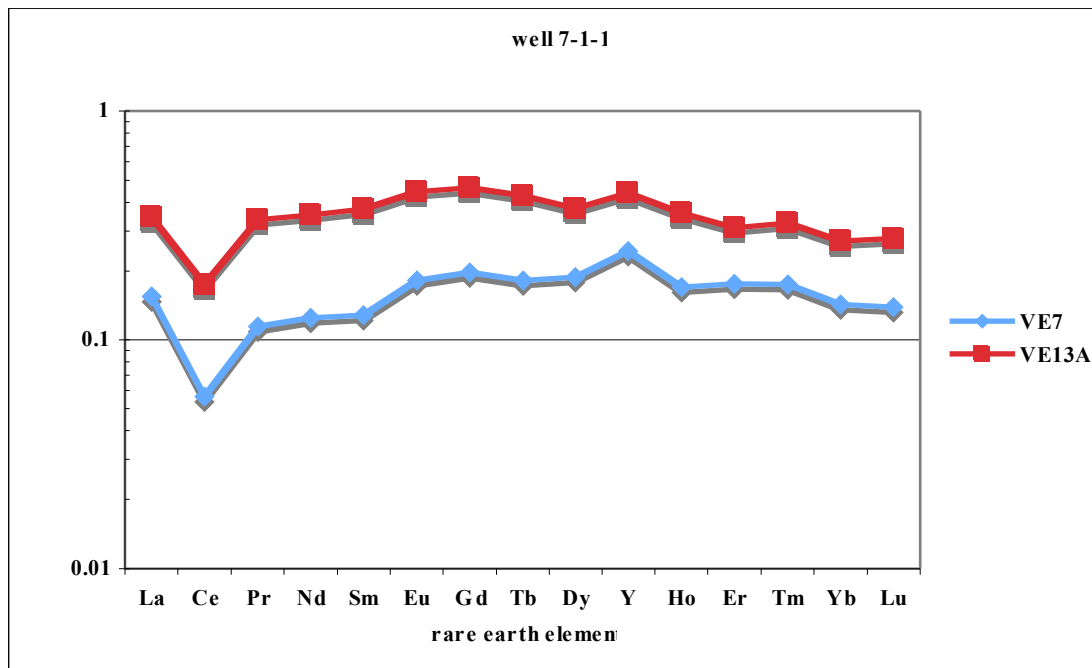


Figure 4.2: The geochemical difference between Chalk from the Hod Formation (red) and the Tor Formation (blue) is obvious in this plot with REE (rare earth elements and Y). The latter reflects a stronger original pattern related to seawater composition, while the Hod Formation is affected by clastic input and/or different fluid flow (sample normalisation on the y-axis to PAAS [Post-Archean Australian Average Shale after Taylor and McLennan, 1985]).

Well 15-12-4:

Here, only one sample was so far analysed and shows resemblance to the Hod Formation of well 7-1-1 with enriched concentrations in silica, Zr, Rb, Y, Σ REE and lower Y/Ho ratios than Chalk further south in wells 2-4, although values are even a little bit higher. However, the sample is affected by enrichment in middle REE that might be a result of the existence of clay minerals.

Well 16-2-3:

Again, the Hod Formation shows a different geochemical character with increased non-carbonate element concentrations and lower Y/Ho ratios than the overlying Tor Formation Chalk. However, the Chalk of the Tor Formation shows the highest Y/Ho ratios with very low Σ REE.

Well 25-11-17:

The Tor Formation is very pure but possibly at the top affected by secondary fluid flow, which decreased the Y/Ho ratios, clastic input is negligible.

Plotting average REE pattern of the different wells against each other the relatively similarity is visible and the typical seawater pattern obvious, with a strong negative Ce anomaly and a positive Y anomaly (Fig. 4.3). However, some samples differ slightly like those from well 15-12-4 and well 7-1-1.

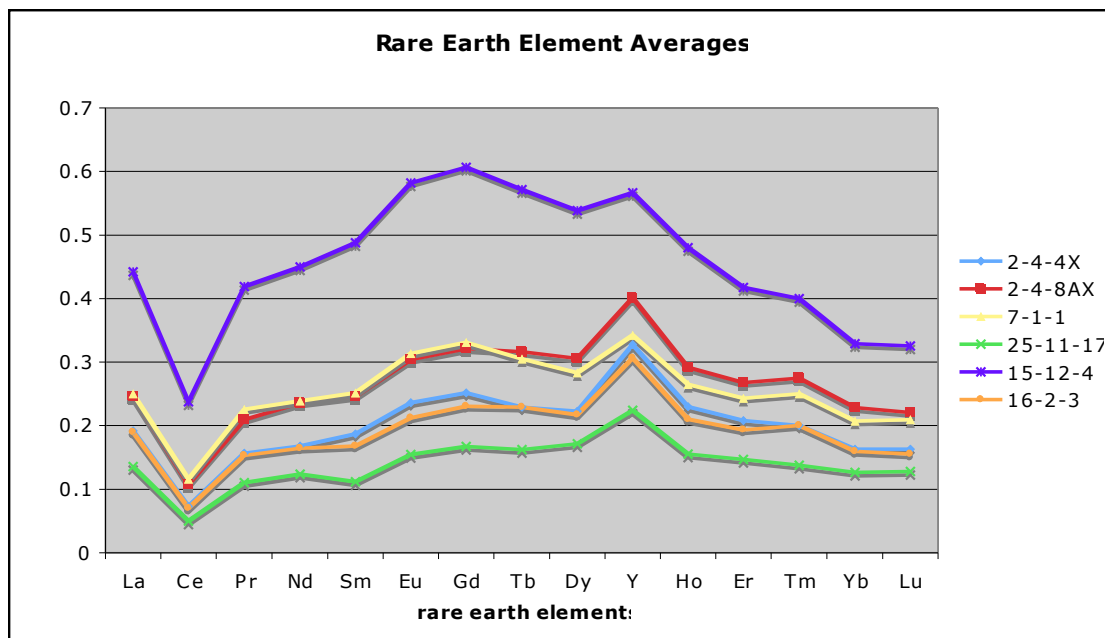


Figure 4.3: REE (including Y) averages for the different wells with a strong enrichment in middle REE (Eu to Ho) for the sample from well 15-12-4; as only one sample was so far analysed this trend needs to be treated carefully (sample normalisation on the y-axis to PAAS [Post-Archean Australian Average Shale after Taylor and McLennan, 1985]).

Conclusively, REE chemistry shows that the entire sample set is influenced by post-depositional fluid flow. The composition points to a freshwater source and is mostly different from onshore samples (see below). Earlier it was proposed (e.g. Scholle, 1977) that freshwater did not circulate in the reservoir

Chalk as this circulation would minimize the porosity. However, these data show that the secondary fluid phase had a very different composition and that high or low porosity is related to other factors than this specific fluid flow as Table 2 shows: there is no correlation between high porosity and high Y/Ho ratios. Hence, if freshwater circulated it would not have affected the porosities.

4.1.1.7 Isotope geochemistry

The C-O isotope values are here demonstrated in delta notation after (see S 200) and routine. Values are written in this notation to avoid complicated discussions. Generally, positive $\delta^{13}\text{C}$ and negative $\delta^{18}\text{O}$ point to a warm climate (and high palaeowater temperatures), while negative $\delta^{13}\text{C}$ and positive $\delta^{18}\text{O}$ to a colder climate. Both isotope values are very well understood for the Cretaceous in terms of secular curves, meaning global water composition. This is argued based on the fact that isotopic differences in seawater are quickly homogenized on a geological time-scale. However, $\delta^{13}\text{C}$ are difficult to re-set and interpreted to be robust under diagenetic and even metamorphic conditions, while $\delta^{18}\text{O}$ are very sensitive to post-depositional geological processes. (See Hoefs, 2009 for details and further information)

$\delta^{13}\text{C}$ is relatively uniform throughout all samples between 1.582 to 2.445, but both values are extreme values when the average of all samples is 1.953 with a standard deviation of only 0.20 (Table 4.3). Values around 2 are comparable to the global C isotope variation curve in seawater (after Arthur et al. 1985, and others)

In contrast, $\delta^{18}\text{O}$ are variable and negative between -0.564 and -6.336. These values are not in concordance with the benthic $\delta^{18}\text{O}$ record on fossils (see Royer et al., 2011 and references therein) and would lead to mostly unrealistic palaeowater-temperatures. Expected $\delta^{18}\text{O}$ for the Late Cretaceous are 0 to 2 ‰ and surface water temperatures vary between 27 and 35°C in tropical areas (Royer et al., 2011). As the North Sea basin was located further north lower temperatures are expected. Only few samples would point to an original O isotope concentration and are marked in green in Table 4.3. This would imply a single crystallization event, as in fossil shells, which is here not the case as Chalk is composed of largest numbers of fossil debris. Secondary cementation is reported and the new growth had happened under different conditions, ideally. Commonly, it is argued that cementation takes place under colder water conditions and a result for palaeowater-temperatures in Chalk during the Late Cretaceous would be around 16-20°C when calculating primary $\delta^{18}\text{O}$ from Surlyk et al. (2010) from deep-water Chalk after

Gómez et al. (2008). Similar results are available for other onshore Chalks (see below and Morosova et al., 2011). Weathering of the Chalk and dolomitisation can be excluded as reasons for secondary alteration of primary $\delta^{18}\text{O}$ values. Hence, disturbed primary $\delta^{18}\text{O}$ values are mainly controlled by a second circulating fluid (see above), from which secondary carbonate phases precipitated. This coincides with the petrographic observation, which pointed to new growth of carbonate cement.

More samples are necessary to gain more insight into the O isotope evolution of these rocks.

FORMATION	SAMPLE	POROSITY	$\delta^{13}\text{C}$	$\delta^{18}\text{O}$	T
	2-4-4X	%	‰	‰	°C
Ekofisk	VE 45	15	1.94	-4.28	32.93
Ekofisk	VE 47	32	1.99	-3.10	26.08
Tor	VE 48	17	1.76	-5.09	38.14
Tor	VE 49	15	1.91	-4.26	32.80
Tor	VE 51	5	1.93	-4.58	34.81
Tor	VE 52A	9	1.95	-4.76	35.98
	2-4-8Ax				
Ekofisk	VE 31	22	1.89	-4.70	35.53
Ekofisk	VE 33	6	1.77	-5.53	41.15
Ekofisk	VE 32	11	1.97	-5.25	39.21
Tor	VE 34	13	2.09	-5.00	37.55
Tor	VE 35	25	1.88	-5.51	40.99
Tor	VE 36	11	1.76	-5.77	42.79
Tor	VE 38	33	1.64	-4.58	34.77
Tor	VE 39	8	1.84	-5.67	42.11
Tor	VE 42	27	2.15	-4.86	36.62
Tor	VE 43	3	1.75	-5.85	43.39
	7-1-1				
Tor	VE 6		2.00	-5.27	39.36
Tor	VE 9		2.06	-5.15	38.49
Hod	VE 13 B		2.44	-3.87	30.45
	16/2-3				
Tor	VE 16		1.98	-0.56	14.25
Tor	VE 17		1.58	-4.95	37.21
Tor	VE 18		1.74	-5.06	37.95
Hod	VE 25		2.26	-6.34	46.92
	15/12-4				
Tor	VE 27	13	1.89	-6.21	45.97
Tor	VE 29 A	9	1.97	-5.67	42.07
Tor	VE 30	15	2.33	-6.25	46.30
	25/11-17				
Tor	VE 3		2.26	-1.18	18.77
Tor	VE 4		1.95	-4.60	34.92
	VE 5		2.18	-4.58	34.81

Table 4.3: C-O isotope variations of off-shore Chalk. Palaeowatertemperatures ($T^{\circ}\text{C}$) after Gómez et al. (2008). Temperatures marked in green might reflect surface watertemperatures of the North Sea but this implies no new growth of calcite under colder conditions. In blue temperatures are marked which could reflect average palaeoseawatertemperatures.

4.1.1.8 Correlating porosity with other geochemical values

Plotting the different porosities versus $\delta^{18}\text{O}$ values does not reveal a systematic trend. The unknown fluid or the secondary carbonate phase hence did not affect the porosity. Comparing porosity values with the total of REE (ΣREE) shows a slight negative trend with lower ΣREE the higher the porosity (see Table 4.3). This is interesting for samples with low to negligible clastic content like Chalk in wells 2/04-4X and 7/01-1. However, more samples are necessary to develop a trend in this regard.

4.1.1.9 Preliminary comments

REE analyses shows that most of the Chalk was affected by secondary fluid flow which lowered Y/Ho ratios towards freshwater values. $\delta^{18}\text{O}$ values are affected by secondary fluid flow. In few samples significant clay minerals were detected as such that ΣREE and $\delta^{18}\text{O}$ values as well as porosity were controlled by other factors, like fluid flow. The variety of porosity through the stratigraphy might be explainable by an inhomogeneous fluid flow so possibly rather local events than basin wide flooding. However, this is speculation and more data are needed for a proper interpretation.

4.1.2 Onshore Chalk

A lot is known about onshore Chalk, which is studied here. The main focus for this short report was therefore not the general description, as this can be read in a large number of publications elsewhere (see e.g. Hjuler (2007), Omdal (2010) and references therein). Therefore, only compelling new observations are mentioned here.

4.1.2.1 Geochemistry

Besides the exposure in Aalborg all onshore Chalk have very low silica concentrations below 1.6 % and with the low trace element composition (Table 4.4) it is relatively clear that clastic material is not abundant in a significant amount. The silica concentrations are related to chert, which is either primary or secondary and still matter of debate.

Onshore Chalk reflects nearly pristine seawater compositions in their REE pattern (Figure 4.3) and is different from off-shore Chalk in this regard (Figure 4.2). Σ REE concentrations are lower in onshore Chalk and Y/Ho ratios are mostly higher. The only matching onshore Chalk in this regard is from Liege and Kansas, although their Σ REE are lower pointing to a less amount of clastic material. Porosities of these two exposures are described as c. 36% for Kansas and 41% for Liege (Hjuler, 2007).

Sample	OUTCROP	Σ REE	Y/Ho	Zr (ppm)	Rb (ppm)	Y (ppm)	Porosity (%)
V5A	STEVNS KLINT	20.79	46.2	8.70	5.3	9.70	53
V5B	STEVNS KLINT	16.32	47.9	3.60	1.1	9.10	53
V5C	STEVNS KLINT	18.46	53.3	6.50	0.9	9.60	53
V5D	STEVNS KLINT	15.24	51.7	7.30	0.6	9.30	53
V12	STEVNS KLINT	15.91	51.6	5.00	4.3	9.80	53
V11A	AALBORG	17.25	43.3	9.20	4	6.50	47
V11B	AALBORG	18.54	45.3	10.10	5	6.80	47
V11C	AALBORG	16.05	49.2	7.50	5.1	5.90	47
V11D	AALBORG	16.72	45.0	10.50	5.2	6.30	47
V13	AALBORG	15.34	42.3	15.90	0.4	5.50	47
V14	LIEGE	21.26	37.9	11.30	2.6	7.20	41
V15	MONS	13.5	48.3	3.30	1.4	5.80	39
V16	KANSAS	15.43	39.3	11.00	3.4	5.50	36

Table 4.4: General data for onshore Chalk with porosity data after Hjuler (2007) and chemical value from Morosova (2011).

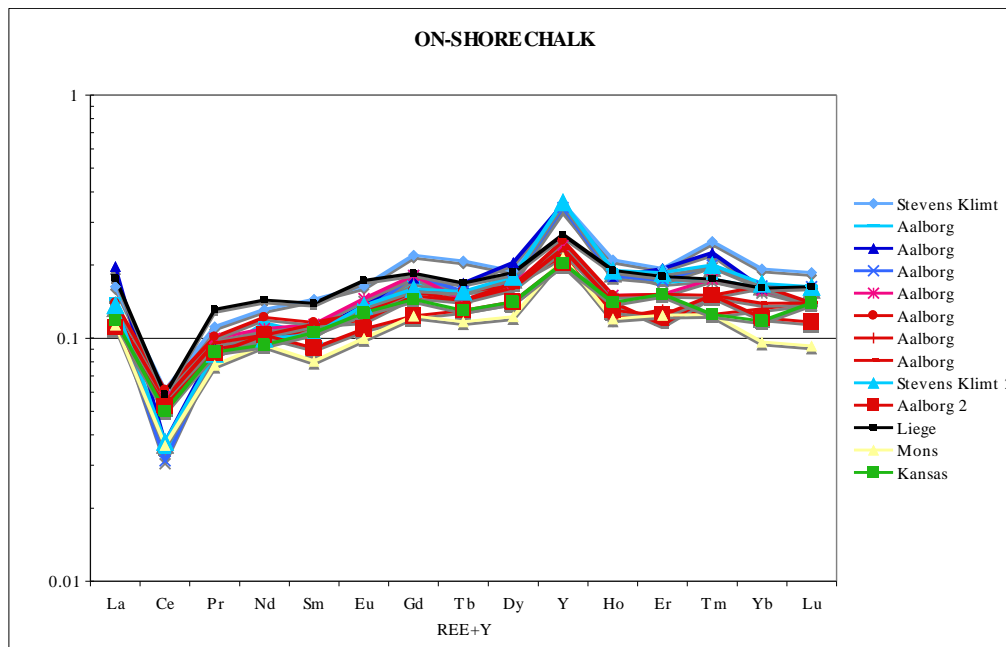


Figure 4.4: Onshore Chalk REE (rare earth elements) pattern, which mimics seawater composition. Note the strong positive anomaly of Y and negative anomaly of Ce (sample normalization on the y-axis to PAAS [Post-Archean Australian Average Shale after Taylor and McLennan, 1985]) and lower REE concentrations than in off-shore Chalk (see Figure 4.1).

4.1.2.2 Isotope geochemistry

$\delta^{13}\text{C}$ values are mostly between 1 and 2 and comparable with global trends during the Late Cretaceous (Arthur et al., 1985). The sample from Kansas varies slightly and more data are necessary to interpret here a trend, which might be different. However, as reported the exact stratigraphic position of the sample is unknown and values as low as 1 are described for the Early Maastricht (Arthur et al., 1985). Surprising are $\delta^{18}\text{O}$ values, which do reflect nearly seawater temperatures during the Late Cretaceous. This implies that (i) no secondary fluid flow took place, (ii) no cementation was developed, (iii) the cement has a similar same isotopic composition as the organisms or (iv) the average of both, cement and fossil debris, is by chance the same as the average palaeoseawater composition. However, similar results are described from Stevns Klint, where $\delta^{18}\text{O}$ values seem to be primary (Surlyk et al., 2010). This can only be resolved on nano-scale level, which is out of the scope here.

Sample	outcrop	$\delta^{13}\text{C}$ (‰)	$\delta^{18}\text{O}$ (‰)
V5A	STEVNS KLINT	1.771	-1.482
V5B	STEVNS KLINT	1.743	-1.596
V5C	STEVNS KLINT	1.772	-1.480
V5D	STEVNS KLINT	1.723	-1.512
V12	STEVNS KLINT	1.548	-1.238
V11A	AALBORG	2.055	-1.159
V11B	AALBORG	2.145	-1.047
V11C	AALBORG	2.166	-1.051
V11D	AALBORG	2.219	-0.713
V13	AALBORG	2.153	-0.953
V14	LIEGE	1.648	-1.349
V15	MONS	2.014	-1.070
V16	KANSAS	1.077	-5.018

Table 4.5: C-O isotope values for onshore Chalk (after Morosova, 2011).

Remarkably and important here is that the Chalk from Kansas, in contrary, has disturbed $\delta^{18}\text{O}$ values similar to the Chalk from the North Sea (see Tables 4.3 and 4.5). Generally, the Chalk from Kansas is not affected by clastic material and shows comparable Y/Ho ratios as off-shore Chalk, hence would be influenced by fluid flow not recognized in other onshore Chalk. Why such a resemblance exist is not clear and need more sample material to substantiate.

4.1.3 Northern Ireland Chalk

14 members of the Ulster White Limestone Formation were sampled, which is the most complete Chalk section onshore in Europe of Late Maastrichtian age (Mitchell, 2004). The litho- and biostratigraphy of the Chalk succession is very well understood and the exposures are well documented (Hancock, 1961; Fletcher, 1977).

4.1.3.1 Petrography

Most of the samples comprise fine shell debris of coccolith but as well echinodermata (crinoids and echinoidea), inocerams (extinct bivalves), and few brachiopods and bryozoans ammonites while belemnites are abundant. First studies show fine secondary cementation filling pore-space and around debris of coccoliths and other organisms. The rocks are often affected by styloliths and chert nodules generation, while most of the members have even developed chert bands, traceable over the preserved basin in Northern Ireland (Fletcher, 1977). The origin of the chert is unknown and interpreted to be of diagenetic origin around trace fossils (Simms and Ruffell, in prep.).

4.1.3.2 Porosity

These values match partly the Tor and Hod Formation but are lower than reservoir and onshore Chalk. It seems that at the base and at the top the porosity is the highest, while within the formation it is much lower. Hence, similar to off-shore Chalk the porosity does not increase with depth and seems to be affected by other processes than simple loading and mechanical reduction of porosity.

The measured porosities are shown in the table below. It was observed a large variation between 1 and 18% (Table 4.6).

Member	Sample	Sample Weight		Porosity		
		Dry	Saturated	P1 calculated	P2 measured	Deviation
		[g]	[g]	%	%	%
Ballycastle	W20	118.18	121.53	6.16	6.44	3.89
Port Calliagh	W16	132.13	141.68	16.19	16.36	6.78
Tanderagee	W15	94.3	98.92	11.89	11.55	2.89
Ballymagaree	W18	21.65	22.66	11.03	11.22	1.72
Portrush	W27	74	75.59	5.29	5.30	0.10
Garron	W10	73.43	73.91	1.48	1.45	1.61
Glenarm	W9	76.66	78.03	1.22	1.23	1.27
Larry Bane	W19	30.4	30.94	4.81	4.91	1.94
Cloghastucan	W24	30.4	30.94	1.06	1.08	1.73
Galboly North	W23	122.69	122.69	8.44	8.44	0.01
Galboly South	W13	81.06	85.58	12.35	12.91	4.33
Cloghfin Sponge Bed	W3	183.15	184.8	2.30	2.36	2.45

Table 4.6: Porosity measurements for the Chalk of the Ulster White Limestone Formation from bottom (Cloghfin Sponge bed Member) to the stratigraphic top (Ballycastle Member) (data courtesy M. Larsen).

4.1.3.3 Geochemistry

The Chalk from Northern Ireland is extremely pure and has less abundance of silica than most of the North Sea and onshore Chalk. Influence of clastic material monitored by Rb, Zr and Y is extremely low above the Galboly Member (Table 4.7). This can be explained by the lithostratigraphic position of the two oldest members, which were uncomfortably deposited on clastic material. Hence, slight reworking or exposure to clastic material had been the case during deposition of the old members, but disappeared later.

Σ EE are relatively low and Y/Ho ratios do not point to a strong influence of freshwater but as clastic material can be excluded as carrier of REE, freshwater fluid flow was present (Table 4.7). These values are comparable with onshore Chalk, but higher than off-shore samples. REE patterns are typical for seawater carbonates besides one sample, the oldest member, which has been deposited uncomfortably on clastic successions and is therefore affected by higher clastic material (Figure 4.4).

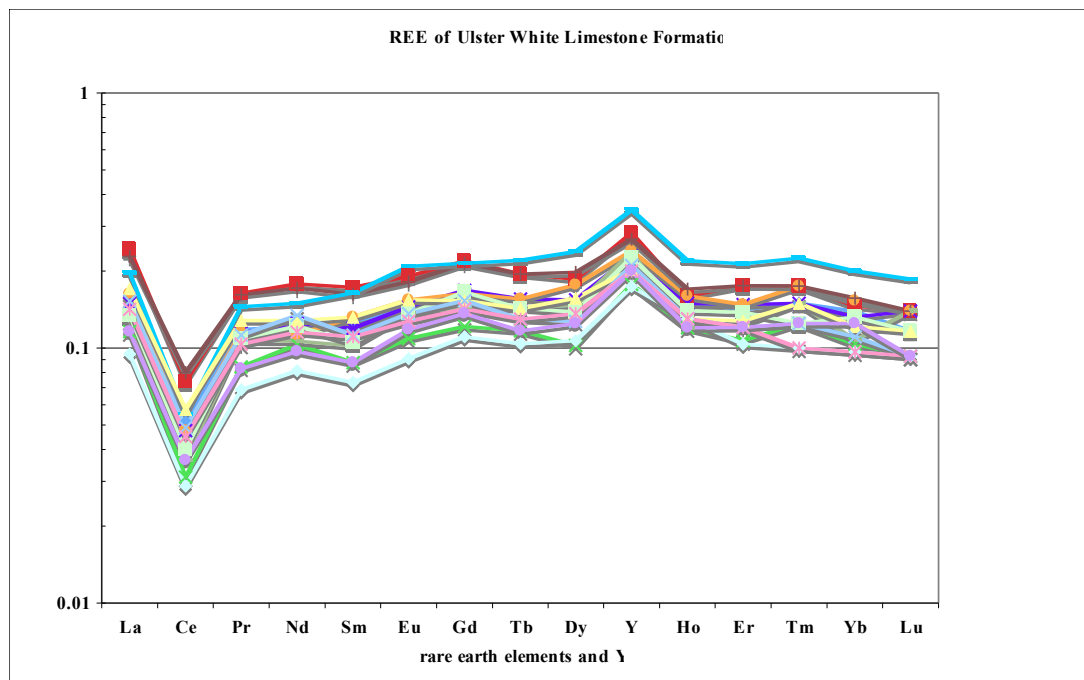


Figure 4.5: REE pattern for Chalk of the Ulster White Limestone Formation. The oldest sample (blue line) shows the less resemblance to normal seawater composition, which can be explained by its stratigraphic position deposited on underlying clastic rocks.

It shows that the samples are less concentrated in clay minerals, although styloliths are very common. Most of the samples were selected carefully avoiding styloliths. The low silica concentrations and the abundant styloliths might reflect the diagenetic effects, which concentrated non-carbonate material in distinct areas of the Chalk. However, this interpretation needs to be substantiated by detailed work on chert and styloliths, which does not exist at this time.

sample	Member	SiO ₂ (%)	ΣREE	Y/Ho	Zr (ppm)	Rb (ppm)	Y (ppm)	δ ¹³ C (‰)	δ ¹⁸ O (‰)
top									
W20	Ballycastle	0.4	16.82	43.6	1.6	0.7	6.1	1.632	-5.388
W16	Port Calliagh	0.34	23.28	42.7	1.2	0.5	9.4	0.887	-5.053
W15	Tandergee	0.47	15.68	53.3	1.7	0.5	6.4	1.409	-5.213
W18	Ballymagarry	0.2	11.67	36.2	1.9	0.3	4.7	1.188	-5.715
W27	Portrush	0.34	14.29	45.0	0.9	0.5	5.4	2.365	-5.689
W11	Garron	0.36	18.72	40.6	1.5	0.8	6.5	1.578	-4.879
W9	Glenarm	0.2	18.21	41.3	0.8	0.7	6.2	1.591	-5.290
W7	Ballintoy	0.27	13.75	40.0	1.5	0.4	4.8	1.938	-5.589
	Larry Bane							1.660	-5.970
W2	Boheeshane	0.32	19.12	39.3	1.1	0.9	5.9	1.558	-4.893
W26	Greggan	0.46	17.04	41.5	1.1	1.1	5.4	1.448	-5.902
W25A	Cloghastucan	0.44	18.48	43.8	1.3	1.1	5.7	2.107	-5.748
W13	Galboly	2.4	28.83	42.4	7.8	4.1	7.2	1.775	-5.097
W23	Galboly	1.14	20.86	42.3	3.3	3	5.5	1.586	-4.398
W04	Cloghfin	1.71	28.46	47.5	5.2	3.6	7.6	1.698	-5.465
bottom									

Table 4.7: *Geochemistry and isotope geochemistry of the members of the Late Cretaceous White Ulster Limestone Formation. The youngest member is at the top of the table, while the oldest is at the bottom.*

4.1.3.4 Isotope geochemistry

δ¹³C values are similar to those in the North Sea and for onshore samples and typical for the Late Cretaceous. δ¹⁸O isotopes are, as expected, disturbed. Tests on belemnite shells gave the same disturbed results. This is surprising as belemnites are ideal primary seawater indicators. The effect might be explained by fluid flow during diagenesis, which also affected the calcite crystals in belemnites. However, more research is necessary in this specific regard. Generally, the samples resemble off-shore Chalk and are different from onshore deposits beside the Kansas Chalk in terms of their disturbed δ¹⁸O values.

4.1.3.5 Compiling remarks

Some samples from Northern Ireland resemble in regard of porosity the off-shore Chalk analyzed, so do their REE composition including Y/Ho ratios and the disturbed $\delta^{18}\text{O}$ values. However, REE concentrations are low and therefore not affected by clastic material. This can be explained by diagenetic effects, which moved clastic phases and silica to distinct location in the Chalk to form styloliths and chert nodules and bands. During this process fluid flow and possibly freshwater fluids circulated in the Chalk, which affected both $\delta^{18}\text{O}$ values and REE pattern.

Therefore, the Chalk itself is a good analog for off-shore Chalk in terms of geological parameter and different from high porosity Chalk from other onshore deposits beside Kansas.

4.1.4 Final considerations: Resemblances of Chalk

The wells in the North Sea, which drilled Late Cretaceous Chalk successions, have different porosities independent of depth and stratigraphic position in the North Sea basin. REE and other geochemical proxies are relatively homogeneous and exclude mostly significant clastic input but point to a freshwater fluid flow. The latter might be responsible for the resetting of $\delta^{18}\text{O}$ values, although this process cannot be observed in all samples and point to local processes.

Onshore Chalks differ in the ability of preserving $\delta^{18}\text{O}$ values and seem to be less affected by freshwater fluid flow with partly higher Y/Ho ratios. However, here more samples need to be analyzed to substantiate this trend. An exception is the Chalk from Kansas, which seems to be the most comparable to the off-shore Chalk in regard of the presented geological data.

All studied sections are depleted in chert nodules or chert bands, but show well developed styloliths. Onshore Late Cretaceous Chalk in Northern Ireland, in contrast, has a lower porosity than other onshore Chalk but shows partly similar values to the low porosity Chalk in the North Sea wells. However, on an outcrop scale the most compelling difference to off-shore and other onshore Chalk is the abundance of chert, as nodules or partly basin-wide bands. Nevertheless, it needs to be kept in mind that drilling possibly miss a number of chert and the existing open pit exposures in onshore deposits like in Denmark and Belgium comprise mostly chert-free Chalk, as chert-rich Chalk would not be mined.

Chert abundances are reported of being more abundant towards the north of the Central Graben in the North Sea, but only perforation cannot account for anything else than a guess. Chert and the development of styloliths might be a consequence of diagenetic processes but here more detailed work is necessary.

If a specific Chalk should be selected for rheological analysis based on geological data as a whole and not only porosity, then Kansas Chalk (for medium porosity) and Ulster Chalk (for lower porosity) are the most similar ones. Onshore Chalk here studied, besides those from Ulster, has generally high porosity and different REE abundances and undisturbed $\delta^{18}\text{O}$ values.

4.2 Kansas outcrop description

The Kansas Chalk proved to be the most comparable sample to off-shore Chalk in regard of the earlier presented geological data. The primary focus in this thesis was to find a Chalk suitable for the Ekofisk field in order to run simulations in a sample as close to reality as possible.

The Kansas outcrop Chalk available at the University of Stavanger was provided by Conoco Phillips five years ago. It was sampled from The Niobrara Formation at the Mermaris Quarry in Kansas. The Niobrara Formation and laterally equivalent rocks were deposited during a Late Cretaceous marine transgressive cycle that created conditions favorable for the deposition of fine-grained marine carbonate rocks and the preservation of organic matter. It was a period of high eustatic sea level and crustal subsidence in the Western Interior Seaway. The Niobrara ranges in thickness from 275 to 550 m and consists mainly of interbedded organic-rich shale, calcareous shale, and marl, with minor amounts of sandstone, siltstone, limestone and Chalk.

The Kansas Chalk has following properties:

- High Porosity (27-34%)
- Low Permeability (
- Bulk density (1.3-1.6 g/cc)
- Low UCS (3,000 psi)
- Calcite % >95%

After selecting the most comparable Chalk for the Ekofisk field, it was decided to run triaxial test to investigate its hardness and abrasiveness. This is important factors that will decide the bit design.

The Chalk was sent to Terratek, a rock laboratory in Utah, and tested together with a Niobrara Chalk already available. The purpose was mainly to see if there were any differences between the samples. The Kansas Chalk provided by UIS will further be referred to as Chalk-B, while the Terratek sample is called Chalk-A.

4.2.1 Mineralogical description

Chalk-A and Chalk-B are both sampled from the Niobrara formation in Kansas. However, the extraction depth and exact GPS location of the Chalk samples are unknown. An X-Ray diffraction analysis was performed on the two different samples in order to find similarities and differences in mineralogy. The results are showed in the table below.

Sample ID	Chalk-A	Chalk- B
Quartz	0,8	0,4
K-Feldspar	1,3	0,0
Plagioclase	0,0	0,0
Calcite	97,3	99,6
TOTAL NON-CLAY	99	100
Kaolinite	0,3	0,0
TOTAL CLAY	0	0
GRAND TOTAL	100	100

Table 4.8: *Whole rock mineralogy of Kansas Chalk A and B.*

As illustrated in the table, there are small differences in Quartz, K-Feldspar, Plagioclase, Kaolite and Calcite content between the two samples. The total non-clay content only varies with one percent. This doesn't prove anything since the calcite content is normally high in pure, homogenous Chalk. The mineralogy was only determined to estimate its homogeneity.

4.2.2 Hardness

As mentioned in chapter 3.2.4, the hardness of a rock sample can be defined by its unconfined compressive strength. Two triaxial tests were performed in the rock laboratory of Terratek in Utah. - One for each of the Kansas Chalks (A and B). Below is a table showing the summary results for the triaxial tests performed.

Sample ID	Depth (ft)	As-Received Bulk Density (g/cm ³)	Effective Confining Pressure (psi)	Effective Compressive Strength (psi)	Residual Effective Compressive Strength (psi)	Quasi-Static Young's Modulus (x10 ⁶ psi)	Quasi-Static Poisson's Ratio
DKCA-5	N/A	1.630	0	2005	N/A	0.878	0.15
DKCA-1	N/A	1.667	500	3795	N/A	1.026	0.18
DKCA-2	N/A	1.669	1000	4575	N/A	0.988	0.16
DKCA-3	N/A	1.669	1500	5575 ²	N/A	1.018	0.17
DKCB-5	N/A	1.389	0	1015	N/A	0.544	0.10
DKCB-3	N/A	1.364	500	2075	N/A	0.634	0.23
DKCB-6	N/A	1.379	1000	2500 ³	N/A	0.586	0.18
DKCB-2	N/A	1.401	1500	3245 ³	N/A	0.817	0.17

Table 4.9: DCS Kansas Chalk- Summary of Triaxial Compression Tests [Terratek].

Quasi static Young's modulus and Poisson's ratio are determined using very low strain rates to eliminate any inertial effects during the tests. Young's modulus is basically the stiffness of the rock determined from the linear portion of the stress-strain curve. Poisson's ratio is the ratio of axial strain to radial strain.

The changes in these values over the ranges of confining pressures are most likely due to variation in the samples. All of the samples for each material were taken very close to one another, but with geologic materials minor variations in structure like the presence of fossils, variation in porosity and depositional texture will affect the mechanical properties.

For Chalk-A the effective confining pressure was increased in steps from 0 to 1500 psi. The effective compressive strength is 2005 psi without applied confining pressure. Later the confining pressure was increased with 500 psi for each step. The effective compressive strength naturally increases with increased confining pressure (ref 3.2.4). When an effective confining pressure of 1500 psi was applied, the maximum effective compressive strength was 5575 psi. This is the effective volumetric yield compressive strength (psi) of the rock sample. The average bulk density of Chalk-A is 1.659 g/cm³.

For Chalk- B the effective confining pressure was increased in equal steps. The effective compressive strength of Chalk-B is approximate 1000 psi lower at initial confining pressure and does therefore not reach the same level of effective UCS as Chalk-A at confining pressure of 1500 psi. The maximum compressive strength of Chalk-B is 3245 psi. This is the effective axial yield compressive strength of the rock sample. The average bulk density of Chalk-B is 1.383 g/cm³.

In summary, the two samples have different unconfined compressive strengths even though the mineralogical composition is quite similar. Chalk-A has a UCS 2330 psi higher than Chalk-B. This indicates that the rock properties of the Kansas Chalk are inhomogeneous. However, both of the Chalk types are considered non-abrasive.

The other method used for hardness measurements was the Coulomb Mohr Failure Envelope Criterion.

Sample ID	Depth (m)	Stress Regime	Effective Confining Pressures (psi)	c' (psi)	φ' (°)	Equation
DKCA-5	N/A	High	500, 1000, 1500	1070	16.4	$\tau' = 0.29364\sigma' + 1071.900$
DKCA-1						
DKCA-2		Entire	0, 500, 1000, 1500	730	23.6	$\tau' = 0.437521\sigma' + 730.527$
DCKA-3						
DKCB-5	N/A	Entire	0, 500, 1000, 1500	470	10.4	$\tau' = 0.18427\sigma' + 469.050$
DKCB-3						
DKCB-6						
DKCB-2						

Table 4.10: DCS Kansas Chalk- Coulomb Mohr Failure Parameters [Terratek]

For the “A” samples the unconfined test had much lower shear strength than the confined tests, probably for the same reasons listed above. Also when confining stress is applied any pre-existing micro fractures will be closed and shear strength will increase.

The failure mode also changes from a more brittle type failure to a ductile/plastic failure as confining stress is applied. The fit of the line, plotted tangent to the Mohr’s circles, is used to define the failure envelope. The two plots below show the results of the conducted tests. Four different samples of Chalk A & B were tested, one for each step of confining pressure.

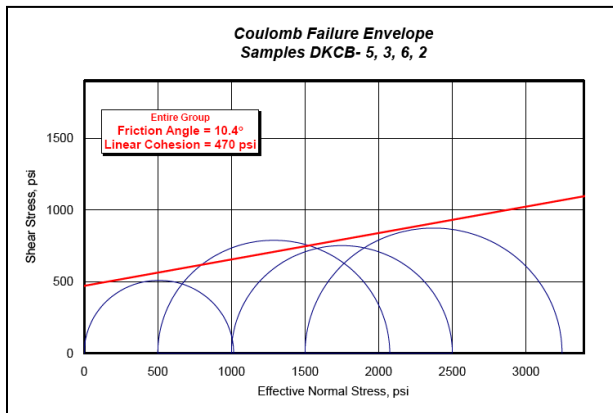


Figure 4.6: CFE results, Chalk-B

The fit of the line, plotted tangent to the Mohr’s circles, is used to define the failure envelope. In this case, the fit is not very good when using all of the Mohr’s circles and it is much better when using the #3 confined tests. The only way to improve this is to run more samples to get a better statistical line. However, when comparing the two CFE plots, it is visible that the linear cohesion and the friction angle for Chalk-A is much higher when compared to Chalk-B. This is pretty much the same result as observed for the triaxial compression test mentioned above.

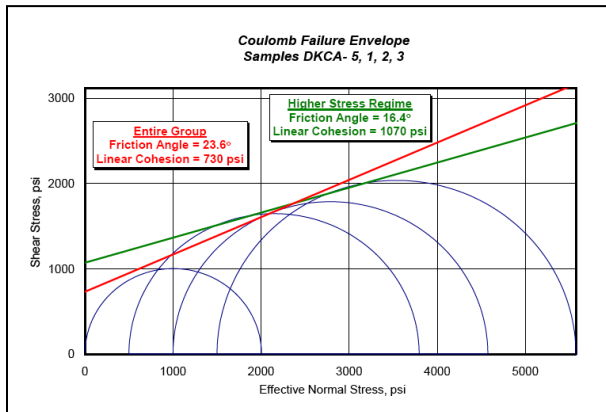


Figure 4.7: CFE results for Chalk-A [Terratek].

5 The Drilling Assembly

The drill string includes several components making each drill string design unique. However, the main components are the same, including a drill pipe, a bottom-hole assembly (BHA) and a bit. Its main function is to deploy and retrieve equipment.

A correctly designed drill string can:

1. Produce a high quality hole
2. Maximize performance of components
3. Maximize drilling and production problems

The drill string components are manufactured with various mechanical properties. The application of drill string design principals will reduce the risk of failures and damage during operations.

The drill string serves four basic functions:

1. Transmit and support axial loads
2. Transmit and support torsional loads
3. Withstand potential fatigue damage
4. Transmit hydraulics to clean the hole and cool the bit

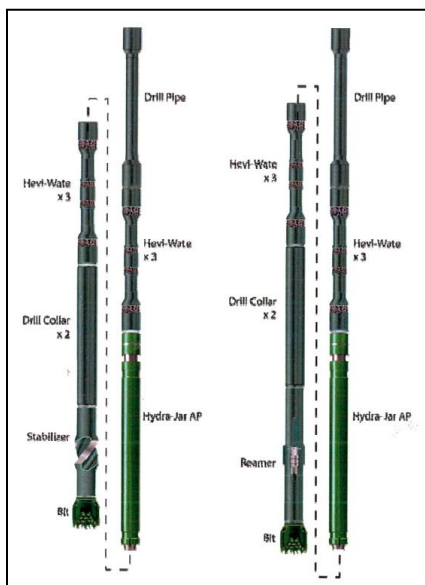


Figure 5.1: *Illustration of two different drill string designs [36].*

5.1 Drill pipe

The drill pipe is one of the largest parts of the drilling assembly. It is located at the very top of the drill string (above the transition pipe) and transmits the rotation of the rig's rotary or top drive down to the drill string. It also serves as a conduit for the drilling fluid.

The most important factor in selecting the correct drill pipe is the strength considerations. The drill string including the tool joints needs to endure torsional, and both burst and collapse pressure during drilling or tripping. The drill pipe strength is calculated based on the outer diameter (OD) and the internal diameter (ID) of the pipe. There are many sizes of drill pipe available. The most common sizes ranges from 2 3/8 in to 6 5/8 in outer diameter (OD). The weight is given in nominal weight in lb/ft and refers to the wall thickness of the pipe, not the drill pipe's actual weight.

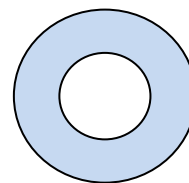
Therefore drill pipes are given grades to indicate how much force they can withstand before damage. Drill pipe grade is indicative of the yield strength in thousands of pounds per square inch. The yield is the maximum pull a joint of pipe can withstand without receiving permanent damage. For each grade of steel pipe, API has established a range of minimum yield strengths. For example, grade E pipe must fall within its established range of 75,000 psi and 105,000 psi [36].

Common grades	Yield Strength [psi]		Tensile strength [psi]	Elongation [%]
	Minimum	Maximum	Minimum	Minimum
Grade E	75,000	105,000	100,000	0.5
Grade X	95,000	125,000	105,000	0.5
Grade G	105,000	135,000	115,000	0.6
Grade S	135,000	165,000	145,000	0.7

Table 5.1: Some common grades of drill pipe with its respective properties.

As the pipe is used, the pipe is worn. Wear and erosion on the outer side of the pipe increases as the pipe is used. The four usable classes of pipe are separated by the remaining wall limits, with premium being the most widely specified class:

1. New- 86.5% nominal wall
2. Premium- 80% nominal wall
3. Class 2-70% nominal wall
4. Class 3-less than 70% nominal wall



Tube cross section

5.2 Bottomhole Assemblies

The bottomhole assembly (BHA) is the lowermost part of the drill string consisting of everything except the drill pipes. The BHA must provide weight on bit (to make the bit able to penetrate the formation), survive hostile mechanical environment and provide directional control of the well.

The components in the BHA vary depending on the application of the drilling operation. Typical factors that need to be considered when designing a BHA are hole-diameter, stiffness, hole-size and formation type. A typical assembly setup include a mud motor, the drill bit, bit sub, rotary steerable (RSS), stabilizers, drill collar, heavy weight drill pipe, jarring devices and various crossovers for various thread forms and dimensions. Other important components that often are included are measurement equipment (MWD tools) and various logging tools (LWD tools); including data storage and equipment for data transmission to surface, usually mud pressure pulses.

There are two major design considerations regarding the BHA configuration. Either a packed hole assembly or a pendulum assembly. The packed assembly has three or more points of stabilization and a near bit contact point. The pendulum assembly has an extended length from the bit to the first stabilizer. It uses the gravity to drop in angle. This chapter will cover the basic components and their functions [36].



Figure 5.2: Example of a typical BHA.

5.2.1 Stabilizers

Stabilizers are tools in the BHA that help maintain hole-direction. They usually have three blades, straight or spiraled out from the body of the stabilizer. These blades may be welded on or machined into the tool body. Non-rotating sleeve stabilizers work best in hard formations such as lime and dolomite. Rotating blade Stabilizers have straight or spiral blades which can be short or long.

Rotating blade stabilizers come in five distinct types:

1. Integral Blade Stabilizers (IBS)
 - High-strength alloy steel as a single piece tool.
 - Used in very hard formations because pieces and parts of the stabilizer can't detach.
2. Welded- Blade Stabilizers
 - Low cost alternative to the IBS.
 - Used in soft and medium formations
3. Shrunk on Sleeve Stabilizer
 - Integral stabilizer composed of two pieces- a body and a sleeve.
 - Has replaceable sleeve
4. Replaceable-Blade Stabilizer
 - Used near the bit to maintain hole gauge in hard and abrasive formations.
5. Sleeve Stabilizer
 - Provide stabilization services in a remote area.
 - Applicable in all formations.

5.2.2 Jars

A jar is a telescopic hammer that is placed in the string above the stuck point. Its function is to free stuck drill stem components during drilling or work-over operations. This is done by “jarring” both up and down with an impact force controllable by the driller. It can be placed almost anywhere in the BHA for optimal performance. Accelerator is often used in addition to improve the jarring energy and impact force. There are many types of jars. The three most common jars are briefly described below.

Three main types of jars:

- 1 The Mechanical Jar
- 2 Hydraulic Jar
- 3 Hydro-mechanical Jar:

[1]Mechanical jars have a mechanical latch with a preset release force. This impact force is constant, independent of pull. It fires as soon as the overpull exceeds the release force.

Mechanical jars work best in vertical wells with less than 30° hole angle.

[2]Hydraulic jars have no actual preset force but is determined by the actual overpull. These types of jars work best in vertical and directional with elevated torque and drag; they can also be used in horizontal and extended reach wells.

[3]Hydro-mechanical jars are hybrid jars that combine method 1 and 2 described above [36].



Figure 5.3: Hydra-jar [36]

5.2.3 Rotary Steerable Systems

Rotary steerable systems (RSS) are designed for directional control while drilling. It provides continuous rotation of the drill string while steering the bit. The system has many benefits compared to conventional bent housing displacement motors.

The main benefits are:

- Continuous rotation while steering means less friction between wellbore and pipe resulting in faster rates of penetration and extended reach.
- Better weight transfer to the bit allows faster rates of penetration, and the use of more aggressive bits leading to yet greater gains in penetration rates.
- Smoother “in gauge” non-spiraled borehole (common for rotated bent housing) means reduced friction for additional extended reach, and easier casing, wireline and completion operations
- Constantly rotating pipe means improved cuttings removal, reducing the need for backreaming and reducing the chances of stuck pipe.

There are two steering concepts used in RSS;

1. Point-the-bit
2. Push-the-bit

1] Point-the-bit uses the same technique as in bent housing motor systems. The bent housing is contained inside a drill collar. It can then be oriented in the desired direction while rotating the drillstring. The PowerDrive Exceed is an example of a point-the-bit RSS (Property of Schlumberger).

2] Push-the-bit uses the principal of applying side force to the bit, pushing the bit against the borehole wall and achieving the desired trajectory. The force is a force that can either be hydraulically or mechanically generated. The PowerDrive X5 is an example of a point-the-bit RSS (Property of Schlumberger) [1, 35].

5.2.3.1 Powerdrive X5

The PowerDrive X5 is a push-the-bit system designed for full directional control while rotating the drillstring. It provides an automatic inclination hold and has downlink functions that maintain directional control while drilling. [37]

It consists of five main components (see figure):

1. The Bias unit
2. The Control unit
3. The stabilizer
4. The E Mag
5. The Flex Joint

1] *The Bias unit* consists of an internal rotary valve controlling the hydraulic actuation of 3 externally mounted pads.

2] *The Control Unit* is a geostationary electronics package mounted within the collar

3] *The Stabilizer* acts as a third point of borehole wall contact for directional control. Selecting the option of string, integral blade, or sleeve type stabilizers allows the position and size to be varied to fine tune the behavior in different environments.

4] *The E Mag* link consists of an electronics assembly with an antenna and modem mounted within a stabilizer mandrel. It receives real-time data from the *Control Unit* via an electromagnetic link and sends it to the MWD across an LTB connection for onward sending up hole.

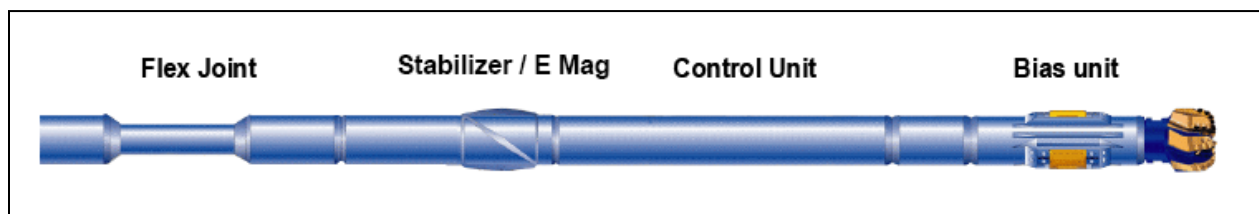


Figure 5.4: Illustration of Schlumberger's Powerdrive X5 with its main components [37].

The Control unit, mounted inside a Control Collar derives power from the flow of drilling fluid across an impeller. It houses the control electronics and directional instrumentation required to control the tools behavior, and is able to hold itself stationary inside the rotating collar. Attached to the downhole end of the Control Unit is a control shaft. This runs down into the Bias unit.

When the Control Unit is stationary, the control shaft is too. A valve on the end of this rod sears over 3 ports that rotate along with the rest of the Bias Unit. As the ports pass underneath the stationary valve drilling fluid is diverted into them. The fluid then activates each of the #3 pads in turn such that they always push out the same relative position in the borehole. The action of the pads on the same point of the borehole wall forces the bit in the opposite direction. The amount of time that the Control unit is held stationary over a given period of time determines the dogleg capability of the tool [37].

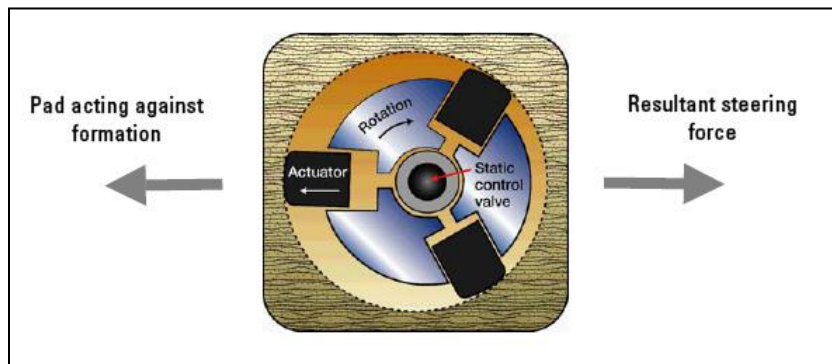


Figure 5.5: *Cross sectional view of the Bias unit [37].*

5.3 Drill Bit

At the bottom of all BHAs is a drill bit. The bit design will vary depending on the formation. Its primary function is creating the hole by digging into the earth. The correct bit will provide a good rate of penetration (ROP), last a reasonable number of hours, and drill holes the same size as the bit.

There are three basic types of bit in use in today's industry; Roller cone bits, Polycrystalline Diamond Compact bits (PDC) and diamond bits. In order to drill a whole section smoothly and efficiently, a number of designs for each type are available. Choosing the correct bit for the various types of formations that will be encountered is not always easy. Selection is based on the expected geology as well as the proven performance of different types of bit in nearby wells [38].

Drill bits can be divided into two major groups:

1. Fixed cutter bit types;
 - Polycrystalline Diamond compact (PDC) bit
 - Natural diamond bit
 - Natural impregnated bit
2. Roller cone bit types;
 - Milled tooth (MT)
 - Tungsten Carbide Insert (TCI)

1] PDC bits have fixed cutters that shear the formation with a continuous scraping action. Rocks typically tend to fracture more easily with shear loading because it requires less energy and WOB. Generally, a shearing cutting mechanism is considered more mechanically efficient than a crushing action, assuming that the bits that being compared is drilling under identical conditions. Best performance in terms of ROP and wear is observed in relatively soft, non-abrasive rocks such as shale.

A diamond impregnated bit is a sintered, powder metal matrix bit with diamonds distributed throughout the entire crown selection. The matrix wear down at a rate whereby when active diamonds become worn and blunt, the diamonds will be discarded enabling new fresh diamonds to be exposed to the

substance being drilled. Together with natural diamond bits, impregnated bits are used for very hard and abrasive formations [3, 4, 6].

2] A roller cone bit is a tri- cone bit designed to crush the rock. The cutting process can be divided in two main steps; Indentation and fracturing achieved by the applied weight on bit, and tooth displacement achieved by cone- and drill string rotation. The roller- cone bit has conical cutters or cones that have spiked teeth around them. When the drill string is rotated, the bit cones roll along the bottom of the hole in a circle. During cone rotation, new teeth gets in contact with the bottom of the hole, crushing the rock immediately below and around the bit tooth [3, 5].

Milled tooth bits and tungsten carbide bits are both roller cone bits with similar cutting action. But there are many other significant differences between them. The MT has steel teeth that are premilled and covered with hardfacing. It is less resistant to wear than TCI bits, but is applicable in very soft low-compressive strength, unconsolidated formations such as clay, gypsum and sands.

Tungsten Carbide Insert roller cone bits have inserts pressed into the cone. The inserts are made of tungsten carbide which makes it wear resistant. TCI bits are effective in within a range from soft, low compressive strength, fairly abrasive formation to very hard and abrasive formation [2, 5].

Generally, a chipping & crushing drilling mechanism requires more energy, in the form of increased WOB, to fracture the rock with compressive loading. Hence, it is fair to say that in the majority of drilling applications, roller-cone bits require more WOB to drill efficiently than PDC bits. Milled tooth bits and tungsten carbide insert (TCI) bits are designed for long interval rotary drilling or steerable mud motor runs where extended bearing life, directional responsiveness and/or gauge life are of primary concern.

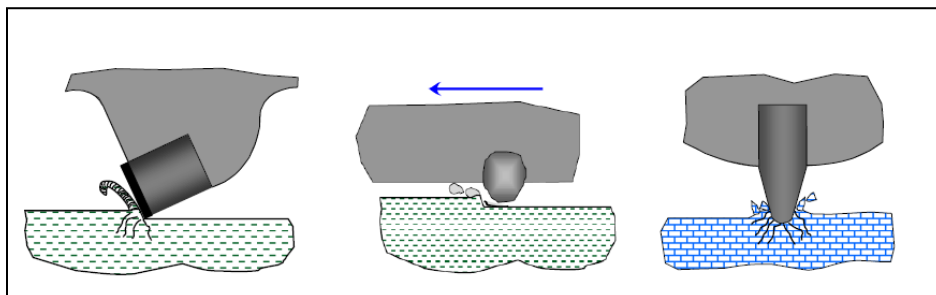


Figure 5.6: Illustrates the different drilling mechanisms for PDC bits, impregnated bits and rock bits respectively [5].

5.3.1 Bit Terminology and Features

The figures below are illustrating the main characteristics for PDCs, Rock bits and Impreg bits respectively. Since the main focus of the thesis was to design a PDC bit for Chalk applications, its terminology should be studied in detail.

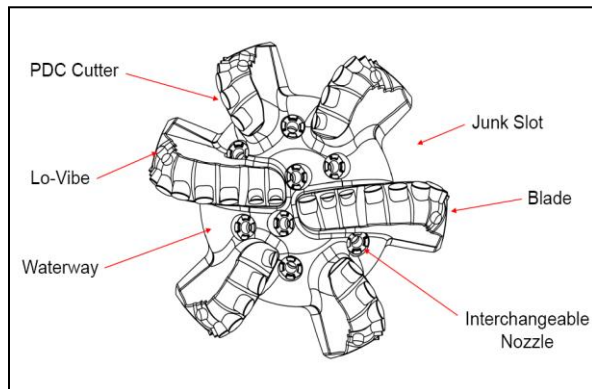


Figure 5.7: Top view, PDC terminology

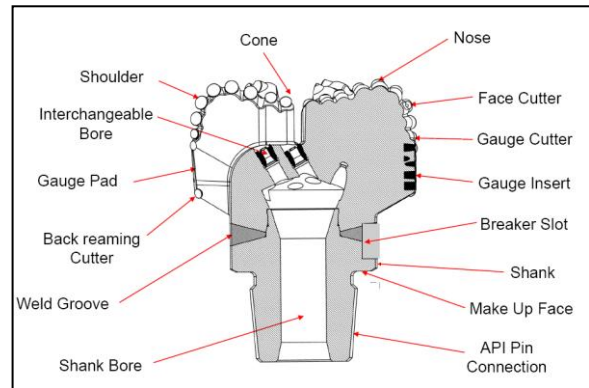


Figure 5.8: cross sectional view, PDC terminology

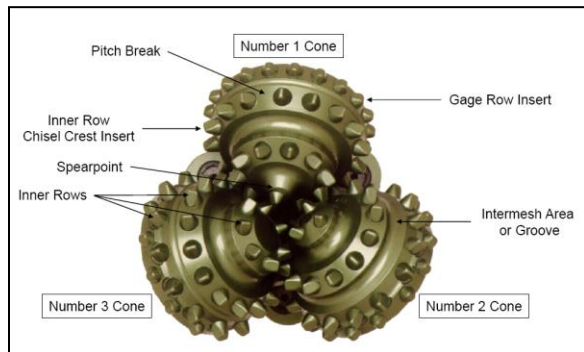


Figure 5.9: Tungsten Carbide nomenclature

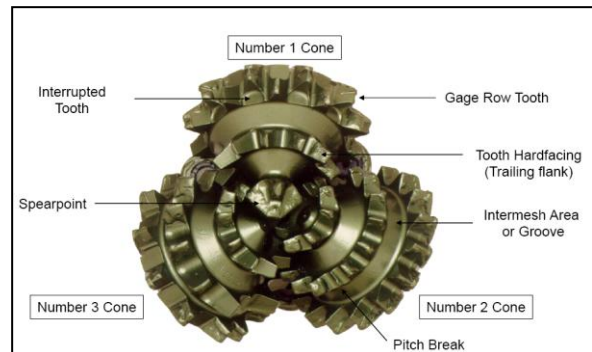


Figure 5.10: Milled tooth nomenclature

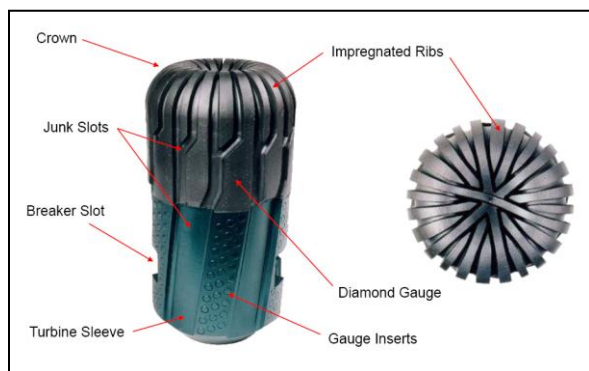


Figure 5.11: Impreg nomenclature

6 PDC bit

6.1 Introduction

Polycrystalline Diamond Compact (PDC) cutters and bits have been a significant contributor to the greatly improved efficiencies and economics of oil and gas drilling over the last 30 years.

It all started in the 1970s, when the first PDC drill bit was introduced to the market. It increased the average rate of penetration in soft formations, but had one significant limitation; it required oil- based drilling fluids. This limited the products' market potential and, by 1982 they still were responsible for less than 2% of all footage drilled. In the late 1980s this problem was solved. A bladed bit design with deeper junk slots combined with improved jet nozzle hydraulics, made the PDC bit applicable for drilling with water-based fluids.

The next major obstacle was overcoming the effects of impact damage to the PDC cutter. The diamond table had a tendency to get delaminated from the cutter substrate, leading to breakage or cracking of cutter substrates. The initial solution to this problem was the development of non-planar diamond to substrate interfaces. By introducing patterns or grooves on the face of the tungsten carbide substrate, a transition zone between the diamond table and substrate was created. These interfaces resulted in reduced diamond table delamination. At this stage of development, PDC bits had increased their market presence to about 15% of all footage drilled.

Later a major advancement was made due to a phenomenon recognized as "bit whirl". Bit whirl is a self regenerating off-center rotation condition that causes PDC drill bits to experience high lateral forces. When the problem was recognized, drill bit companies started to develop technologies and methods to mitigate it, including blade asymmetry, force balancing, blade and gage spiraling, cutter tracking, smooth gage configurations and penetration limiters.

These developments increased the potential for the economic application of PDC bits and started the next development; improved rock analysis tools to better program and apply PDC bits. In Smith bits, this is the IDEAS [Integrated dynamic engineering analysis system] software that will be discussed in detail later. By the late 1990s, PDC bits accounted for about 45% of all footage drilled in the oilfield.

The next challenge was to make the PDC bit resistant to abrasive wear. This was mainly done by reducing the cobalt content in the outermost layer of the diamond table. This process (later referred to as leaching) significantly improved the cutters abrasion resistance and thermal stability.

In 2010, PDC bits account for 65% of footage drilled in oil and gas applications and still do not have peaked in their development. More research than ever is going into PDC bits, and especially into PDC cutters.

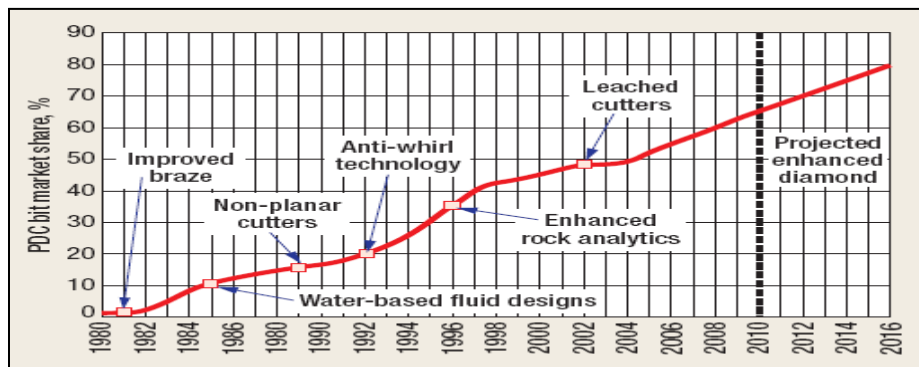


Figure 6.1: PDC bit market adoption “S” curve, from 1980 to projected 2016.

6.2 PDC Applications

Generally PDC bits are used in soft formation such as mudstone, claystone and unconsolidated sands. Analysis [7] has established the maximum value for PDC drilling at a confined compressive strength of about 310 MPA for conventional PDC bits. This limit relates to the effectiveness of a PDC bit in overcoming the shear strength of the formation, without failure of the cutter itself. However, high cutter-density PDC bits can drill harder formations.

PDC bits have been continuously improved in technology and design since the first introduction in 1976. Today they are today nearly as common as roller cone bits. Roller cone bits have most widely been used in hard rock drilling. However, the seal and bearing assemblies that allows for rotation of the cones can fail at high temperatures. The PDC bit rotate as one piece and contain no separately moving parts. Furthermore, roller cone bits often suffer from slow penetration rates in hard formations as when compared to PDC bits. [42]

6.3 PDC Cutter Technology

Polycrystalline diamond compact (PDC) is a durable material directly related to the cutting structure of a drill bit. The material is a synthetic composite comprised of diamond grit (PCD) and tungsten carbide bonded together with cobalt.

PDC is important to drilling since it aggregates tiny, inexpensive (compared to natural diamond) man-made diamonds into relatively large masses of randomly oriented crystals that can be formed into useful shapes called diamond tables. PDC also bonds effectively with tungsten carbide which is essential in the process where the PDC cutter is brazed to the bit body. (See 6.3.1 for further description of the PDC cutter manufacturing process)

The raw material for PDC cutters is polycrystalline diamond (PDC). It is a powder of tiny monocrystalline particles, with a diameter of 100 or less [3]. Each man-made diamond is chemically and property wise, identical to natural diamond. They are hard, sharp and extremely wear resistant. However, the difference in orientation of diamond crystals creates inequalities

In the diamond grit, the individual diamond crystals are diversely oriented giving the man-made diamond better performance in shear than natural diamond. This is because the natural diamonds are cubic crystals and will therefore fracture more easily along their orderly crystalline boundaries.

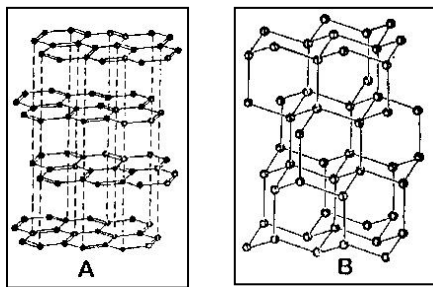


Figure 6.2: Atomic structure of graphite (A) and Diamond (B) [23]

On the other hand, the diamond compacts have limited heat resistance. At atmospheric pressure, a diamond's surface turns to graphite (Figure6.2) at 900 C or higher. But during use, conventional PDC cutters experience a decline in tool performance around 750 C, which the cutting edge can easily reach due to frictional heating in hard, abrasive rock.

The limited heat resistance is believed to be due the cobalt that is present in the PDC cutter. The cobalt is necessary in the manufacturing process since it acts as a catalyst during the ultra-high-pressure

sintering of PDC. The catalytic effect creates the diamond-to-diamond bonds and unitizes the diamond layer to the tungsten carbide structure.

Critically, the presence of cobalt is believed to be the reason that PDC converts to graphite at a lower temperatures than natural diamond. As temperatures increases, graphitization of the diamond in the presence of cobalt becomes a dominant effect.

Graphitization can be explained by two factors:

1. Localized frictional heating
2. Difference between thermal expansion coefficients

1] Diamond wear is due to a transformation into graphite under the influence of localized frictional heating. When drilling, the part that becomes hottest is the cutting tip that comes into contact with the formation. The cutting tip is the PDC layer consisting of diamond grit, tungsten carbide and cobalt.

The transformation is accelerated in the presence of cobalt through a combination of mechanical and chemical effects. The frictional heating causes the shear resistance of cobalt to drop rapidly, and the grains are not strongly held. The real area of contact also depends on the velocity with which plastic strains are propagated in the metal binder. The shearing occurs so rapidly that full plastic yielding under the normal load is not possible.

2] In addition, there is a significant difference between the thermal expansion coefficients of cobalt and diamond. During heating, cobalt expands at a higher rate than diamond. The amount of thermal stress increases, and the structure breaks down. The reduced thermal stability causes diamond-to-diamond bonds to break under high temperatures. If the loads get high enough, it causes failure and the diamonds are quickly lost. The PDC cutter then loses its hardness and sharpness and becomes ineffective. [6, 11, 24]

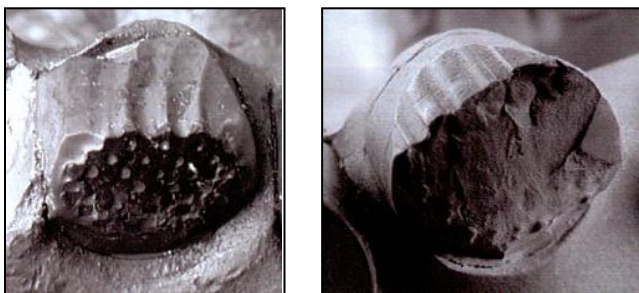
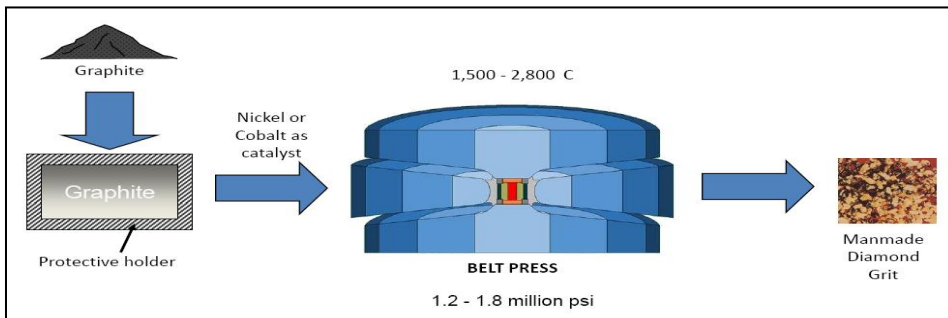


Figure 6.3: *Lost diamond tables (delamination) due to high axial loading.*

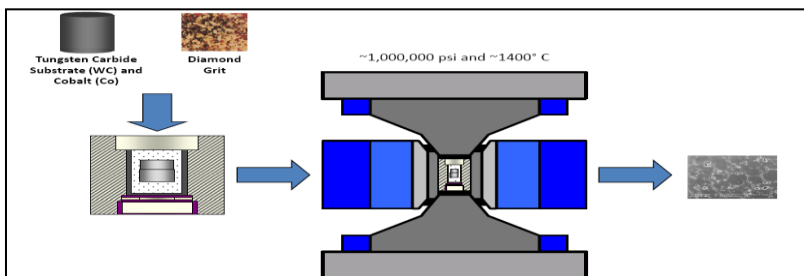
6.3.1 PDC cutter manufacturing process

Man-made diamonds have been made since the early 1950's, by a process called high-pressure, high-temperature synthesis (HPHT). Making diamond grit is only the first step in the PDC cutter manufacturing cycle. The process of making the entire PDC cutter can be described by following steps:

1. Graphite is put into a huge hydraulic belt press and is subjected to 1.5 million psi and 2,200°F in the presence of a catalyst (cobalt, nickel) to replace time, and manmade diamond grit is produced.



2. The diamond grit, with a pre-determined particle size, is then placed into a refractory metal can.
3. A tungsten carbide substrate is then placed on top of the diamond grit and the bottom of the refractory metal can is put into place. The can is mechanically sealed and placed within a graphite heater tube.
4. The assembly is then placed in the diamond press and the sintering process is commenced. At approximately 1,000,000 psi and 1400° C diamond to diamond bonding occurs.



5. The Cobalt from the Tungsten Carbide substrate sweeps through the Diamond grit catalyzing the bonding process. The Cobalt also forms a bond with the Tungsten Carbide substrate resulting in one integral component.
6. The PDC cutter is then subjected to leaching, as described in 6.3.3.

6.3.2 Thermally Stable Polycrystalline cutters

As means of improving heat resistance, polycrystalline diamonds have been created that not bound to ultra-hard alloy base materials. The cutters are then immersed in acid and heat treated. The acid treatment dissolves the metal binder phase in the polycrystalline diamond. With the absence of cobalt, the PCD material is thermally stable to a temperature of 1,200 C and is then termed TSP, or Thermally Stable Polycrystalline. TSP can then be cut into the desired shapes and sizes depending on the proposed application.

However, the material created by this process has additional problems. With the cobalt phase removed, cavities remain in the TSP, degrading the strength of the sintered material. The result is a material that lacks sufficient hardness and impact strength to be used as a cutting tool. Without the cobalt phase, it is also difficult to create a strong bond between the TSP and the tool.

It is the tip of the cutter that becomes hottest during drilling, as stated earlier. Cutting tool studies in the late 1950s found that the temperature a few microns from the contact point is 12% of the (absolute) temperature at the point of contact [11]. In other words; the temperature decreases rapidly with increasing distance from the contact point. Therefore, improving heat resistance of just the cutting edge of a PDC would significantly improve drilling performance.

6.3.3 Leached cutters

The new PDC has a conventional diamond table with a surface layer from which the cobalt has been removed. After the PDC is finished, its cutting surface is exposed to powerful acids that remove the cobalt phase by an etching process called leaching. The cobalt is removed up to 200 microns deep into the PDC layer (meaning just the cutting edge). By leaching a thin layer at the working surface it reduces diamond degradation and improves the tools thermal resistance. First, when cobalt is removed from the cutter tip, the diamond-to-diamond bonds remain strong and little graphitization occurs. Second, when the leached layer consists of diamond alone, it transmits heat away from the cutting tip more efficiently. Also, since cobalt still remains inside the PDC diamond table, it is less loss of overall strength in the sintered object.

6.3.4 ONYX cutters

Recent technological developments have produced a new, highly abrasion resistant cutter that has increased rate of penetration and total footage drilled. The ONYX cutter is manufactured by a two-step high pressure/high temperature (HPHT) process (Figure 6.4) which gives it two main advantages compared to the conventional one-step process:

1. The residual stress in the PDC table is reduced by the additional process
2. The two-step HPHT process increases the microstructure strength of the PCD.

During the first step, a premium PCD (diamond) table is made using a conventional HPHT process. The PCD table is then treated in acid to make the diamond disc catalyst free. The disc is then assembled again with a WC substrate and subjected to a modified HPHT process which is different from the first. The end product is then treated again to remove infiltrate material from the second HPHT process.

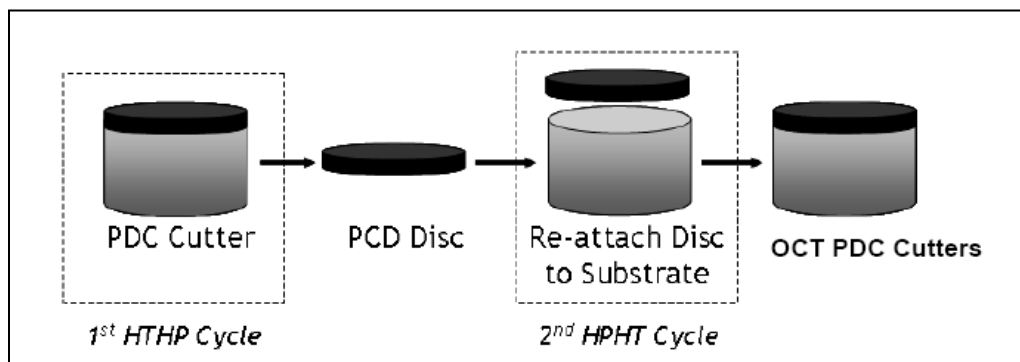


Figure 6.4: Steps to manufacture ONYX Technology cutters (OCT).

A very important property of a PDC cutter is abrasion resistance. A cutter with high abrasion resistance stays sharper longer and minimizes frictional heat which leads to thermal/mechanic breakdown in diamond. Field tests [SPE 132143] document that the new OCT cutters have outstanding thermal wear properties and are therefore applicable in hard/abrasive formations.

The ONYX cutters perform well in abrasive formations. However, when the cutter stays sharp and round it will be more impact resistant than a cutter with a big wear flat that is overheating and pulling itself apart. In addition, OCT cutters are run with larger bevels (ref that significantly increase impact resistance [45]).

6.3.5 PDC cutter design

PDC cutter development is crucial to bit optimization. A cutter that is inappropriate for any given application will be extremely detrimental to PDC performance, no matter how good the bit design is. A cutter designed to have excellent impact resistance may not necessarily have good abrasion resistance. Placing such cutter in a PDC bit that is programmed to drill through highly abrasive sandstone, can easily lead to premature bit wear. Hence, it is fair to say that cutter characteristics directly impact bit performance and durability. These properties are impact and abrasion resistance, shear strength and thermal stabilization.

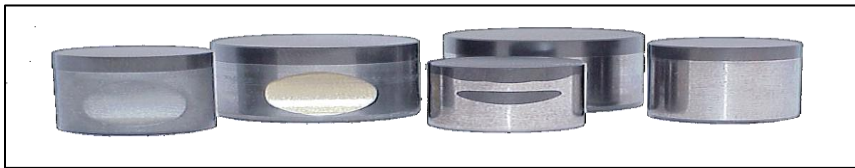


Figure 6.5: A selection of PDC cutters from Smith Bits product Catalogue

All bit companies have patented cutters with different features. This section contains a brief description of the main features of PDC cutters.

PDC cutters consist of a 0.15 to 1.5 mm thick PDC diamond table and a tungsten carbide cylinder. The diamond table is the part of the cutter that is intended to be in contact with the formation. The main PDC cutter that Smith manufactures is the conventional cutter.

6.3.5.1 Conventional cutter

A PDC layer is sintered onto a tungsten carbide substrate. The tungsten carbide substrate acts as a support for the diamond table and provides toughness. The substrate can be a one piece or a two piece cylinder as illustrated in picture above. In the two piece example, the two carbide substrates are cemented together forming an LS bond line.

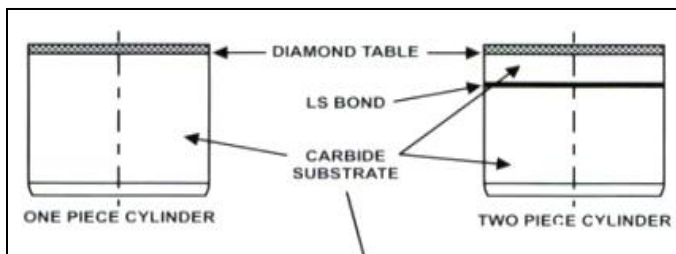


Figure 6.6: Illustration showing conventional cutter characteristics.

6.3.5.2 Beveled cutters

A beveled cutter is a cutter where the edge is cut at 45 degrees (i.e a modified edge). In general, they have the advantage of increasing the impact resistance of a cutter. The downside is that it also decreases the aggression of the bit, which can have the net result of reducing the rate of penetration of the bit.

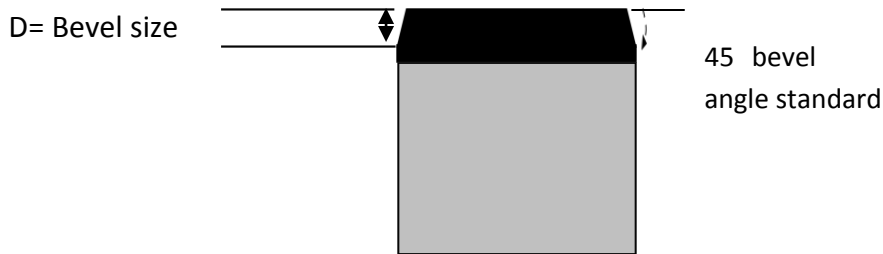


Figure 6.7: Illustration of a beveled cutter.

Cutter bevels come in a variety of sizes that can be selected to match application requirements.

6.3.5.3 Non- planar interface

When the cutter is manufactured, it is exposed to high temperature and pressure. This treatment results in a residual stress field in and around the diamond to tungsten carbide substrate. Having a non-planar interface, similar to what is shown in Figure 6.8, influences the residual stress state within the cutter. Many types of interfaces between the diamond table and the substrate exist, all of which are specifically engineered to improve cutter performance.

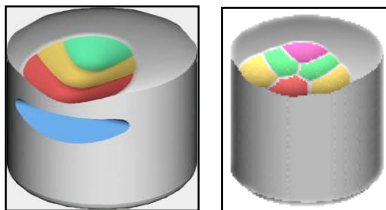


Figure 6.8: Interface examples for PDC cutters [40].

6.4 PDC bit design

As new reservoirs are getting smaller, deeper and more difficult to reach, bit vendors are pressured to continually improve and develop bits that can drill faster through hard and abrasive formations.

It is evident that the drill bit is one of the most important oilfield technologies due to its significant impact on drilling cost per foot. The procedure today is to provide a bit that is designed for a specific formation instead of providing a great bit with multiple advanced features. This is believed to reduce costs due to increased safety and efficiency in the formation to be drilled.

Four considerations primarily influence bit design and performance:

1. Mechanical design parameters
2. Materials
3. Hydraulic conditions, and
4. The properties of the rock being drilled

Bit design includes geometric parameters (bit profile and shape) and cutting structure characteristics. This chapter will briefly address the effect of blade count, blade layout, bit material and bit profile. Cutter characteristics are described in detail in chapter 6.5.

6.4.1 Blade count

The blade count is an important aspect in the design of a bit for a specific application. General terms used to describe the blade count on a bit is “light” set, “medium” set and “heavy” set. Each of the terms addresses how many blades a specific bit has. A light set bit has between three and five blades; a medium bit has six or seven blades, while a heavy set bit has eight or more blades. How many blades a bit has, influence its performance potential. For a light set bit, the force applied by WOB is divided by a smaller area providing a high ROP potential. It’s most applicable area is in soft, non-abrasive formations due to the low cutter density. For a heavy set bit, the force applied by WOB is naturally divided on a bigger area, restricting the ROP potential, but making it applicable for hard and abrasive formations due to high cutter density.

6.4.2 Blade Layout

An important factor in bit design is bit stability. Blade geometry and layout has an influence on bit vibration reduction. By reducing the gage stress on a bit, it lowers the probability that a bit will pivot about its gage and start causing vibrations. This chapter will briefly discuss the advantages and disadvantages between straight and spiraled blade geometries and the effect of having symmetrical versus asymmetrical blade layouts.

6.4.2.1 Straight vs. Spiraled blade designs

With straight blades, the cutter radial forces are summed up as whole on the gauge. With spiral blades, only a component of each radial force is used and the net effect on the gauge is less than that of straight blades. A spiraled blade design has therefore following advantages as compared to straight blade design in challenging formations; the gauge stresses are reduced, and the vibrations are minimized and bit stability is promoted.

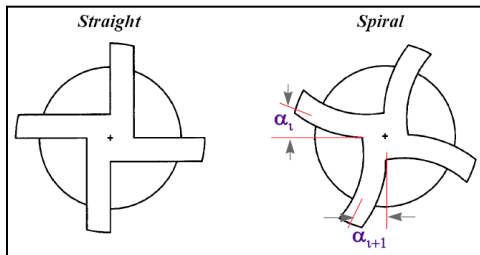


Figure 6.9: Straight blade and spiral blade designs.

6.4.2.2 Symmetrical vs. Asymmetrical blade layout

With symmetrical layout, the angle between consecutive blades is equal. Due to the symmetry, induced vibration is repeated and amplified. With asymmetrical layout, the angle between any consecutive blades is different. Harmonics is broken and the elapsed time between signals is maximized

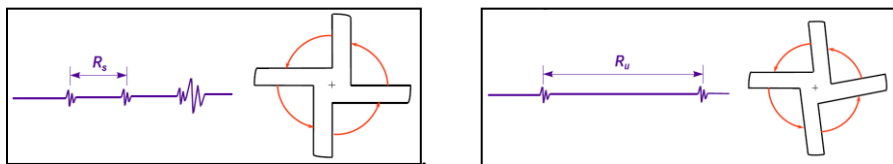


Figure 6.10: Symmetrical vs. asymmetrical blade layout.

6.4.3 PDC Materials

The PDC bit body is manufactured and designed in either steel or matrix. Both of the materials provide significantly capabilities. A choice between them is therefore decided by the nature of ends, both types having certain advantages.

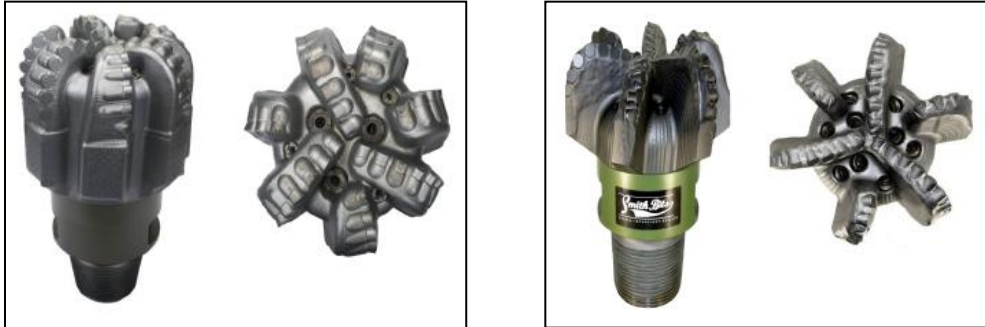


Figure 6.11: Illustration of bit body materials, matrix to the left and steel to the right [6.]

“Matrix” is a very hard, rather brittle material comprised of tungsten carbide grains bonded together with a softer, tougher, metallic binder. The hardness of the “Matrix” material makes the bit erosion resistant in abrasive formations. The matrix is also capable of withstanding relatively high compressive loads, but is not as strong in tension as steel. Steel is relatively soft, and without protection. This makes it capable of withstanding high impact loads, but tends to fail in abrasive formations. With steel bodied PDC bits, the use of steel allows a greater blade stand-off to be achieved which can improve the hydraulic properties of a PDC bit in certain formations and applications. Relatively high and thin blades can be useful in applications with water based mud where bit balling often occur [3, 4].

Bit Body Materials		
Type	Matrix	Steel
Advantage	Erosion resistant and applicable in abrasive formations. Capable of withstanding relatively high compressive loads.	Capable of withstanding high impact loads. Can be incorporated to relatively thin blades.
Disadvantage	Not as strong in tension as steel. Has low resistance to impact loading.	Relatively soft and without protection. Fail quickly by erosion in abrasive formations.

Table 6.1: Schematic overview illustrating characteristics for matrix and steel body bits.

6.4.4 Bit Profile

The profile of the bit is seen when the bit is viewed from the side (see Figure 6.12). The profile shape is one of the most important characteristics of fixed cutter bits, having direct influence on the possibilities for cutter densities, cutter placement patterns and hydraulic layouts.

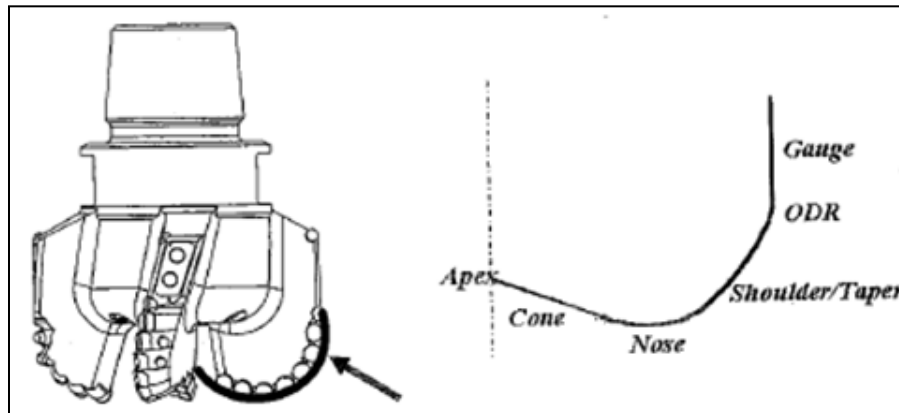


Figure 6.12: Cross sectional view of the bit profile showing the location of the six components that makes up the profile.

Operationally, the bit profile has a direct influence on bit performance in terms of:

- Stability
- steerability (e.g. directional responsiveness),
- cutter density in key areas of the profile,
- rate of penetration (ROP),
- hydraulic properties of the profile (e.g. how well the bit cleans and cools the cutting structure).

Six components make up the profile of a PDC bit. Firstly, there is the Apex of the bit which is the geometrical center of the bit. This does also define the cone. The cone is then followed by the nose, the shoulder, the outside diameter radius (ODR) and the gage.

6.4.4.1 Cone Angle

The cone is highlighted in Figure 6.12. The two legs of the cone join at the apex and form an angle referred to as the cone angle. Cones with an approximately 90 degree angle are termed “deep”, while those with a much larger angle, approx 150 deg, are termed “shallow”. The cone angle affects bit stability, cuttings removal characteristics, cutter densities, steerability, and bit aggressiveness.

A PDC bit with a deep cone profile has a high degree of bit stability (larger accumulation of formation in the center of the bit) and increased room for higher cutter densities in the centre of the bit (see picture above). However, a deep cone angle result in a decrease in bit steerability decreased cleaning efficiency and a decrease in bit aggressiveness.

In contrast to bits with deep cone profiles, bits with shallow cone profiles tend to have increased steerability, increased bit cleaning and increased aggressiveness (due to the WOB being distributed over a smaller area). However, this has the corresponding disadvantage of decreasing the bits stability and decreasing the diamond volume in the cone.

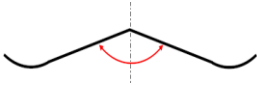

Cone Profiles		
Type	Shallow cone	Deep cone
Advantage	Increased bit cleaning. Increased aggressiveness. Increased steerability.	High degree of bit stability. Increased diamond volume in center.
Disadvantage	Decreased stability. Decreased diamond volume.	Less steerable. Less aggressive. Poor cleaning efficiency.
Illustration		

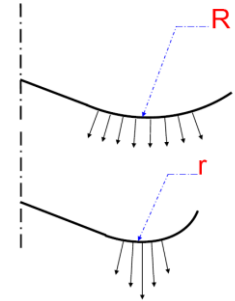
Table 6.2: Schematic overview illustrating characteristics for shallow and deep cone profiles.

6.4.4.2 Nose location

The nose is described by the radius (R) of its curvature and the horizontal distance, or location (L), from the bit centerline at which the curvature begins, (see figures below). The location of a bit nose and the sharpness of the nose radius curvature influences bit aggressiveness and durability of the design.

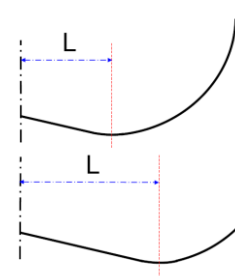
Radius (R)

- Large radius (R) provides higher surface area for better load distribution in hard and transitional drilling.
- Small or sharp radius (r) provides higher point loading on cutters and are suitable for soft homogeneous formations



Location (L)

- Nose location closer to the center provides more surface area and cutter density on the shoulder.
 - Suitable for soft but abrasive formations
- Nose location closer to the gage provides more surface area on the bit face for better load distribution
 - Suitable for harder formation.



6.4.4.3 Shoulder, ODR and Gage

The bit shoulder extends from the outside nose tangent to the start of the Outside diameter radius. The shoulder connects the nose with the outside diameter radius and the ODR provides a smooth transition between the shoulder and the gage. Lastly, the gage is the outward most part of the bit. Cutters located on the gage cut and maintain an in-gage wellbore and help to prevent unstable drilling properties such as bit whirl. Various gage types and lengths are available to achieve maximum drilling efficiency. The gage features are vertical and parallel to the bit centerline.

6.4.5 Bit Profile shapes

There are four general categories of PDC bit profile shapes that range from long, parabolic curves to flat shapes with narrow radius, compressed curves.

The four types are described as:

1. Flat profiles.
2. Short parabolic profiles.
3. Medium parabolic profiles.
4. Long parabolic profiles.

The profile of any given PDC design needs to be matched to the particular application and formation, resulting in a large degree of design flexibility. However, the most frequently used bit profile shapes are the medium and short parabolic shapes. Cutter density can be increased if surface area is increased. Higher cutter density results in more widely distributed cutter workload and wear but decreased ROP. ROP reductions can be partially offset with more aggressive profiles. The different profiles are presented in subchapter's 6.4.5.1-6.4.5.4.

6.4.5.1 Flat profile

The flat parabolic profile is less commonly used than short and medium parabolic. Flat profiles with relatively sharper noses are used for drilling soft, less abrasive formations such as limestones and dolomites. It is also less aggressive than parabolic profiles (see Table 6.3), however, flat profiles provides good resistance to impact loading of the cutters due to their blunt nose.

6.4.5.2 Short parabolic

The short profile is one of the most versatile bit profiles because it provides an effective compromise between ROP, wear, and cleaning. The surface area is not significantly increased, relative to cleaning and cooling, so thermal wear and cleaning problems are not significant drilling problems with this profile. Short parabolic profiles have the sharpest nose of the three types of parabolic profiles.

This makes the profile not that aggressive and is therefore generally used to drill softer, less abrasive formations such as calcareous sandstones, limestones and cherts.

6.4.5.3 Medium parabolic

Medium parabolic profiles with relatively wide noses are rather aggressive and are used to drill harder and more abrasive formations such as sandstones, limestones and hard shales. Medium parabolic profiles clean better than short parabolic profiles.

6.4.5.4 Long parabolic

The long parabolic profile is less commonly used than medium and short parabolic profiles. Long parabolic profiles are comprised of series of curves beginning at the cone to nose intersection and continuing to the outside diameter radius and gage intersection. The long parabolic profiles with wider noses are used to drill harder and more abrasive formations such as silicious shales and clays. "

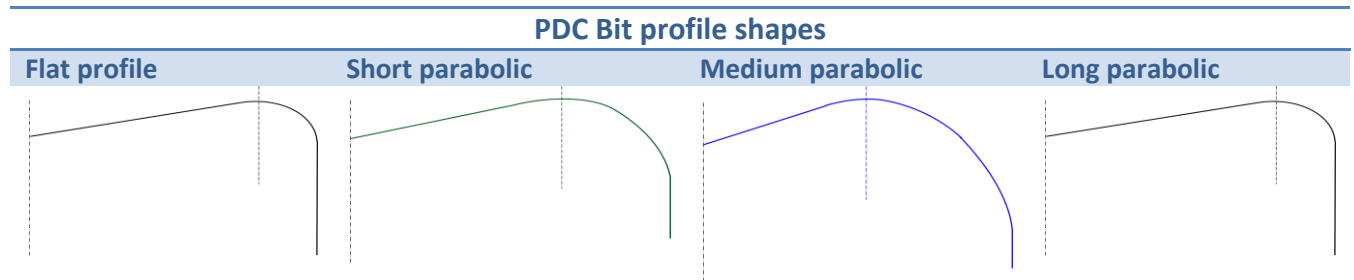


Table 6.3: Illustrating the four different bit profiles. The vertical dotted line is the central axis of the drill string.

6.5 PDC cutting structure characteristics

A PDC bit cutting structure is defined as a unique cutter arrangement designed to achieve particular performance and durability characteristics. Cutting structures must provide adequate bottomhole coverage to address formation hardness, abrasiveness, potential vibrations, and satisfy production needs.

6.5.1 Mechanical Specific Energy (MSE)

Low rate of penetration and reduced drilling efficiencies have always been a challenge to the drilling industry. To overcome this challenge, a fundamental understanding of the mechanics of the rock-cutting process is necessary. The rock drilling process can be analyzed through an energy point of view, Simon (1963) and Teale (1965) using the concept of MSE.

MSE is defined as the amount of mechanical energy required to extract a unit volume of rock. The MSE for drilling rocks under atmospheric conditions is close to the unconfined compressive strength (UCS) of the rock. A measure for the efficiency of drilling is created by comparing the MSE of the atmospheric drilling process to the UCS of the rock.

MSE is calculated through the following equation:

Equation 6.1

Equation 6.2

6.5.2 PDC Cutting structure

The cutting structure i.e. the cutter distribution is a non visible feature that directly influence bit behavior (stability) and drilling efficiency (ROP). A multitude of arrangements are possible to achieve particular performance and durability goals. This chapter will briefly address the two existing types of cutting structures; the single set and the plural set.

6.5.2.1 Single set cutter arrangement

The single set cutting structure is the earliest and most utilized form of cutter arrangement. The distribution is called “single set” as every cutter has a unique radial position. It has one PDC cutter in each radial position and cutters are distributed along the profile for complete bottom-hole coverage. Picture 5 illustrates the basics of a single set cutting structure on a 6 bladed bit. Notice that there is no redundancy.

There are two different types of single set layouts:

1. Forward spiral
 - Advance outward radially in clockwise direction
2. Reverse spiral
 - Advance outward radially in counterclockwise direction

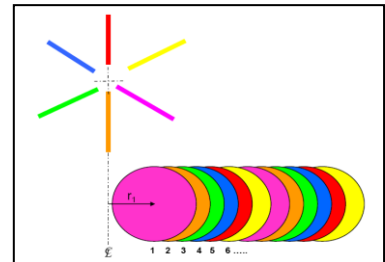


Figure 6.13: Illustration of a single set layout.

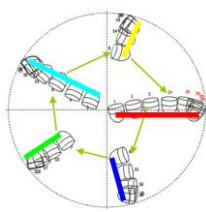
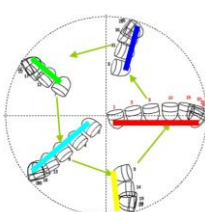
Single set cutter arrangements		
Type	Forward spiral	Reverse spiral
Advantage	More aggressive	Considered very stable
Disadvantage	Less stable than reverse spiral and harder for designers to stabilize	Less aggressive than Forward Spiral
Illustration		

Table 6.4: Schematic overview illustrating characteristics for different single set cutter arrangements.

6.5.2.2 Plural set cutter arrangement

The plural set cutting structure stand out from the single set with other properties and capabilities. The distribution is called “plural set” as its exhibits sets of cutters where each set can consist of multiple cutters (2, 3, and 4). Plural set structures employ sets of cutters comprised of two or more cutters per set having identical radial position. Picture 6 illustrates two different redundancy layouts for a #6 bladed bit.

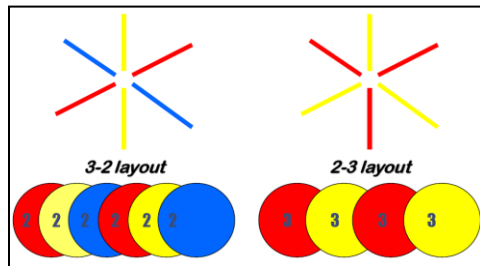


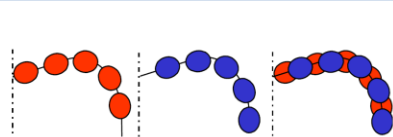
Figure 6.14: Illustration of 3-2 and 2-3 plural set layouts

A plural set can have a variety of redundancy option depending on following features:

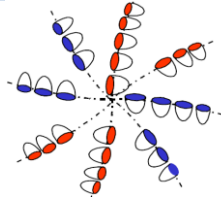
1. Lead number
 - Number of blades on a bit that complete bottom-hole coverage without redundancy.
2. Set number
 - Maximum number of cutters having identical radial position
3. Trailing
 - Blades with duplicate radial cutter locations are grouped together and placed adjacently.
4. Opposing
 - Blades with duplicate radial cutter locations are angularly spaced at approximately equal distance

Plural set cutter arrangements

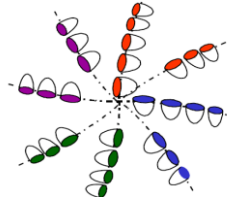
1] Lead number



2] Set number



3] Trailing



4] Opposing

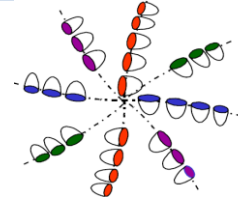


Table 6.5: Schematic overview illustrating different plural set cutter arrangements

As mentioned, cutter structures influence the bit behavior in terms of stability. How stable a bit is can be described by its ridge height. Increasing ridge height increases the stability of the bit. In this case, is more stable than (ref picture). The shape and size of the formed ridges have considerable effect on bit stability and to a certain extent penetration rate.

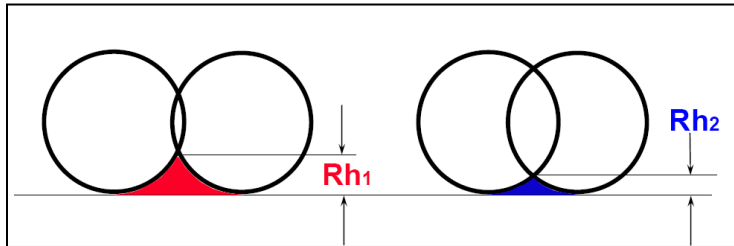


Figure 6.15: Illustration of high and low ridge heights.

The numbers of leads (see description above) in plural cutter arrangement will influence the ridge height, hence the stability. A lower number of leads generate high ridges and hence greater stability factor. A higher number of leads generate small ridges and most of the load supplied to the cutter is used for drilling. This arrangement is more aggressive but highly unstable. Plural cutter arrangement generates more pronounced ridges as compared with single set. Ridges generated from plural arrangement also offer greater resistance to off-center movement.

The cutting structure also influences the drilling efficiency. The effect of number of sets determines the bits durability because the spatial arrangement of these cutters determines the bits aggressiveness, hence penetration rate.

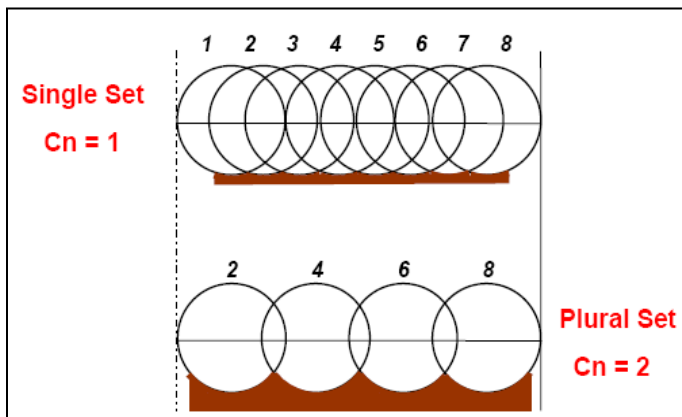


Figure 6.16: Illustration of single set vs. plural set cutting structure.

6.5.3 PDC cutter orientation

Cutters are placed onto the bit to give specific attack angles relative to the formation. The orientation of the cutters influence bit performance in terms of aggressiveness and stabilization. In general we differentiate between two main cutter orientation principals, namely back- rake angle and side-rake angle.

6.5.3.1 Back- Rake Angle

In general, cutter back-rake can be considered as the angle at which a PDC cutter attacks the formation, as shown in Table 6.6. It can also be defined as the angle the cutter face makes from a vertical plane through the cutter that is perpendicular to the formation being drilled. The rate of penetration and torque response with PDC bits is primarily controlled by the aggressiveness of the cutter i.e. the back rake angle.

As mentioned above, the back-rake angle affects the aggressiveness of the cutter. When the back-rake angle is high, a decreased amount of the cutter is in contact with the formation. This leads to a less aggressive cutter and a decreased rate of penetration (ROP). When the back- rake angle is low, the rate of penetration is higher due to higher Depth of Cut (DOC).

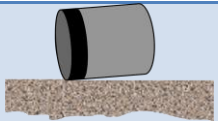

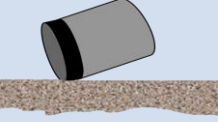
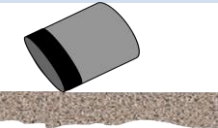
Back-rake Angle	Formation Hardness	Back-rake illustration
5-10	Very soft clays/shales. Low angle produces highest ROP's	
15	All formations. Best in soft formations (e.g.. shale)	
20	All formations. Improves cutter life. Best in abrasive/sand formations	
30	Harder formations Typically used on gauge	

Table 6.6: Schematic overview presenting application areas for different back-rake angles. [4]

Certain back- rake angles are used in certain formations. In very soft formations such as soft claystone and shale formations, an aggressive back-rake angle enables high rate of penetration. In abrasive formations a higher back-rake angle is favorable. See Table 6.6 back-rake angle illustrations.

As a rule, higher back-rake angles improve impact and wear resistance, while lower back-rakes increase ROP. Furthermore, back-rakes can be varied to achieve maximum ROP and durability.

In general, individual cutters on a blade have different back-rake angles to provide a stable and efficient drill bit. By having a variation of back-rake angles on each blade, the workload of the drilling action is evenly distributed. This produces uniform cutter wear-rates and maximizes bit life. Low, more aggressive angles are used at the center where linear speed is low. Higher, less aggressive angles are used at the gage where linear speed is high, cooling more difficult, and durability an issue. At the shoulder, back rake angles and cutter density are both increased because of high linear distances shoulder cutters travel, and cooling complexity.

Back-rake angles from 5 to 30 degrees are presented in the table above. In practice, the back- rake angle is limited by different factors. In order to drill efficient with a decent ROP, a certain amount of DOC is necessary. To achieve sufficient DOC, the weight applied to the bit (WOB) must be very high with back rake angles exceeding 30 deg. This makes PDC cutters most effective in the back rake range between 15 - 20 depending on the formation being drilled. However, special requirements such as steerability during sliding may require high back-rake angles [4, 25].

6.5.3.2 Side Rake Angle

In general, side rake angle can be considered as the side-to-side orientation of a cutter. It is defined by the angle between a cutter face and the radial plane of the bit (Figure 6.16). Cutters that incorporate side rake are believed to provide a radial and tangential cutting structure as the bit rotates. Cutters with no side rake cut only in the tangential direction.

Because of the side-to-side orientation, such cutters are also less inclined to sticking problems than cutters with no side rake. In addition, cutters with side rake give a mechanical displacement of cuttings towards the outer radius of the bit of the bit in conjunction with the fluid velocity of the mud system, creates increased cleaning efficiency. This minimizes regrinding of cuttings and the incidence of balling, which again lead to increased penetration rate. However, the main reason for incorporate is to stabilize the bit [4, 25-27].

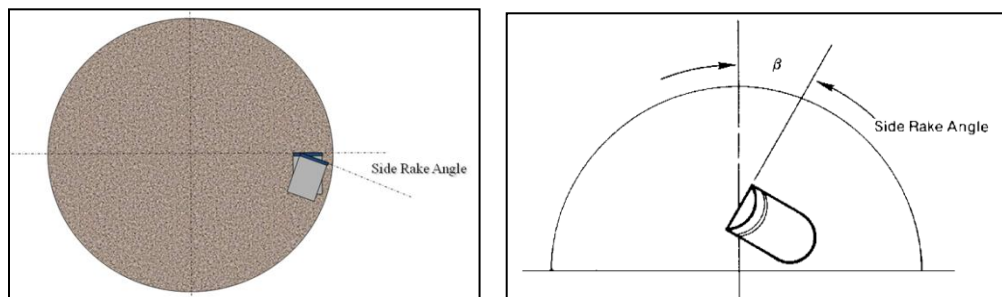


Figure 6.17: illustration of side rake angle [26].

6.5.4 Cutter Density

Cutters are strategically placed on a bit face to ensure complete bottomhole coverage and to facilitate uniform wear and extended bit life. The term cutter density refers to the number of cutters used in a particular bit design.

PDC cutter density is a function of profile shape and length, cutter size, shape and quantity. General procedure is to increase amount of cutters from the center of the bit to the gage because of requirements for work as the distance from the centerline increases. Cutters closer to the gage must travel faster and farther than cutters in the center of the bit to achieve an equal depth of cut. As a result, cutters closer to the gage remove more rock and have higher work rates.

To equalize the work rate on the inner and outer cutting structure (to achieve a stabilized bit), the penetrating force supported by each cutter must be reduced as radial position increases. A general rule is to have higher cutter density in areas with higher wear (taper, gage) and lower cutter density in the area of lower wear (cone, nose).

A common industry practice is to use PDC bits with more cutters when drilling firmer formations. It is believed that increased diamond content (cutter density) will help minimize cutter breakage and abrasive wear. The workload distribution (WOB) is then divided by more cutters and the unit load per cutter is decreased. This reduced the wear rate to result in longer bit life.

By reducing the number of cutters on a bit face, the downward force will be distributed over fewer cutters causing unit load per cutter to increase. As result, cutters are pushed deeper into the formation (greater depth of cut) and the rate of penetration is increases and higher torque results. In other words, ROP and cleaning efficiency will increase as cutter density decreases. A low cutter density is normally applied on softer and less abrasive formations. [4, 25, 26]

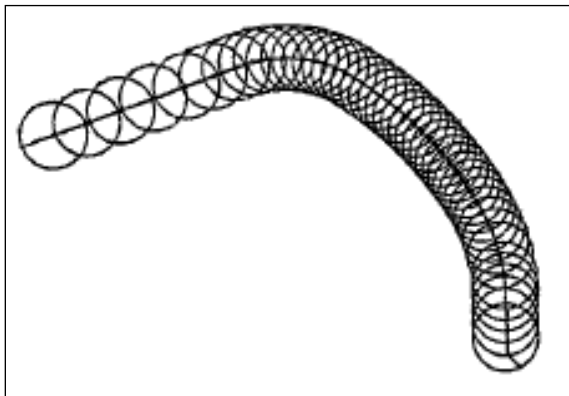


Figure 6.18: *Planar representation of cutter density increase with radial position* [4].

6.5.5 Cutter exposure

Cutter exposure is the distance from a bit's face to the tip of a particular cutter. It has an impact on bit performance and is considered an important element of bit design. Cutter exposure is considered for its effect on cleaning and mechanical strength. In general, cutter exposure is discussed in terms of full or partial exposure of the PDC cutter.

6.5.5.1 Full cutter exposure

In full cutter bit designs, the entire cutter face is exposed to the formation, (Figure 6.18). Huang and discussed the advantages and disadvantages of full and partial cutter exposure by comparing the effect of chip clearance and hydraulic properties. With a full cutter exposure, more space is created for chip clearance that minimizes interference between larger chips and the bit. However, the large clearance created for the chip means large fluid areas, which in turn lead to decreased flow velocity. This low flow velocity may cause the formation to be trapped in the large fluid area and bit balling can occur. The majority of modern bits employ full cutter exposure.

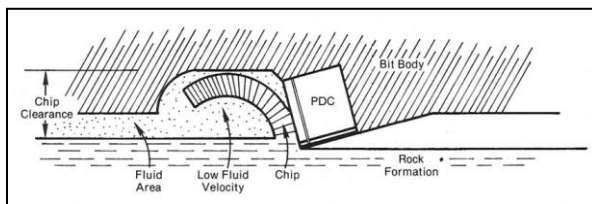


Figure 6.19: Fully exposed cutter creating big chip clearance and low flow velocity [27].

6.5.5.2 Partial Cutter Exposure

A cutter is partially exposed when a portion of the cutter face is mounted within the bit body, (Figure 6.20). With a partial cutting structure, less space is created for chip clearance and less rock is removed. When the chip clearance is small, the flow velocity induced is higher leading to better removal of cuttings. It also provides a mechanical backing to the PDC cutter for increased resistance to impact loads. However, the low clearance can cause the chip to be trapped between the bit body and the rock formation. If the formation is very soft, the chip can be packed tight in front of the cutter leading to poor hole cleaning. Another negative effect of chip interference is that the chip will push the bit upwards and reduce the actual weight applied to the formation.

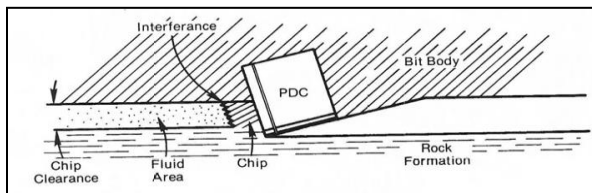


Figure 6.20: Partially exposed cutter creating low chip clearance and high flow velocity [27].

7 IDEAS [Integrated Dynamic Engineering Analysis System]

[IDEAS] is a simulation software used to design, test and analyze bit performance in specific applications. The software provides an expert bit selection tool because it can accurately predict how several different bit designs will perform in particular formation types, with a specific drive type, under various operating parameters and with a specific BHA configuration.

The IDEAS software utilizes a suite of Finite Element Analysis (FEA) to achieve Virtual Prototyping (VP). VP allows the engineers to virtually drill through the same interval multiple times with different bits and then choose the most appropriate bit and BHA combination for the application. This significantly shortens the development cycle thus reducing new product “time to market”. Most importantly it allows the running of “what if” scenarios rather than the traditional trial and error method of bit/BHA development. As oil and gas well requirements become more and more complex and tool strings become more correspondingly more sophisticated, the use of IDEAS make commercial sense.

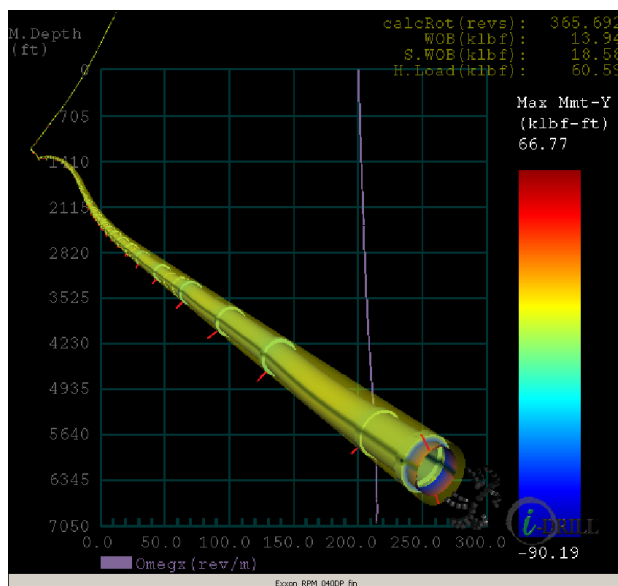


Figure 7.1: Example of FEA Mesh [35].

The program simulates transient performance of the entire drill-string and is able to predict rate of penetration, directional tendency, lateral-, torsional- and axial vibrations, stick-slip, torque, moments, forces and displacement at any point along the string. The model accounts for well surveys, formation and mud properties, geometry and configuration of BHA components and detailed cutting structure information [31-35].

7.1 The system Approach Applied to Drilling

Vibrations and accelerations have detrimental effects on directional control, tool reliability, drill string integrity, and drilling performance. To address severe down-hole vibrations, torque and RPM fluctuations a holistic modeling approach to vibration prediction and drilling system design is necessary. To accurately predict the performance of the drilling system, it is essential to consider the sum of all forces affecting the system.

In the IDEAS software, the bit and every string component are first modeled individually. The exact interaction between the bit and the formation drilled are modeled using lab derived rock mechanics. A series of shearing (for PDC) and indentation (for RB) tests are performed to replicate the exact interaction between a bits cutting structure and the applicable rock sample. If a specific formation is to be drilled (and not available in the rock lab), an outcrop sample similar to the formation must be drilled to give as accurate modeling as possible. The result gives and understanding of the excitation forces needed to destroy the rock. The information is further processed by an Integrated Dynamic Engineering Analysis System that generates 4D outputs.



Figure 7.2: *Shearing test applied to a PDC cutter on desired formation [35].*

The last step in the IDEAS process is to apply the dynamics (time based FEA) to each component of the drillstring. This delivers the opportunity to model, analyze and predict the behavior and performance of the entire drilling system. The multiple interactions achieved can capture the effect of the bit on BHA and vice versa. This modeling help predict which tool that causes vibrations and accelerations which in turn have detrimental effects on directional control, tool reliability, drill string integrity, and drilling performance [31-35].

7.2 FEA Mesh Model Contents

Finite Element Analysis (FEA) is a numerical method of solving engineering problems. It is used in problems where analytical solutions are difficult to obtain. FEA uses a complex system of points (usually displacements) called *nodes* which make a grid called a *mesh* (Figure 7.3). The mesh is programmed to contain the material and structural properties which define how the structure will react to certain loading conditions. Nodes are assigned at a certain density throughout the material depending on the anticipated stress levels of a particular area. Regions which will receive large amounts of stress usually have a higher node density than those which experience little or no stress. Points of interest may consist of: fracture point of previously tested material, fillets, corners, complex detail, and high stress areas. The mesh acts like a spider web in that from each node, there extends a mesh element to each of the adjacent nodes. This web of vectors is what carries the material properties to the object, creating many elements.

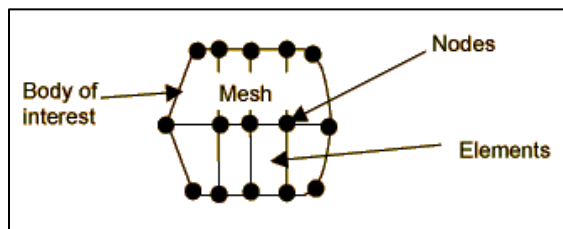


Figure 7.3: Mesh structure [35].

The behaviour of an individual element can be described with a relatively simple set of equations. Just as the set of elements would be joined together to build the whole structure, the equations describing the behaviours of the individual elements are joined into an extremely large set of equations that describe the behaviour of the whole structure. The computer can solve this large set of simultaneous equations. From the solution, the computer extracts the behaviour of the individual elements. From this, it can get the stress and deflection of all the parts of the structure. The stresses will be compared to allow values of stress for the materials to be used, to see if the structure is strong enough.

The variable to be determined in the analysis is assumed to act over each element in a predefined (e.g. quadratic) manner. The number and type of elements is chosen to ensure that the variable distribution over the whole body is adequately approximated by the combined elemental representations. After the problem has been divided into the discrete units, the governing equations for each element are calculated and then assembled to give system equations that describe the behaviour of the body as a whole.

In a stress analysis problem, the finite element software calculates the displacements of the nodes and from this information, the stresses and strains in the elements are determined. In order to prevent unlimited rigid body motion, boundary conditions are applied.

The basic concept of FEA is to break a complex system down to a large but simple set of elements. A BHA component is represented as group of elements. Each element is made up of several nodes. At each intersection (Figure 7.4) there would be a node. And for each node the behavioral equations are simple and easily solved because we may consider forces on neighboring nodes only.

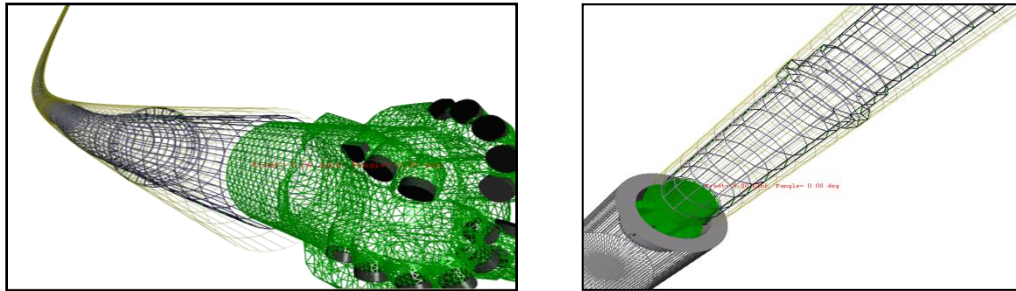


Figure 7.4: Illustration of a BHA component with its respective nodes.

The IDEAS model offers an approach to focus on any drillstring component in order to optimize and understand the components contribution and effect.

The model includes the following components:

- PDC or Roller Cone cutting structure and body geometry
- Formation type and hardness
- RSS (Rotary steerable system)
- PDM (Positive displacement motor)
- Turbo drills
- Stabilizers
- Jars
- Shock Subs
- DC (Drill collars)
- HWDP (Heavy weight drillpipe)
- DP (Drillpipe) including tool joints

The nodes in the FE mesh that represent the cutting structure (bit or reamer) are governed by rock mechanics and behave in a highly non linear manner. Rock mechanics data are empirically derived in a laboratory test program and implemented within the model to establish rock/bit dynamic output.

The interaction of nodes is described by Newtonian dynamics, and a general form is given in the following equation:

Equation 7.1

Where M, C and K are matrix coefficients that hold information pertaining to mass, dampening and spring/elasticity for the node in question. The matrices are also conducted from material properties and include viscous dampening from drilling fluids.

Each node has six degrees of freedom, represented by x , which yields a vector length of six. A large degree of freedom in the system is necessary since the drillstring is flexible and energy transfer finite. If a drilling parameter is changed on surface it will take finite time to make an effect down hole. Other external forces acting on the FE mesh such as contact forces between cutters and formation, and borehole wall contact with the drillstring, are modeled and included as the term F_{ext} in equation 7.1. Internal and external forces are time dependent and therefore solved dynamically. A dynamic solution requires boundary conditions that can be changed during the simulation. Therefore restrictions on node positions x are imposed in the software. The interaction of the drillstring with the well bore is modeled as a nonlinear relation of contact force relative to free motion of unrestricted displacement. These conditions confine the string within the well bore and ensure a well supported FE mesh such that a feasible solution for the entire system can be obtained [34, 35].

7.3 Simulation Approach for Chalk Drilling Challenge

As mentioned above, IDEAS can simulate the behavior of the entire drillstring (including the drill bit) in a particular formation. However, the magnitude of PDC bit selection is extremely large. The blade count ranges from six to twelve blades. There are also numerous different cutting structures available due to the complexity of side-rakes, back-rakes, radial position etc. To be able to narrow down the simulations, Alberto Caycedo (Senior FE, Smith bits) was consulted in the bit selection process. It was decided to choose five bits with design properties suitable for drilling in the Chalk formation. Even though there are three similar bit types, different bill of materials was used. The six first numbers in each BOM number represent the cutting structure, while the remaining numbers represent different aspect such as blade geometry, bit profile, gage length etc.

Following bits were used in the simulations:

Bit information			Back rake angles				Features	
Bit_nbr	Bit_type	BOM	Cone	Nose	Shoulder	Gage	Radial nose	Cone angle
1	MDi716LUBPX	6425250504	18-20	20	25	30	2.625	16.5
2	MDi716LUBPX	64867A0002	18-20	20-25	25	30	2.625	16.5
3	MDi716LUBPX	65024A0001	15-16	16-20	25	30	2.625	16.5
4	MDi619LBPX	6422190701	18-20	20	20-25	30	-	16.5
5	MDi619MPX	65057A0001	10-13	15-20	20-25	27-30	2.4	20

Table 7.1: Selected bit designs with their back-rake angles and features respectively.

The project scope includes looking at Schlumberger’s Powerdrive (RSS) and its relation to the different bit designs. Several drill pipe geometries will be simulated to understand the importance of pipe stiffness in relation to stick slip and other vibration failure modes. Identifying optimal drilling parameters in relation to both ROP potential and vibration levels will also be part of the project scope. Impact of different bit designs will also be considered.

The objective of this project was to design an 8 ½” PDC bit that could drill through the Chalk formations in one effective run with high penetration rate and limited vibration levels. NPD cores from the selected formations were first tested in terms of mineralogy, petrology, isotope properties etc and later compared to outcrops to find a compatible Chalk for extraction. The Kansas Chalk proved to be the most compatible sample (see 4.3.2), but weren’t used directly in the simulations due to extraction difficulties.

The ideal simulation procedure would be to:

1. Drill through the Kansas Chalk in the rock lab
2. Integrate the results in the software
3. Simulate drilling action through the formation with various drilling parameters.

Through extensive laboratory testing, rock files have been developed on different lithologies. These rock files include confining pressure, compressive strength etc. Since the Kansas Chalk was unavailable, rock files couldn’t be develop. Instead, different Chalk samples already tested in the rock lab were considered. It was decided to select two different Chalk formations for simulations; Lueders Limestone and Austin Chalk. The Lueders Limestone represents a hard and abrasive Chalk formation with high compressive strength. The Austin Chalk has lower compressive strength and is softer and less abrasive to drill.

The new simulation approach:

1. Simulate drilling action in Lueders Limestone (LL).
 - Use different bit designs and drilling parameters and use on particular BHA and well path throughout the simulations.
 - Analyze results and find best bit in “worst case scenario”
2. Simulate drilling action in Austin Chalk.
 - Use bit with best performance in LL in addition with a similar bit design (for reference).
 - Analyze results and find best bit in Ekofisk comparable Chalk.

8. Applied Lab results to Virtual Drilling Environments

8.1 IAP Method

In order to find the best suitable bit with its most effective dynamic parameters, an IAP was decided to be used as a tool. IAP is an abbreviation for IDEAS Analysis Project, which is a highly detailed program that includes different BHA's, well profiles, bit designs, multiple lithology layers, etc. It is a time consuming project due to the level of detail needed for all input parameters. When all input parameters are filled in, it is sent to China to be run in a hardware that can handle the information. The simulation than take two days to finish.

The first stage of the simulation process was to perform an IAP, as previously described. The purpose of this analysis is to compare and contrast the dynamic drilling characteristics of the PDC bits examined. It was decided to run two IAP's as mentioned in Chapter #6. First IAP simulates drilling through Lueders Limestone (worst case) and second IAP simulates drilling through Austin Chalk (most compatible with Kansas and Ekofisk). All variable parameters such as well path, BHA and drilling parameters remain unchanged. The only difference between the two IAP's is the formation and the bit selection design.

8.2 IDEAS Program Description

The IDEAS program includes several important parameter aspects such as well trajectory, BHA structure and also a much more in depth description of the bit. These input parameters are of great importance for the accuracy of the results from the simulations.

All of the parameters used in the simulations are presented in this chapter to give a comprehensive understanding of the entire process.

8.2.1 BHA Input

The next step was to choose a suitable BHA for directional control in the Chalk formations. The BHA can consist of many different components depending on the application. It was decided to use Schlumberger's PowerDrive as rotary steerable together with the components listed in the table below. General dynamics are included.

From top to bottom:

Tool [Type]	Length [ft]	OD [in]	ID [in]	Weight [lbs/ft]	Unit l [ft]	Tool joint l [ft]	Tool joint OD [in]	Tool joint ID [in]
Drillpipe	14100	5,5	4,778	30,0	30,0	1,833	7,25	3,5
Cross-over	2,850	7,0	2,81	82,40	-	-	-	-
HWPD	275,7	5,0	3,0	57,420	31,0	4,0	7,0	4,0
Drill collar	34,02	6,5	2,75	106,5	-	-	-	-
HWDP	154,0	5,0	3,0	57,420	31,0	4,0	7,0	4,0
Drill Collar	31,030	6,5	2,75	106,5	-	-	-	-
HWPD	59,780	5,0	2,75	41,150	31,0	4,0	6,25	2,81
Stabilizer	28,080	6,75	3,280	100,64	15,0	1,083	8,25	-
Stabilizer	32,580	6,75	2,809	100,64	15,0	1,083	8,375	-
MWD/LWD	27,330	6,75	2,25	110	-	-	-	-
Stabilizer	25,980	6,75	2,809	100,64	15,0	1,083	8,375	-
Drill Collar	9,380	5,5	3,250	60,30	-	-	-	-
Stabilizer	5,7	6,75	3,0	100,64	2,0	2,0	8,313	-
Powerdrive	13,480	6,75	2,280	80,0	-	-	-	-

Table 8.1: BHA components with general dynamics.

8.2.2 Drilling Parameters

Another important aspect was selecting the parameters for the simulations. A PDC bit may experience vibrations at a certain weight on bit. A bit can vibrate with a certain WOB and rotational speed, but can be prevented if one or both of the parameters are changed. Therefore, #4 different WOB were simulated on #3 different RPM's. The weight applied on bit was decided to range from 15 to 30 Klbs (see table below) while the rotational speed was decided to range from 100 to 160 rotations per minute (RPM).

Selected bits		Drilling Parameters				
BIT	BOM	Depth [m]	Formation	WOB [klbs]	RPM	Steering
MDi716LUBPX	6425250504	4513 5825	Lueders Limestone Pierre Shale	15, 20, 25, 30	100, 130, 160	NO
MDi716LUBPX	64867A0002	4513 5825	Lueders Limestone Pierre Shale	15, 20, 25, 30	100, 130, 160	NO
MDi716LUBPX	65024A0001	4513 5825	Lueders Limestone Pierre Shale	15, 20, 25, 30	100, 130, 160	NO
MDi619LBPX	6422190701	4513 5825	Lueders Limestone Pierre Shale	15, 20, 25, 30	100, 130, 160	NO
MDi619MPX	65057A0001	4513 5825	Lueders Limestone Pierre Shale	15, 20, 25, 30	100, 130, 160	NO

Table 8.2: Selected drilling parameters for the simulation.

Another important aspect regarding this is the possibility of observing how the vibrations will propagate or degrade as the drilling parameters are changed. Operating parameters can then be suggested to the customer when they choose to run the bit in hole.

8.2.3 Bit Selection

There are several PDC bits available today. Numerous different cutting structures and other features can be incorporated in each bit type. Therefore, a certain Bill of Material (BOM) must be selected for the bit types to be tested. The focus was to test on #3 different MDi716's and #2 MDi619. The first bit type is a seven bladed bit with 16 mm cutters, while the MDi619 is a six bladed bit with 19 mm cutters.

Cutting structure	Size [in]	Type	BOM (Cutting Structure)	Make up length	Gauge pads Width	Gauge pads height	Gauge pads Spiral	Gauge pads undercut
1	8,5	MDi716LUBPX	6425250504	9,75	1,25	2,00	5,00	0,01
2	8,5	MDi716LUBPX	64867A0002	9,75	1,25	2,00	5,00	0,01
3	8,5	MDi716LUBPX	65024A0001	8,50	1,25	2,00	5,00	0,01
4	8,5	MDi619LBPX	6422190701	9,75	1,25	2,00	5,00	0,01
5	8,5	MDi619MPX	65057A0001	9,125	1,25	2,0	5,00	0,01

Table 8.3: Selected bit designs with corresponding BOM's.

8.2.4 Well Profile

The Chalk formations in the Ekofisk field are normally drilled horizontally, so this was naturally the focus for the well trajectory inputs in the IAP. The table below represents the well profile used for the simulations. The 9 7/8" casing was set at 11500 ft MD depth (see table).

The 8 1/2" drilling section was simulated from 14 797 ft MD to 19837 ft MD. The Lueders Limestone formation started at 14 797 ft MD and ranged down to 19038ft MD, followed by Pierre shale down to total depth.

Well Profile Directional Surveys				
MD (ft)	Inclination (deg)	Azimuth (deg)	MD (m)	MD (ft)
0,000	0,00	0,00	0,000	0
1000,000	10,00	240,00	305,000	1000
5000,000	25,00	240,00	1525,000	5000
8000,000	40,00	240,00	2440,000	8000
9000,000	50,00	240,00	2745,000	9000
10534,777	52,38	242,40	3211,000	10534,78
10702,100	59,76	241,70	3262,000	10702,1
10767,717	62,72	241,23	3282,000	10767,72
10954,725	68,16	238,64	3339,000	10954,72
11154,856	73,55	236,46	3400,000	11154,86
11440,289	82,93	235,41	3487,000	11440,29
11646,982	87,11	235,13	3550,000	11646,98
11935,696	86,34	235,57	3638,000	11935,7
13047,901	85,52	237,61	3977,000	13047,9
13736,877	86,06	236,97	4187,000	13736,88
14632,546	85,84	238,03	4460,000	14632,55
16450,132	85,43	237,01	5014,000	16450,13
16633,859	82,07	237,04	5070,000	16633,86
16843,833	81,27	236,96	5134,000	16843,83
16965,224	75,94	236,37	5171,000	16965,22
17244,095	64,88	238,06	5256,000	17244,1
17532,809	57,42	239,93	5344,000	17532,81
17752,625	52,71	238,18	5411,000	17752,63
17946,195	47,08	237,33	5470,000	17946,19
17979,003	45,98	237,33	5480,000	17979
18087,271	42,17	238,97	5513,000	18087,27
18180,414	39,47	239,34	5541,390	18180,41
18369,423	33,69	238,89	5599,000	18369,42
18465,256	30,77	238,39	5628,210	18465,26
18753,085	26,64	247,32	5715,940	18753,08
19038,124	27,46	250,44	5802,820	19038,12
19454,955	29,60	249,28	5929,870	19454,95
19737,533	24,22	245,03	6016,000	19737,53
19837,927	21,05	244,15	6046,600	19837,93

Table 8.4: Chosen well profile.

9. Report on Virtual Results

Since the overall goal was to find a stable and effective bit, the results were analyzed in terms of vibrations (axial, lateral, and torsional) and rate of penetration (ROP). The results for the different vibrations modes were plotted as g forces as a function of WOB_RPM. This made it easier to analyze the results and find the best bit design with its most suitable drilling parameter. The penetration rates were naturally plotted as feet/hour as a function of WOB_RPM to find most effective bit with the most suitable drilling parameters.

In order to differentiate between safe and unsafe vibration levels, following differentiation chart recommended by Field Engineers was used:

Vibration Mode	FE Recommended Ranges		
	Safe	Moderate	Unsafe
Lateral	<5g	5 to 10g	>10g
Axial	<0.5g	0,5 to 1g	>1g
Torsional [Delta torque at bit]	<1 kft/lbs	1 to 5 kft/lbs	>5kft/lbs

Table 9.1 *Vibration level Differentiation chart.*

As can be seen from the table above, the recommended ranges for safe, moderate and unsafe vibration levels, varies between the different vibration modes. Lateral and Axial vibrations are measured in g forces, while torsional vibrations are measured in Kft/lbs. The torsional vibration equals the delta torque at bit.

9.1 Lueders Limestone & Pierre Shale II

The first step was to simulate through hard Lueders Limestone with high compressive strength to simulate worst case scenario (Norman E. Garner et al [52]). After the hard section, a soft shale section was included to make the drilling process more realistic, in this case low compressive Pierre Shale. Two different drilling depths were used; 14797 ft and 19100 ft. Simulation for both depths are presented in this chapter.

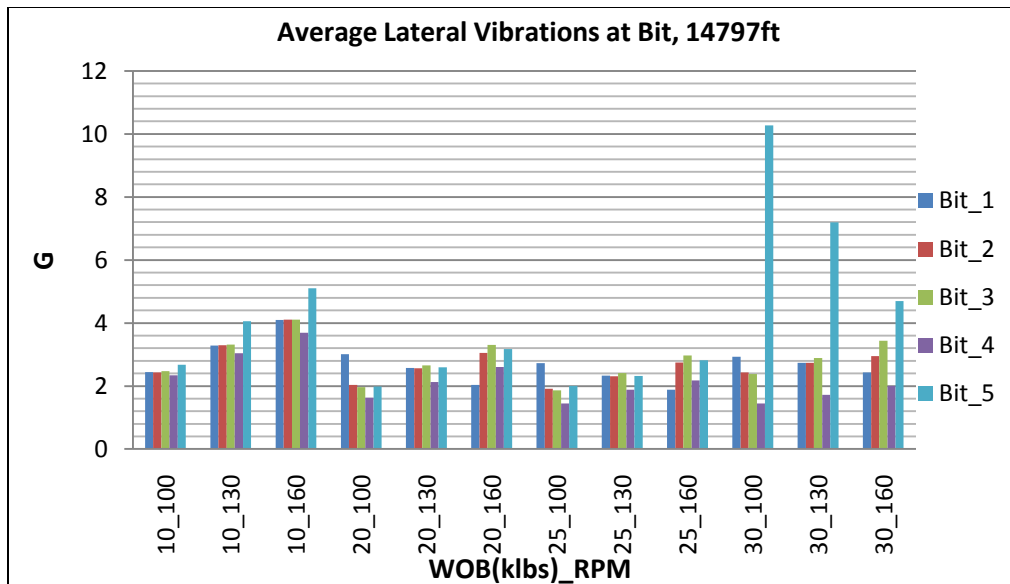


Figure 9.1: Lateral vibrations at bit, 14797ft (Lueders Limestone).

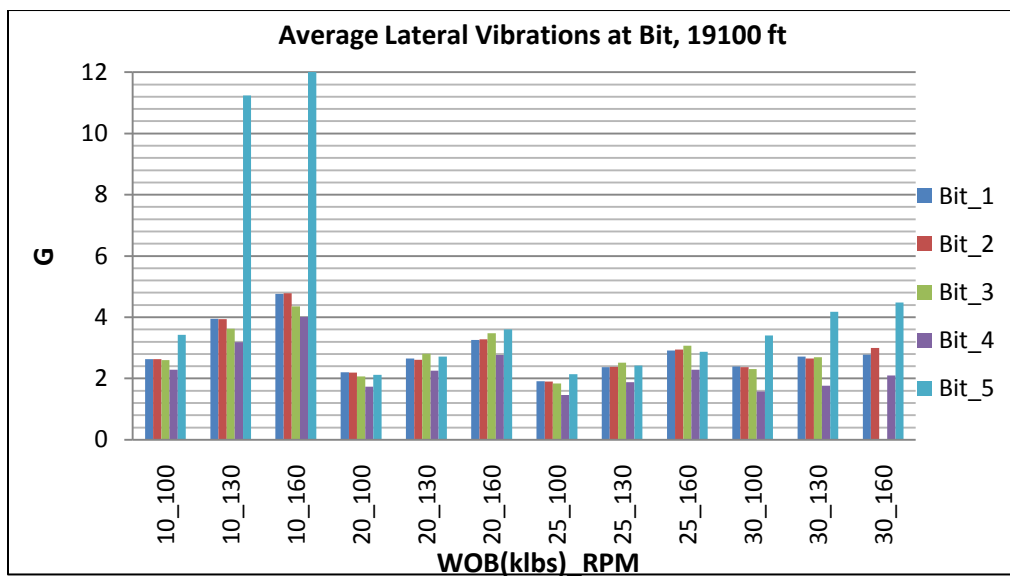


Figure 9.2: Average Lateral Vibrations at Bit, 19100ft (Lueders Limestone).

The average lateral vibrations for both drilling depths are at an acceptable level for Bit_1 to Bit_4. Unsafe values of lateral vibrations are observed with Bit_5 at 14797ft (30WOB_100RPM) and at 19100 ft (10WOB_130-160RPM). Bit_5 shows in addition the overall worst performance for both drilling depths. With 10 klbs WOB the average lateral vibrations exceed 36 g forces with Bit_5, which is considered unsafe. The best drilling performance is achieved with bit_4 (MDi619LBPX). It is also observed that the best performance in terms of lateral vibrations is with a weight on bit between 20-25 klbs and between 100-130 rotations per minute.

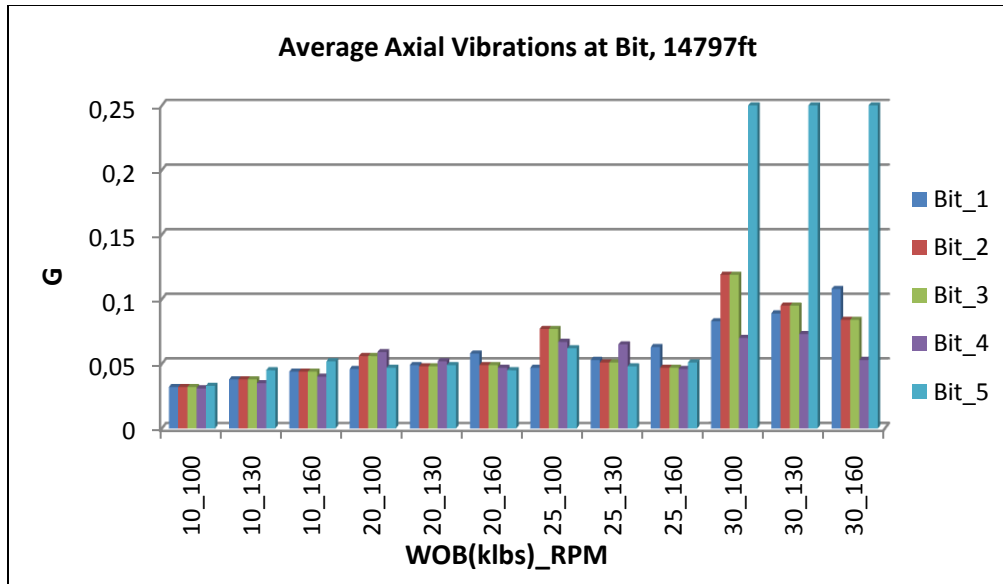


Figure 9.3: Average Axial Vibrations at Bit, 14797ft (Lueders Limestone).

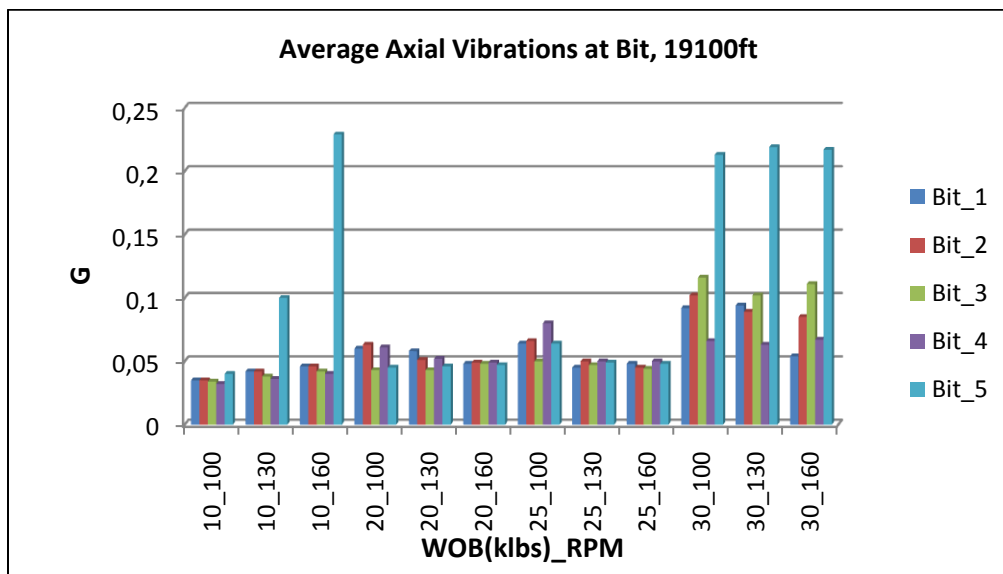


Figure 9.4: Average Axial Vibrations at Bit, 19100ft (Lueders Limestone)

The average axial vibrations for both drilling depths are at an acceptable level for all bit designs. This was expected since the axial vibrations are generally at a low level for PDC bits. However, Bit_5 shows the overall worst performance for both drilling depths. With 30 klbs WOB the average axial vibrations exceed 0.683 g forces for Bit_5, which is considered as a moderate range, but not recommended. The best drilling performance is achieved with bit_4 (MDi619LBPX). It is also observed that the best performance in terms of lateral vibrations is with a weight on bit between 20-25 klbs and with all RPM parameters.

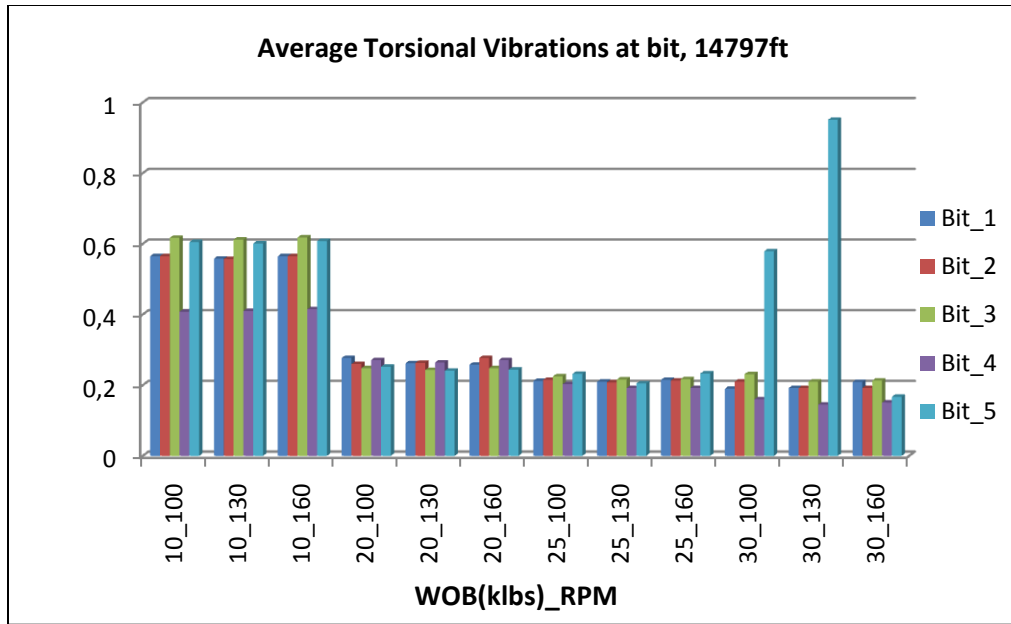


Figure 9.5: Average Torsional Vibrations at bit, 14797 ft (Lueders Limestone).

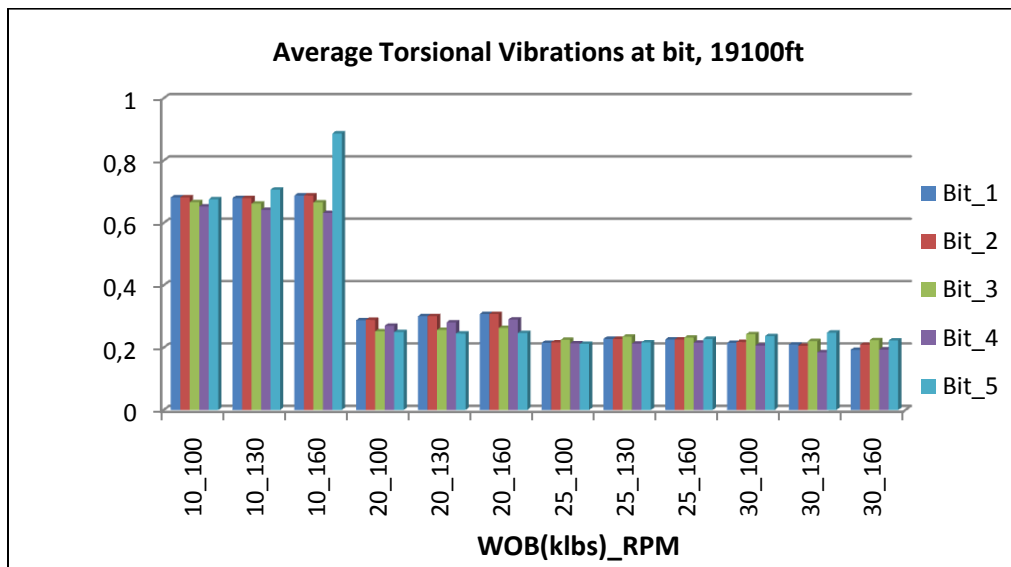


Figure 9.6: Average Torsional Vibrations at bit, 19100 ft (Lueders Limestone).

The average torsional vibrations for both drilling depths are at an acceptable level for Bit_1 to Bit_4. Unsafe values of lateral vibrations are observed with Bit_5 at 14797ft (30WOB_130RPM) and at 19100 ft (10WOB_160RPM). Bit_5 shows in addition the overall worst performance for both drilling depths. The best drilling performance is achieved with bit_4 (MDi619LBPX). It is also observed that the best performance in terms of lateral vibrations is with a weight on bit between 20-30 klbs and with all RPM parameters.

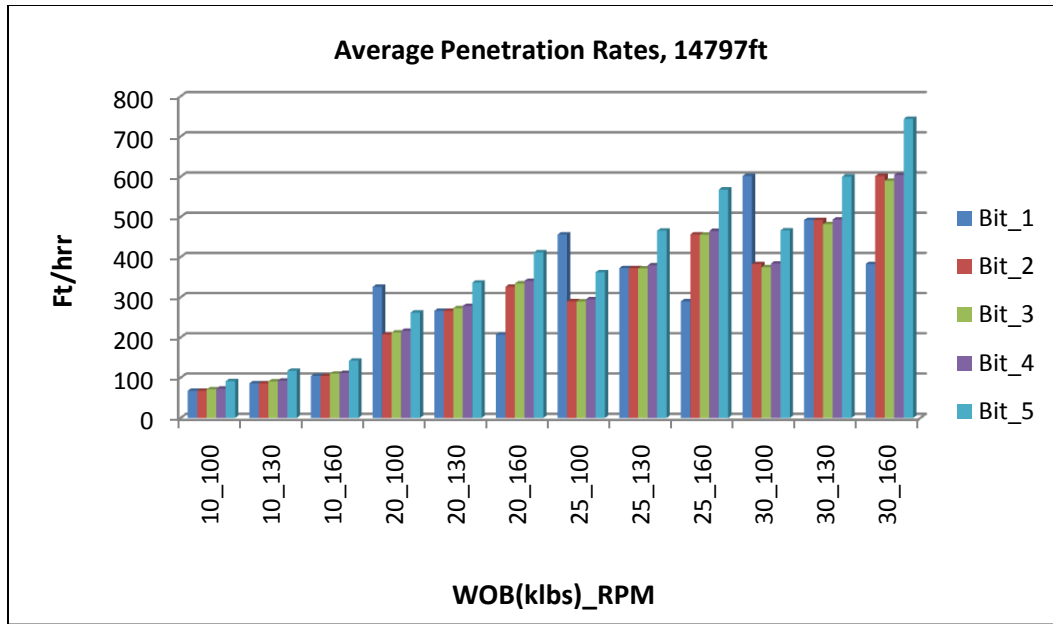


Figure 9.7: Average penetration rates achieved with the different bit designs, 14797ft (LL)

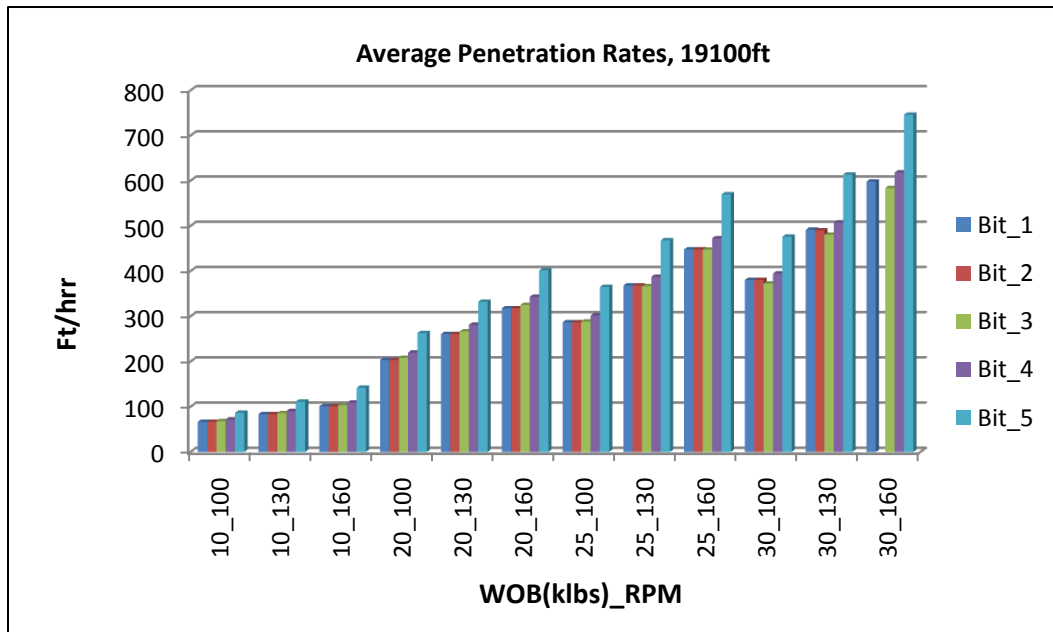


Figure 9.8: Average penetration rates achieved with the different bit designs, 19100ft (LL)

The penetration rates naturally increases with increased weight on bit. Bit_5 shows best overall performance, but due to high vibration levels it's not a desirable bit design. A penetration rate above 300ft/hr is desirable, and this is achieved with 20 klbs weight on bit and with a RPM level higher than 130 rotations per minute. Bit_4 shows the next best overall performance in terms of penetration rate.

9.1.1 Primary results

The MDi619LBPX (Bit_4) showed best performance in terms of lateral, axial and torsional vibrations. Bit_5 showed best performance with regards to average penetration rates. However, Bit_5 had the overall worst performance in terms of vibration levels. Since Bit_5 was considered least stable, a bit with low vibration levels and acceptable penetration rates was selected. Bit_4 had low vibration levels and high penetration rates, making it the best bit design in Lueders Limestone (considered being the worst case scenario for Chalk drilling). Bit_4 was therefore selected for simulations in the Austin Chalk.

In order to test the MDi619LBPX in Austin Chalk, another bit design had to be included for simulation references. Since the best performance for the majority of the bit designs were observed with a weight on bit between 15-25 klbs, these values were the one used for the next simulation.

Following bits and drilling parameters were selected:

Selected bits		Drilling Parameters				
BIT	BOM	Depth [ft]	Formation	WOB [klbs]	RPM	Steering
MDi619LBPX*	6422190603	14797 19100	Austin Chalk	15,20,25	100,130,160	NO
MDi619LBPX	64664B0002	14797 19100	Austin Chalk	15,20,25	100,130,160	No

Table 9.2: Selected bits for secondary Simulation, Austin Chalk. * Same bit as in first simulation.

The RPM's remained unchanged as well as the well path and BHA selection. The same drilling depths were used, but Pierre shale II was not included.

9.2 Austin Chalk

The next step was to simulate through a softer Chalk with low compressive strength (0-2). The Austin Chalk is compatible with the initially desired Kansas Chalk (Melvin Friedman et al [53]), and was therefore used to simulate the actual drilling action in the Ekofisk Chalk. Two different drilling depths were used; 14797 ft and 19100 ft. Drilling simulation for both depths are presented in this chapter.

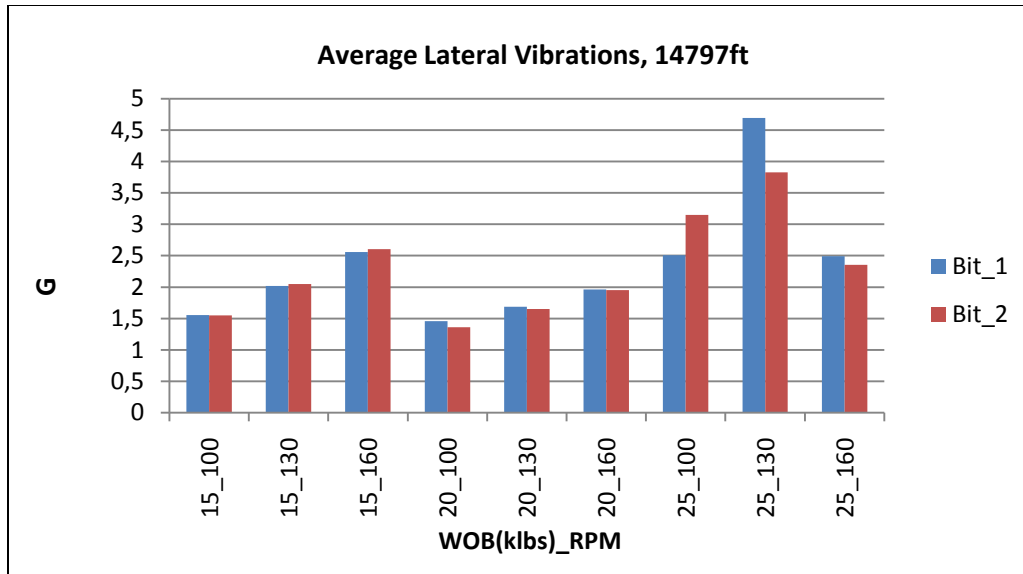


Figure 9.9: Lateral vibrations at bit, 14797ft (Austin Chalk).

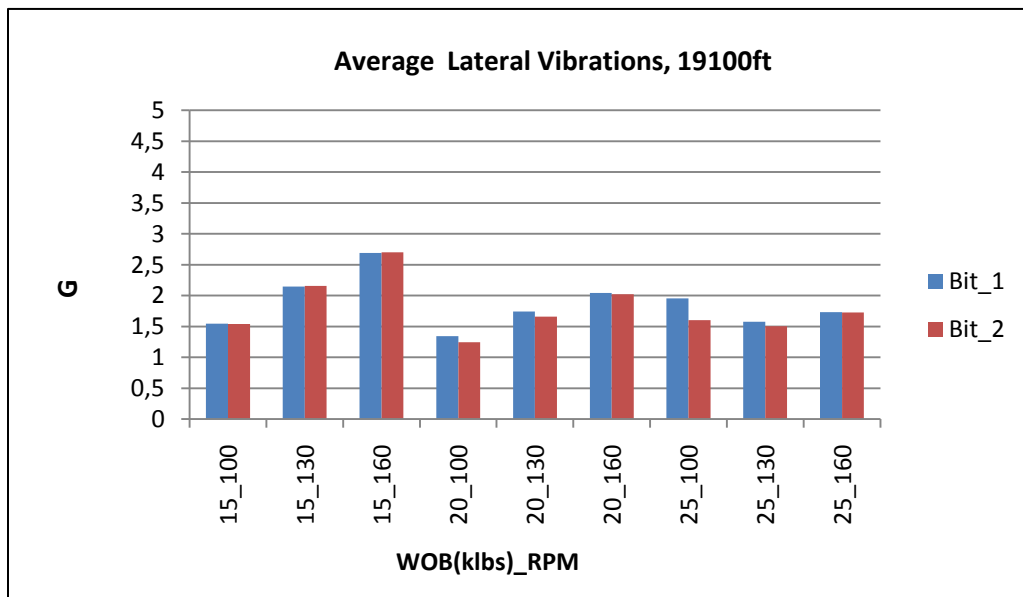


Figure 9.10: Average lateral vibrations at bit, 19100 ft (Austin Chalk).

The average lateral vibrations for both drilling depths are at an acceptable level (<5g) for both bit designs. The results are quite similar for Bit_1 (MDi619LBPX*) and bit_2 (MDi619LBPX) in terms of lateral vibrations. The best performance in terms of lateral vibrations is with a weight on bit of 20 klbs and between 100-130 rotations per minute.

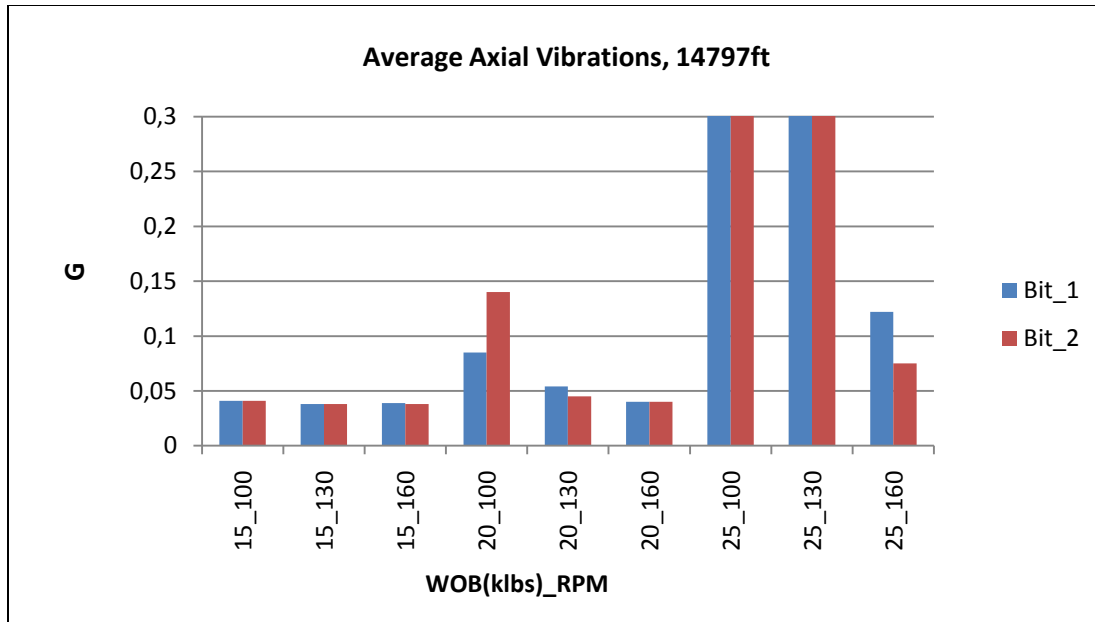


Figure 9.11: Average Axial vibrations at bit, 14797ft (Austin Chalk).

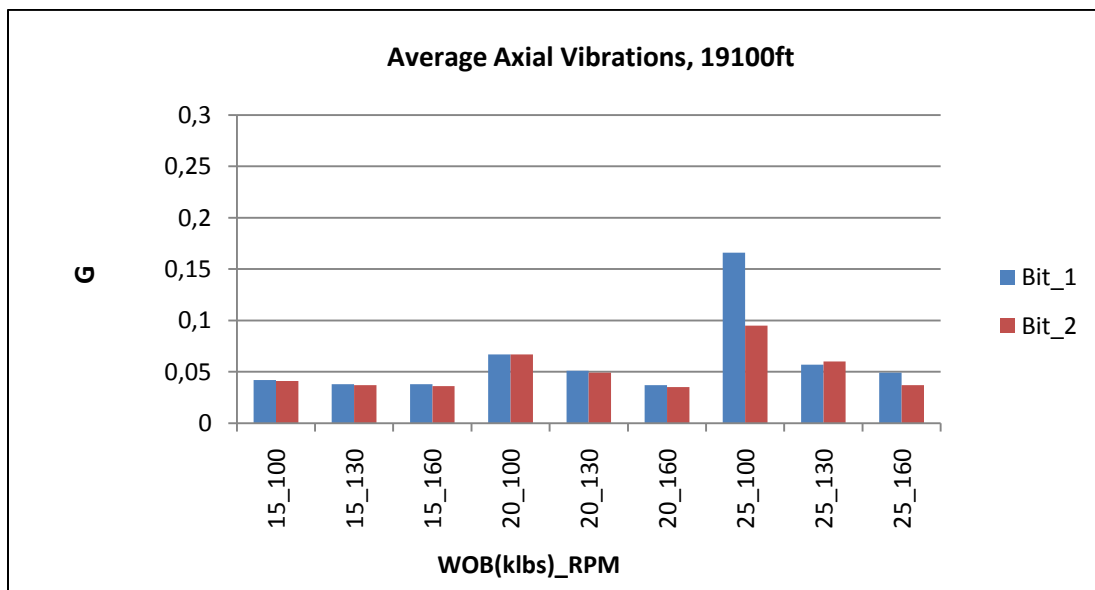


Figure 9.12: Average Axial vibrations at bit, 19100ft (Austin Chalk).

The average axial vibrations are at an acceptable level for both bit design with majority of drilling parameters. However, a very unstable condition is observed with 25 klbs weight on bit and between 100-130 rotations per minute for the first depth (14797 ft). Both bit designs exceeds an average axial vibration above 2g's which is considered unsafe. Bit_1 shows best overall performance with a WOB between 15-20 klbs and all RPM's.

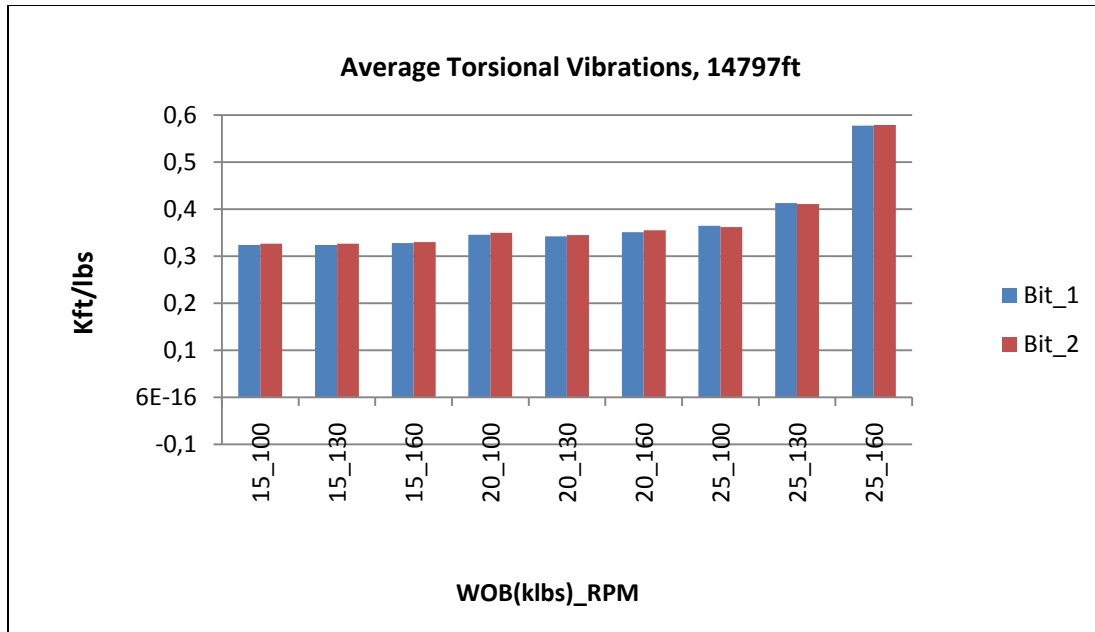


Figure 9.13: Average Torsional Vibrations, 14797 ft (Austin Chalk).

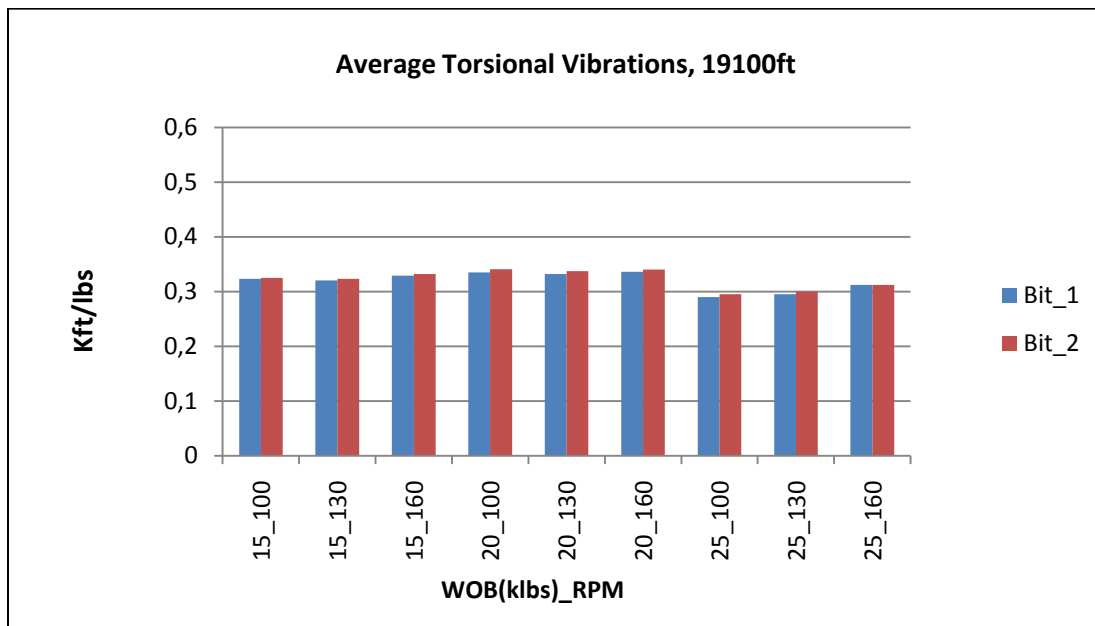


Figure 9.14: Average torsional Vibrations, 19100 ft (Austin Chalk).

The average torsional vibrations for both drilling depths are at an acceptable level (<1 kft/lbs) for both bit designs. The best drilling performance in terms of torsional vibrations is achieved with Bit_1 (MDi619LBPX*). Desirable drilling parameters for depth_1 (14797ft) is achieved with a WOB between 15-20 klbs, and all simulated RPM values. The best performance at 19100 ft is achieved with a weight on bit of 25 klbs and between 100-160 rotations per minute.

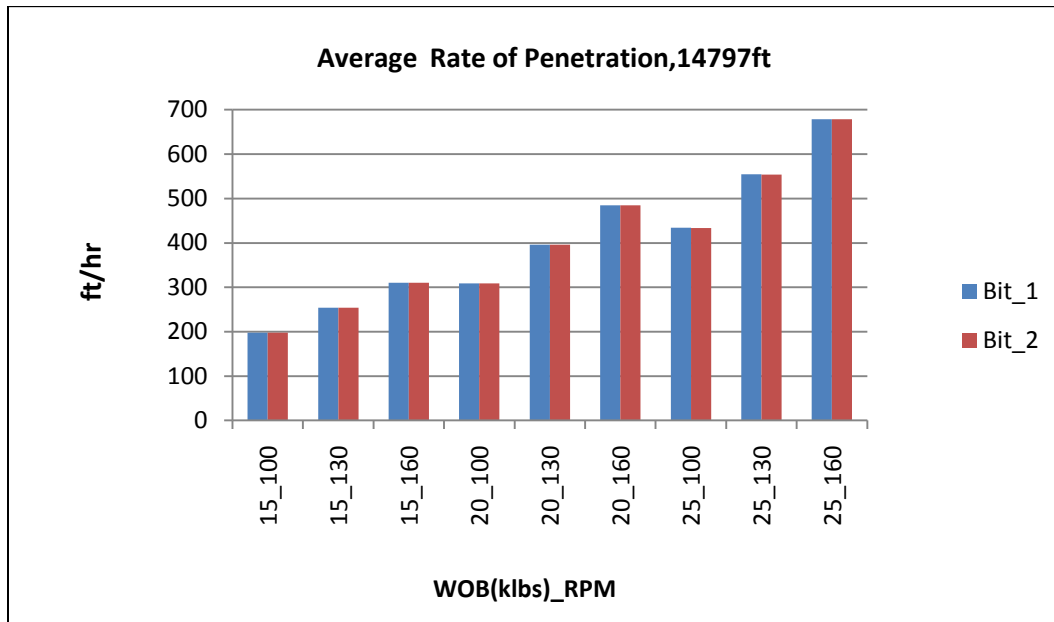


Figure 9.15: Average Rate of Penetration, 14797 ft (Austin Chalk)

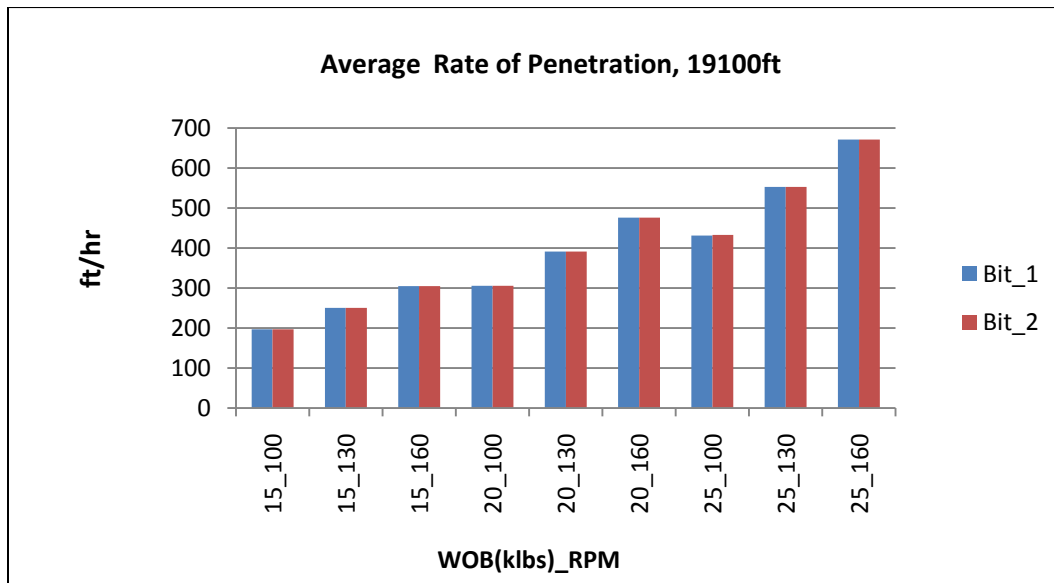


Figure 9.16: Average Rate of Penetration, 19100 ft (Austin Chalk)

The penetration rates naturally increases with increased weight on bit. A penetration rate above 300ft/hr is desirable, and this is achieved with 20 klbs weight on bit and with 100 rotations per minute or higher. The penetration rates for both bit designs are quite similar. The bit selection should then mainly be based on the stability of the bit.

9.2.1 Final Results

After the first simulation in Lueders Limestone and Pierre shale, the MDi619LBPX (6422190603) proved to be the best bit option for hard, compressive Chalk. The same bit was then tested in Austin Chalk to investigate a trend for this bit design in Chalk applications. The vibration levels were even lower and the penetration rates increased. This indicates that this particular bit is highly suitable in Chalk applications, i.e. the Chalk formations in the Ekofisk field.

9.2.1.1 MDi619LBPX

The MDi619LBPX (BOM 6422190603) is the most suitable bit for Chalk applications based on the simulation results. A short description of the selected bit is presented in this chapter to give an understanding of its design and specifications.



Figure 9.17 Illustration of an MDi619 bit design, side and top view.

A number of abbreviations are used to describe the design of a certain bit type. The #3 first letters represent general bit information while the remaining letters describe additional features. In this case, the **M** stands for a bit composed of matrix, the **D** stands for directional certified through IDEAS and the **L** stand for IDEAS certified (meaning that the bit has been designed and verified through the IDEAS software). **619** can be read as a #6 bladed bit with 19mm (in diameter) cutters. The additional features are not presented here since the direct bit input data in the IDEAS software is the cutting structure.

This particular bit (BOM 6422190603) has #27 cutters in total (#13 face cutters, #6 gauge cutters and #8 cone cutters.). The gauge length, make up length and BOM description is described in detail in 8.2.3.

9.2.1.2 Operating parameters

Different operating parameters were used to find the most effective and stable run for the bit. A mud weight of 1200 was used together with variable weights on bit and rotations per minute. The optimal parameters are presented in this chapter.

The desired weight on bit varied between the two simulations. The simulated drilling action through Lueders Limestone required higher weights on bit when compared to simulations through Austin Chalk. This was not surprising due to the fact that Lueders Limestone is a much harder Chalk with higher compressive strength than Austin Chalk. Normal procedure is to apply more weight when formation hardness/abrasiveness increases.

In terms of stability and penetration rates, the best performance in Lueders Limestone was observed to be with a weight on bit between 20-25 klbs (see 9.2). Lower WOB was desirable for MDi619LBPX in Austin Chalk with a WOB level between 15-20 klbs (see 9.3).

The different RPM values did not give any major effects on stability and penetration rates for the suggested WOB values. However, a certain trend was observed. The overall best performance in Lueders Limestone (in terms of stability with WOB levels between 20-25 klbs) was with 100 rotations per minute. The best performance in Austin Chalk (in terms of stability with WOB levels between 15-20 klbs) was with RPM values between 130-160 for axial and torsional vibrations, and 100 for lateral vibrations.

10. Conclusion

The demand for energy and oil has never been higher and neither has the complexity and difficulty of extracting desirable amounts in a cost-effective manner. Reservoirs are getting smaller, deeper and more difficult to reach, continually increasing drilling costs and pressuring manufactures to develop bits that can drill through almost any formation in one effective run. To accommodate this need, Smith bits has started to custom-design effective and stable bits for formations of interest.

Through extensive studies of onshore and offshore Chalk samples, the Kansas Chalk (for medium porosity) and the Ulster Limestone (for low porosity) are the most similar onshore Chalks to North Sea Chalk. In other words The Kansas Chalk is a suitable simulation-substitute for the Ekofisk Field, while the Northern Ireland sample is a suitable simulation substitute for harder offshore Chalks with chert present (like Chalk in the Sleipner Field). The Kansas Chalk was selected for further studies since the main focus in this project was to find a suitable PDC bit for 8 ½" Chalk sections in the Ekofisk Field.

Since the Kansas Chalk was impossible to extract within the timeframe, another solution approach was necessary. Together with Alberto Caycedo (Senior Field Engineer in Smith Bits), different Chalks already available in the IDEAS rock library were studied. The new approach required two simulations instead of one as initially planned.

The first simulation was through Lueders Limestone, which is considered as a hard Chalk with high compressive strength. The Idea was to simulate different drill bit designs in what was believed to be a "worst case scenario" for the drill bit in Chalk applications of the North Sea. The MDi619LBPX had low vibration levels and high penetration rates, making it the best bit design in Lueders Limestone. Optimal drilling parameters were observed with a WOB between 20-25 klbs and with 100 rotations per minute.

The final and last simulation (In Austin Chalk) strengthened the conclusion from the first simulation. The MDi619LBPX had best performance, making it the best suitable bit for Chalk applications in the North Sea.

11. Future Work

For future work it is recommended to trace down the GPS location of the Mermaris quarry and extract enough samples for shearing tests in the rock lab in Houston. The Kansas Chalk proved to be comparable with Chalk from the Ekofisk field, and should be integrated in the IDEAS rock library for future simulations. It is also recommended to test the performance of the MDi619LBPX *(6422190603) in this particular formation.

The results from the entire Chalk study are presented in chapter 5. Material for future work is included and should be studied in detail. The Northern Ireland Chalk was comparable to harder Chalks which is more present in Chalk formations further north (Sleipner area) in the North Sea. It is recommended to extract appropriate samples from this location and integrate rock characteristics into the IDEAS rock library for future simulations.

It is recommended to test drilling performance of the already selected bit design for Chalk applications, as well as simulating other bit design in both Kansas Chalk and Ulster Limestone. The results make it possible to design a PDC bit that can drill through both soft and hard Chalk in one single run, which are desirable in the future when chert beds are present in Chalk.

12. Acknowledgements

I would like to thank Udo Zimmermann for his guidance throughout the work of this thesis. He has inspired me to see the importance of having knowledge about geological aspects even for people in technical environments. His knowledge and inspiration in this work has been crucial for the outcome of this thesis.

I would also like to give a special thanks to Alberto Caycedo in Smith Bits, A Schlumberger Company. Not only is he an inspiring and experienced Field Engineer, he has been the man to turn to through thick and thin. Thanks for providing me with important papers, participation in discussion and for giving me more knowledge about the bit-designing process.

Thanks to Edvard Omdal in Conoco Phillips for giving me a deeper understanding of the Kansas Chalk, for always answering my questions, and for getting me in touch with the right people for possible extraction of the Chalk in the future.

I would also like to thank Christian Utvik, district manager of Smith Bits Norway, who gave me the opportunity to write this thesis. Thank you for the support and commitment which was essential for the outcome of this work.

Smith Bits engineers:

- Olav Larsen.
- Odd Vinsevik
- Eirik Sundfør
- Henrik Gustavsen
- Magnus Lie
- Erik Håland

13. References

[1] Engineer In Training Certification

Smith international internal training session, 2007

[2] Active Damping of Torsional Drillstring Vibrations with a Hydraulic Top Drive

J.D Hansen, SPE, A/A Norske Shell; Leon van den Steen, Shell research; and Erik Zachariasen, Maritime Hydraulics A/S

[3] The Destruction of PDC bits by Severe slip-Stick Vibration

M.J Fear, SPE, BPX Exploration (Colombia) LTd.; F. abbassian, SPE, and S.H.L. Parfitt, SPE, BP Exploration Ltd.; and A. McClean, Hughes Christensen Company

[4] Internal Bit vibration manual, Smith Bits, 2004.

[5] Drillstring Integrity and Vibration Control Guidelines, external edition

W.H.G Keultjes, A.C. Pols, J-M. savignat and L. van den Steen, Shell international exploration and production.

[6] Vibration Suppression Chart

Smith technologies internal document, 2005

[7] A New Approach to Stick-Slip Management Integrating Bit Design and Rotary-Steerable-System Characteristics

M.R. Niznik and A.D. Carson, ExxonMobil Development Co.; K.J. Wise, Schlumberger; and F. Carson, ReedHycalog.

[8] Torsional Resonance of Drill Collars with PDC Bits in Hard Rock

T.M. Warren, SPE, and J.H. Oster, Amoco E&P Technology Group

[9] Rocks: Materials of the Solid Earth

Tarbuck, Edwards & Lutgens, Frederick (authors), Earth science, eleventh edition

[10] The Millennium Atlas

Geology society of London, 2003

[11] The effect of acid stimulation on fractured Chalk"

Omdal, Edvard (editor), Master of Science at the University of Stavanger, 2006,

[12] The mechanical Behavior of Chalk under Laboratory Conditions Simulating Reservoir Operations

Edvard Omdal (editor), PhD thesis UIS no. 104-June 2010

[13] Chalk diagenesis and its relation to petroleum exploration: oil from Chalks, a modern miracle.

Scholle PA (1977) AAPG bull 61: 982-1009

[14] The Making of a Land- GEOLOGY OF NORWAY

Ivar B. Ramberg, Inge Bryhni, Arvid Nøttvedt, Kristin Rangnes

[15] Discussions with Udo Zimmermann

Prof UIS.

[16] Schlumberger oilfield glossary:

<http://www.glossary.oilfield.slb.com>

[17] An Introduction to Porosity

Hook, J.R (editor), Petrophysics, May-June, 2003

[18] Discussions with Alberto Caycedo

Senior Field Engineer, Smith Bits A Schlumberger Company

[19] Strain Hardening of Porous Limestone

J.B. Chatman-member aim, Rice U-Houston Tex, Society of Petroleum Engineers office Dec.6, 1996

[20] Geology of the Norwegian North Sea

Baker Hughes INTEQ Scandinavia, 2009

[21] Petroleum Geology of the North Sea- Basic concepts and recent advances

K.W. Glennie, fourth edition. ISBN 0-632-03845-4

[22] Google Images

[23] A revised Cretaceous and Tertiary lithostratigraphic nomenclature for the Norwegian North Sea

Norwegian Petroleum Department (NPD), Bulletin no 4, 1988

[24] Norwegian Petroleum Department fact pages:

<http://www.npd.no/engelsk/cwi/pbl/en/index.htm>

[25] Landet blir til- The geology of Norway

Norsk geologisk forening (NGF), 2006

[26] Petroleum Geology of the North Sea

K.W. Glennie(editor). 4. Edition, Blackwell science Ltd, 1998

[27] Petroleum Systems and Geological Assessment of Oil and Gas in the Southwestern Wyoming Province, Wyoming, Colorado, and Utah.

Thomas M. Finn and Ronald C. Johnson, chapter 6

[28] Cyclostratigraphy of the upper Cretaceous Niobrara Formation, Western Interior, U.S.A.: A Conician-Santonian orbital timescale.

Robert. E Locklair, Bradley B. Sageman, Department of Earth and planetary sciences, Northwestern University-2008

[29] Microholes for microdarcy reservoirs

Kent Perry and Samih Batarseh, Gas Technology institute, E&P Article,2 006.

[30] Geological Overview of the Niobrara Chalk Natural Gas Play

W. Lynn Watney, Kansas Geological Survey

[31] Dynamic BHA modeling of Hole Enlargement While Drilling leads to ROP Improvement in Gulf of Mexico.

Myles, Barret, Shell International E&P, Molly Compton, Mukul Agnihotri, Fernando Veano, Simon Mitchell and David Fitzmorris, Smith International. OTC 20370, 2007

[32] Deepwater Drilling in Hard and Abrasive Formations; The Challenges of Bit Optimization

Dominic Murphy, Tullow Oil plc, Nick Tetley, Uyen Partin and Denise Licington, Smith Technologies, SPE 12895- 2010

[33] Dynamic Simulations Provide Development Drilling Improvements

Mark. P. Frenzel, Smith Technologies, OTC 19066- 2007

[34] Integrated FEA Modeling Offers System Approach to Drillstring Optimization

H. Aslaksen, SPE, M. Annand, SPE, R. Duncan, SPE, A Fjaere, L Paez, SPE, and U. Tran, Spe, Smith Technologies. IADC/SPE 99018

[35] IDEAS integrated training presentation

Eirik Møgedal, Smith Technologies (Market research analyst Sr)

[36] BHA and Drill String Fundamentals

Schlumberger's training and development document, 2010

[37] PowerDrive Operating Guidelines

Stonehouse Technology Center Sustaining, Copyright 2006 Schlumberger

[38] Basic drilling- technology and equipment

Aberdeen drilling schools & well control training centre

[39] Chert drilling: An experimental and numerical feasibility study

Vigdel, Linda (editor), Master of Science thesis, 2003

[40] Introduction to PDC bits

Smith international internal training document, 2003

[41] Introduction to roller cone bits

Smith international internal training document, 2003

[42] The Current State of PDC bit Technogy, Part 1-3

Federico Bellin, Alfazazi Dourfaye, William King and Mike Thigpen, Varel internation, World Oil, 2010
(Leaching a thin layer at the working surface of a PDC cutter to remove the cobalt dramatically reduces diamond degradation due to frictional heat)

[43] Cutting efficiency of a single PDC cutter on hard rock.

Canadian International Petroleum conference, 2011

[44] PDC drillability study of Conglomerate/breccias formation

Gustavsen, Henrik , Master of Science at the University of Stavanger, 2010

[45] New Cutter Technology for Faster Drilling in Hard/Abrasive Formations

Billy Plemons, Anadarko Petroleum Corp., and Charles Douglas, Yueling Shen, Guodong Zhan, and Youhe Zhang, Smith Internation, SPE 132143

[46] Modified tables created from the associated reference.

Master thesis author, Margodt Marie Larsen

[47] The effect of PDC Cutter Density, back rake, size and speed on performance

L.A Sinor, SPE, and J.R POWERS, SPE, Hughes Christensen CO., and T.M Warren, SPE, Amoco production Co. IADC/SPE 39306

[48] PDC Drill Bit Design and Field Application Evaluation

Callin joe Kett, * SPE, Norton Christensen Canada Ltd. Journal of petroleum technology, march 1988.

[49] The positive Effects of Side Rake in Oilfield Bits Using Polycrystalline diamond compact cutters

Hsin I. Huang, * Robert E. Iversen, * Christensen Diamond Products U.S. a, SPE 10152

[50] Design, application and future of Polycrystalline Diamond compact cutters in Rocky Mountains.

Cerkovnic, J, SPE 10893

[51] Discussions with Knut Eugen Svendsen

Drilling engineer from Conoco Phillips, Ekofisk field

[52] Experimental Study of Crater Formation in Limestone at Elevated Pressures

Norman E. Garner, Augusto Podio, Carl Gatlin, Society of Petroleum Engineers. September 1968

[53] Extrapolation of Fracture Data from Outcrops of the Austin Chalk in Texas to Corresponding Petroleum Reservoirs at Depth.

Melvin Friedman, Desiree E. McKiernan, Department of Geology and Center for Tectonophysics, Texas
Paper No. HWC94-36

APPENDIX A

[1] Raw data from Coulomb Mohr Failure Envelope, Sample A and B.

[1.1] Coulomb Failure Envelope, samples DKCA- 5,1,2,3

```

\      Mohr's   Circle   Data   File:   dkca.dat
\      Program  Version  1.00,  Released May      1991
\
\
\      Mohr's   Circle   Input   Data:   sigma_1  sigma_3
\      5575    1500
\      4575    1000
\      3795    500
\      2005    0
\
\      Linear   Fit:     tau     =      0,437521  sigma   +      730,527
\      Coefficient of   Linear Cohesion =      730,527
\      Angle    of     Internal Friction =      23,6304  degrees
\
\
\

```

```

\      Mohr's   Circle   Data   File:   dkcahigh.dat
\      Program  Version  1.00,  Released May      1991
\
\
\      Mohr's   Circle   Input   Data:   sigma_1  sigma_3
\      5575    1500
\      4575    1000
\      3795    500
\
\      Linear   Fit:     tau     =      0,29364  sigma   +      1071,9
\      Coefficient of   Linear Cohesion =      1071,9
\      Angle    of     Internal Friction =      16,3644  degrees
\
\
\

```

Effective Normal Stress (psi)	Shear Stress (psi)
5575	0
5573,97	64,6457
5570,9	129,226
5565,77	193,677
5558,61	257,932
5549,41	321,928
5538,18	385,599
5524,94	448,883
5509,7	511,714
5492,47	574,03
5473,27	635,768
5452,12	696,866
5429,05	757,262
5404,07	816,896
5377,21	875,707
5348,5	933,637
5317,97	990,626
5285,64	1046,62
5251,55	1101,56
5215,74	1155,38
5178,24	1208,05
5139,08	1259,5
5098,32	1309,68
5055,98	1358,54
5012,11	1406,04
4966,76	1452,11
4919,96	1496,73
4871,78	1539,84
4822,25	1581,4
4771,43	1621,36
4719,37	1659,7
4666,11	1696,36
4611,72	1731,32
4556,25	1764,53
4499,75	1795,96
4442,29	1825,59
4383,91	1853,38
4324,68	1879,3
4264,66	1903,33
4203,9	1925,44
4142,48	1945,61
4080,44	1963,83
4017,86	1980,07
3954,79	1994,31

3891,31	2006,55
3827,47	2016,76
3763,33	2024,95
3698,97	2031,09
3634,45	2035,19
3569,83	2037,24
3505,17	2037,24
3440,55	2035,19
3376,03	2031,09
3311,67	2024,95
3247,53	2016,76
3183,69	2006,55
3120,21	1994,31
3057,14	1980,07
2994,56	1963,83
2932,52	1945,61
2871,1	1925,44
2810,34	1903,33
2750,32	1879,3
2691,09	1853,38
2632,71	1825,59
2575,25	1795,96
2518,75	1764,53
2463,28	1731,32
2408,89	1696,36
2355,63	1659,7
2303,57	1621,36
2252,75	1581,4
2203,22	1539,84
2155,04	1496,73
2108,24	1452,11
2062,89	1406,04
2019,02	1358,54
1976,68	1309,68
1935,92	1259,5
1896,76	1208,05
1859,26	1155,38
1823,45	1101,56
1789,36	1046,62
1757,03	990,626
1726,5	933,637
1697,79	875,707
1670,93	816,896
1645,95	757,262
1622,88	696,866
1601,73	635,768
1582,53	574,03
1565,3	511,714

1550,06	448,883
1536,82	385,599
1525,59	321,928
1516,39	257,932
1509,23	193,677
1504,1	129,226
1501,03	64,6457
1500	0
4575	0
4574,1	56,7137
4571,4	113,37
4566,91	169,913
4560,62	226,284
4552,55	282,427
4542,7	338,287
4531,08	393,805
4517,71	448,927
4502,59	503,597
4485,75	557,76
4467,2	611,361
4446,96	664,347
4425,04	716,663
4401,48	768,258
4376,29	819,08
4349,51	869,077
4321,15	918,198
4291,24	966,395
4259,82	1013,62
4226,92	1059,82
4192,57	1104,96
4156,8	1148,98
4119,66	1191,85
4081,17	1233,52
4041,39	1273,94
4000,34	1313,08
3958,06	1350,9
3914,61	1387,36
3870,03	1422,42
3824,35	1456,05
3777,63	1488,22
3729,92	1518,88
3681,25	1548,02
3631,68	1575,6
3581,27	1601,59
3530,05	1625,97
3478,09	1648,71
3425,43	1669,79
3372,13	1689,19

3318,25	1706,89
3263,82	1722,87
3208,92	1737,11
3153,59	1749,61
3097,9	1760,34
3041,89	1769,31
2985,62	1776,49
2929,16	1781,88
2872,55	1785,48
2815,86	1787,28
2759,14	1787,28
2702,45	1785,48
2645,84	1781,88
2589,38	1776,49
2533,11	1769,31
2477,1	1760,34
2421,41	1749,61
2366,08	1737,11
2311,18	1722,87
2256,75	1706,89
2202,87	1689,19
2149,57	1669,79
2096,91	1648,71
2044,95	1625,97
1993,73	1601,59
1943,32	1575,6
1893,75	1548,02
1845,08	1518,88
1797,37	1488,22
1750,65	1456,05
1704,97	1422,42
1660,39	1387,36
1616,94	1350,9
1574,66	1313,08
1533,61	1273,94
1493,83	1233,52
1455,34	1191,85
1418,2	1148,98
1382,43	1104,96
1348,08	1059,82
1315,18	1013,62
1283,76	966,395
1253,85	918,198
1225,49	869,077
1198,71	819,08
1173,52	768,258
1149,96	716,663
1128,04	664,347

1107,8	611,361
1089,25	557,76
1072,41	503,597
1057,29	448,927
1043,92	393,805
1032,3	338,287
1022,45	282,427
1014,38	226,284
1008,09	169,913
1003,6	113,37
1000,9	56,7137
1000	0
3795	0
3794,17	52,2718
3791,68	104,491
3787,54	156,605
3781,75	208,561
3774,31	260,307
3765,23	311,791
3754,52	362,962
3742,2	413,766
3728,26	464,154
3712,74	514,075
3695,64	563,478
3676,99	612,314
3656,79	660,533
3635,07	708,087
3611,86	754,928
3587,17	801,009
3561,03	846,284
3533,47	890,706
3504,51	934,231
3474,18	976,816
3442,52	1018,42
3409,56	1058,99
3375,32	1098,5
3339,85	1136,91
3303,18	1174,16
3265,34	1210,24
3226,38	1245,1
3186,34	1278,7
3145,24	1311,02
3103,14	1342,01
3060,08	1371,66
3016,1	1399,92
2971,25	1426,78
2925,57	1452,19
2879,1	1476,15

2831,9	1498,62
2784	1519,58
2735,47	1539,01
2686,34	1556,89
2636,68	1573,2
2586,52	1587,93
2535,91	1601,06
2484,92	1612,58
2433,59	1622,47
2381,96	1630,73
2330,11	1637,35
2278,06	1642,32
2225,89	1645,63
2173,64	1647,29
2121,36	1647,29
2069,11	1645,63
2016,94	1642,32
1964,89	1637,35
1913,04	1630,73
1861,41	1622,47
1810,08	1612,58
1759,09	1601,06
1708,48	1587,93
1658,32	1573,2
1608,66	1556,89
1559,53	1539,01
1511	1519,58
1463,1	1498,62
1415,9	1476,15
1369,43	1452,19
1323,75	1426,78
1278,9	1399,92
1234,92	1371,66
1191,86	1342,01
1149,76	1311,02
1108,66	1278,7
1068,62	1245,1
1029,66	1210,24
991,82	1174,16
955,148	1136,91
919,677	1098,5
885,442	1058,99
852,478	1018,42
820,817	976,816
790,493	934,231
761,535	890,706
733,972	846,284
707,833	801,009

683,144	754,928
659,929	708,087
638,211	660,533
618,014	612,314
599,356	563,478
582,258	514,075
566,735	464,154
552,805	413,766
540,479	362,962
529,772	311,791
520,694	260,307
513,254	208,561
507,46	156,605
503,317	104,491
500,829	52,2718
500	0
2005	0
2004,5	31,8073
2002,98	63,5825
2000,46	95,2937
1996,93	126,909
1992,41	158,396
1986,88	189,724
1980,37	220,861
1972,87	251,776
1964,39	282,437
1954,95	312,814
1944,54	342,875
1933,19	372,592
1920,9	401,933
1907,68	430,869
1893,56	459,372
1878,53	487,412
1862,63	514,962
1845,86	541,992
1828,24	568,478
1809,78	594,39
1790,52	619,704
1770,46	644,395
1749,63	668,436
1728,04	691,804
1705,73	714,476
1682,71	736,428
1659	757,639
1634,63	778,087
1609,62	797,751
1584,01	816,612
1557,8	834,651

1531,04	851,85
1503,75	868,19
1475,95	883,657
1447,68	898,234
1418,95	911,906
1389,81	924,66
1360,28	936,483
1330,39	947,363
1300,16	957,289
1269,64	966,252
1238,85	974,241
1207,82	981,249
1176,58	987,27
1145,17	992,296
1113,62	996,323
1081,95	999,347
1050,2	1001,36
1018,41	1002,37
986,594	1002,37
954,799	1001,36
923,052	999,347
891,385	996,323
859,829	992,296
828,418	987,27
797,181	981,249
766,152	974,241
735,36	966,252
704,837	957,289
674,614	947,363
644,722	936,483
615,189	924,66
586,046	911,906
557,323	898,234
529,048	883,657
501,25	868,19
473,956	851,85
447,195	834,651
420,993	816,612
395,376	797,751
370,371	778,087
346,002	757,639
322,294	736,428
299,271	714,476
276,957	691,804
255,372	668,436
234,54	644,395
214,482	619,704
195,217	594,39

176,764	568,478
159,143	541,992
142,372	514,962
126,466	487,412
111,442	459,372
97,3161	430,869
84,1013	401,933
71,8111	372,592
60,4581	342,875
50,0537	312,814
40,6083	282,437
32,1314	251,776
24,6316	220,861
18,1165	189,724
12,5925	158,396
8,0653	126,909
4,5394	95,2937
2,01836	63,5825
0,504716	31,8073
0	0

[I.2] Coulomb Failure Envelope, samples DKCB- 5,3,6,2

```

\      Mohr's   Circle   Data   File:   dkcb.dat
\      Program  Version  1.00,  Released May      1991
\
\
\
\      Mohr's   Circle   Input   Data:   sigma_1  sigma_3
\      3245    1500
\      2500    1000
\      2075    500
\      1015    0
\
\      Linear   Fit:     tau     =     0,18427  sigma  +     469,05
\      Coefficient of   Linear Cohesion =     469,05
\      Angle     of   Internal Friction =     10,4408  degrees

```

Effective Normal Stress, psi	Shear Stress, psi
3245	0
3244,56	27,6826
3243,24	55,3374
3241,05	82,9364
3237,98	110,452
3234,04	137,856
3229,23	165,122
3223,56	192,221
3217,04	219,127
3209,66	245,812
3201,44	272,249
3192,38	298,413
3182,5	324,275
3171,8	349,812
3160,3	374,996
3148,01	399,803
3134,93	424,207
3121,09	448,184
3106,49	471,709
3091,16	494,76
3075,1	517,312
3058,33	539,344
3040,87	560,832
3022,74	581,756
3003,96	602,094
2984,54	621,826
2964,5	640,931

2943,87	659,392
2922,66	677,188
2900,89	694,302
2878,6	710,718
2855,8	726,417
2832,5	741,385
2808,75	755,607
2784,56	769,068
2759,95	781,755
2734,95	793,654
2709,59	804,754
2683,88	815,044
2657,87	824,513
2631,56	833,152
2605	840,952
2578,2	847,906
2551,19	854,005
2524,01	859,245
2496,67	863,619
2469,21	867,124
2441,65	869,756
2414,02	871,512
2386,34	872,39
2358,66	872,39
2330,98	871,512
2303,35	869,756
2275,79	867,124
2248,33	863,619
2220,99	859,245
2193,81	854,005
2166,8	847,906
2140	840,952
2113,44	833,152
2087,13	824,513
2061,12	815,044
2035,41	804,754
2010,05	793,654
1985,05	781,755
1960,44	769,068
1936,25	755,607
1912,5	741,385
1889,2	726,417
1866,4	710,718
1844,11	694,302
1822,34	677,188
1801,13	659,392
1780,5	640,931
1760,46	621,826

1741,04	602,094
1722,26	581,756
1704,13	560,832
1686,67	539,344
1669,9	517,312
1653,84	494,76
1638,51	471,709
1623,91	448,184
1610,07	424,207
1596,99	399,803
1584,7	374,996
1573,2	349,812
1562,5	324,275
1552,62	298,413
1543,56	272,249
1535,34	245,812
1527,96	219,127
1521,44	192,221
1515,77	165,122
1510,96	137,856
1507,02	110,452
1503,95	82,9364
1501,76	55,3374
1500,44	27,6826
1500	0
2500	0
2499,62	23,796
2498,49	47,5679
2496,6	71,292
2493,97	94,9443
2490,58	118,501
2486,45	141,938
2481,57	165,233
2475,96	188,361
2469,62	211,299
2462,55	234,025
2454,77	256,515
2446,28	278,747
2437,08	300,698
2427,19	322,346
2416,63	343,67
2405,39	364,648
2393,49	385,258
2380,94	405,481
2367,76	425,295
2353,95	444,681
2339,54	463,619
2324,53	482,091

2308,95	500,077
2292,8	517,559
2276,11	534,521
2258,88	550,944
2241,15	566,812
2222,91	582,11
2204,21	596,821
2185,04	610,932
2165,44	624,427
2145,42	637,294
2125	649,519
2104,2	661,09
2083,05	671,995
2061,56	682,224
2039,76	691,766
2017,66	700,611
1995,3	708,751
1972,69	716,177
1949,86	722,882
1926,82	728,859
1903,61	734,102
1880,24	738,606
1856,74	742,366
1833,13	745,379
1809,44	747,641
1785,69	749,151
1761,9	749,906
1738,1	749,906
1714,31	749,151
1690,56	747,641
1666,87	745,379
1643,26	742,366
1619,76	738,606
1596,39	734,102
1573,18	728,859
1550,14	722,882
1527,31	716,177
1504,7	708,751
1482,34	700,611
1460,24	691,766
1438,44	682,224
1416,95	671,995
1395,8	661,09
1375	649,519
1354,58	637,294
1334,56	624,427
1314,96	610,932
1295,79	596,821

1277,09	582,11
1258,85	566,812
1241,12	550,944
1223,89	534,521
1207,2	517,559
1191,05	500,077
1175,47	482,091
1160,46	463,619
1146,05	444,681
1132,24	425,295
1119,06	405,481
1106,51	385,258
1094,61	364,648
1083,37	343,67
1072,81	322,346
1062,92	300,698
1053,72	278,747
1045,23	256,515
1037,45	234,025
1030,38	211,299
1024,04	188,361
1018,43	165,233
1013,55	141,938
1009,42	118,501
1006,03	94,9443
1003,4	71,292
1001,51	47,5679
1000,38	23,7959
1000	0
2075	0
2074,6	24,9857
2073,41	49,9463
2071,43	74,8566
2068,66	99,6916
2065,11	124,426
2060,77	149,035
2055,65	173,495
2049,76	197,779
2043,1	221,864
2035,68	245,726
2027,51	269,341
2018,59	292,684
2008,94	315,733
1998,55	338,463
1987,46	360,853
1975,66	382,88
1963,16	404,521
1949,99	425,755

1936,15	446,56
1921,65	466,915
1906,52	486,8
1890,76	506,195
1874,4	525,081
1857,44	543,437
1839,91	561,247
1821,83	578,491
1803,2	595,153
1784,06	611,215
1764,42	626,662
1744,29	641,479
1723,71	655,649
1702,69	669,159
1681,25	681,995
1659,41	694,145
1637,2	705,595
1614,64	716,335
1591,75	726,354
1568,55	735,641
1545,07	744,188
1521,32	751,986
1497,35	759,026
1473,16	765,302
1448,79	770,807
1424,25	775,536
1399,57	779,484
1374,79	782,648
1349,91	785,023
1324,97	786,608
1299,99	787,401
1275,01	787,401
1250,03	786,608
1225,09	785,023
1200,21	782,648
1175,43	779,484
1150,75	775,536
1126,21	770,807
1101,84	765,302
1077,65	759,026
1053,68	751,986
1029,93	744,188
1006,45	735,641
983,253	726,354
960,361	716,335
937,798	705,595
915,587	694,145
893,75	681,995

872,31	669,159
851,288	655,649
830,705	641,479
810,582	626,662
790,94	611,215
771,797	595,153
753,174	578,491
735,089	561,247
717,559	543,437
700,604	525,081
684,24	506,195
668,483	486,8
653,35	466,915
638,855	446,56
625,013	425,755
611,838	404,521
599,344	382,88
587,542	360,853
576,445	338,463
566,065	315,733
556,41	292,684
547,492	269,341
539,319	245,726
531,899	221,864
525,24	197,779
519,349	173,495
514,231	149,035
509,892	124,426
506,336	99,6916
503,566	74,8566
501,585	49,9463
500,396	24,9857
500	0
1015	0
1014,74	16,1019
1013,98	32,1876
1012,7	48,2409
1010,92	64,2457
1008,63	80,1857
1005,83	96,045
1002,53	111,808
998,734	127,458
994,443	142,979
989,661	158,357
984,394	173,575
978,647	188,619
972,425	203,472
965,735	218,121

958,584	232,55
950,979	246,745
942,927	260,691
934,436	274,375
925,516	287,783
916,175	300,901
906,422	313,716
896,268	326,215
885,722	338,385
874,795	350,215
863,499	361,692
851,844	372,805
839,842	383,543
827,505	393,894
814,847	403,849
801,879	413,397
788,614	422,529
775,067	431,236
761,25	439,508
747,178	447,338
732,864	454,717
718,323	461,638
703,57	468,095
688,62	474,08
673,487	479,588
658,187	484,613
642,735	489,15
627,148	493,194
611,439	496,742
595,626	499,79
579,725	502,334
563,75	504,373
547,719	505,904
531,648	506,925
515,552	507,436
499,448	507,436
483,352	506,925
467,281	505,904
451,25	504,373
435,275	502,334
419,374	499,79
403,561	496,742
387,852	493,194
372,265	489,15
356,813	484,613
341,513	479,588
326,38	474,08
311,43	468,095

296,677	461,638
282,136	454,717
267,822	447,338
253,75	439,508
239,933	431,236
226,386	422,529
213,121	413,397
200,153	403,849
187,495	393,894
175,158	383,543
163,156	372,805
151,501	361,692
140,205	350,215
129,278	338,385
118,732	326,215
108,578	313,716
98,8253	300,901
89,4841	287,783
80,5638	274,375
72,0734	260,691
64,0214	246,745
56,416	232,55
49,2648	218,121
42,575	203,472
36,3533	188,619
30,606	173,575
25,3389	158,357
20,5573	142,979
16,266	127,458
12,4694	111,808
9,17119	96,045
6,37476	80,1857
4,08293	64,2457
2,298	48,2409
1,02176	32,1876
0,255505	16,1019
0	0

APPENDIX B

[1]Raw data from vibration simulations

[I.I] IAR Dynamic Results, simulation through Lueders Limestone

IAR Dynamic Results								
Bit TQ (kft-lb) Delta	Surface TQ (kft-lb) 25%- ile	Surface TQ (kft-lb) 75%- ile	Surface TQ (kft-lb) Delta	RPM 25%- ile	RPM 75%- ile	RPM Delta	Build Drop Value + B/D	Walk Value + L/R
0,565	14,07	14,679	0,609	156,866	163,384	6,518	-0,8476	0,2144
0,277	15,851	16,327	0,476	153,316	166,545	13,229	-0,732	0,1766
0,212	16,937	17,311	0,374	154,672	165,144	10,472	-0,6287	0,1378
0,19	18,015	18,46	0,445	153,351	166,23	12,879	-0,616	0,1065
0,558	13,757	14,328	0,571	127,764	132,631	4,867	-0,8648	0,2224
0,262	15,633	15,846	0,213	127,183	132,985	5,802	-0,7256	0,1698
0,21	16,693	16,886	0,193	127,351	132,622	5,271	-0,6227	0,1486
0,192	17,78	18,012	0,232	126,587	133,16	6,573	-0,6187	0,1189
0,565	13,416	13,989	0,573	98,098	102,105	4,007	-0,8936	0,2345
0,258	15,326	15,47	0,144	97,957	102,099	4,142	-0,7405	0,1488
0,215	16,391	16,53	0,139	98,15	102,136	3,986	-0,6363	0,1359
0,209	17,504	17,663	0,159	97,676	102,341	4,665	-0,6326	0,1068
0,688	20,167	20,791	0,624	158,023	162,813	4,79	-0,7143	0,1878
0,308	20,436	20,671	0,235	157,586	163,159	5,573	-0,6141	0,1318
0,226	20,738	20,912	0,174	157,539	162,904	5,365	-0,4471	0,129
0,193	21,147	21,32	0,173	157,656	162,951	5,295	-0,4333	0,0816
0,68	19,56	20,198	0,638	128,091	132,402	4,311	-0,7272	0,1929

[I.I] IAR Dynamic Results, simulation in Austin Chalk

Case Reference #	Depth	Formation	UCS	WOB (klbs)	Rotary RPM	Bit Type
007/Bit1	14797	Austin Chalk Limestone	0-2	15	100	MDi619LBPXX
016/Bit1	19100	Austin Chalk Limestone	0-2	15	100	MDi619LBPXX
004/Bit1	14797	Austin Chalk Limestone	0-2	15	130	MDi619LBPXX
043/Bit3	14797	Austin Chalk Limestone	0-2	15	100	MDi619LBPX
040/Bit3	14797	Austin Chalk Limestone	0-2	15	130	MDi619LBPX
037/Bit3	14797	Austin Chalk Limestone	0-2	15	160	MDi619LBPX
013/Bit1	19100	Austin Chalk Limestone	0-2	15	130	MDi619LBPXX
001/Bit1	14797	Austin Chalk Limestone	0-2	15	160	MDi619LBPXX
010/Bit1	19100	Austin Chalk Limestone	0-2	15	160	MDi619LBPXX
008/Bit1	14797	Austin Chalk Limestone	0-2	20	100	MDi619LBPXX
017/Bit1	19100	Austin Chalk Limestone	0-2	20	100	MDi619LBPXX
005/Bit1	14797	Austin Chalk Limestone	0-2	20	130	MDi619LBPXX
014/Bit1	19100	Austin Chalk Limestone	0-2	20	130	MDi619LBPXX
002/Bit1	14797	Austin Chalk Limestone	0-2	20	160	MDi619LBPXX
011/Bit1	19100	Austin Chalk Limestone	0-2	20	160	MDi619LBPXX
018/Bit1	19100	Austin Chalk Limestone	0-2	25	100	MDi619LBPXX
009/Bit1	14797	Austin Chalk Limestone	0-2	25	100	MDi619LBPXX
015/Bit1	19100	Austin Chalk Limestone	0-2	25	130	MDi619LBPXX
044/Bit3	14797	Austin Chalk Limestone	0-2	20	100	MDi619LBPX
041/Bit3	14797	Austin Chalk Limestone	0-2	20	130	MDi619LBPX
038/Bit3	14797	Austin Chalk Limestone	0-2	20	160	MDi619LBPX
006/Bit1	14797	Austin Chalk Limestone	0-2	25	130	MDi619LBPXX
012/Bit1	19100	Austin Chalk Limestone	0-2	25	160	MDi619LBPXX
003/Bit1	14797	Austin Chalk Limestone	0-2	25	160	MDi619LBPXX
045/Bit3	14797	Austin Chalk Limestone	0-2	25	100	MDi619LBPX
042/Bit3	14797	Austin Chalk Limestone	0-2	25	130	MDi619LBPX
039/Bit3	14797	Austin Chalk Limestone	0-2	25	160	MDi619LBPX
052/Bit3	19100	Austin Chalk Limestone	0-2	15	100	MDi619LBPX
049/Bit3	19100	Austin Chalk Limestone	0-2	15	130	MDi619LBPX
046/Bit3	19100	Austin Chalk Limestone	0-2	15	160	MDi619LBPX
053/Bit3	19100	Austin Chalk Limestone	0-2	20	100	MDi619LBPX
050/Bit3	19100	Austin Chalk Limestone	0-2	20	130	MDi619LBPX
047/Bit3	19100	Austin Chalk Limestone	0-2	20	160	MDi619LBPX
054/Bit3	19100	Austin Chalk Limestone	0-2	25	100	MDi619LBPX
051/Bit3	19100	Austin Chalk Limestone	0-2	25	130	MDi619LBPX
048/Bit3	19100	Austin Chalk Limestone	0-2	25	160	MDi619LBPX

BOM	Lateral Accel. (g)	Axial Accel. (g)	Bit TQ (kft-lb) Delta	Initial ROP (ft/hr)
6422190603	1,555	0,041	0,324	197,82
6422190603	1,544	0,042	0,323	196,42
6422190603	2,021	0,038	0,324	254,23
64664B0002	1,549	0,041	0,327	197,83
64664B0002	2,047	0,038	0,327	254,26
64664B0002	2,604	0,038	0,33	310,25
6422190603	2,144	0,038	0,32	250,22
6422190603	2,556	0,039	0,328	310,24
6422190603	2,689	0,038	0,329	304,45
6422190603	1,46	0,085	0,346	308,66
6422190603	1,343	0,067	0,335	305,21
6422190603	1,687	0,054	0,342	396,1
6422190603	1,744	0,051	0,332	391,13
6422190603	1,964	0,04	0,351	484,78
6422190603	2,043	0,037	0,336	475,79
6422190603	1,956	0,166	0,29	430,93
6422190603	2,51	0,62	0,365	434,59
6422190603	1,578	0,057	0,295	552,74
64664B0002	1,364	0,14	0,35	308,66
64664B0002	1,651	0,045	0,345	396,13
64664B0002	1,952	0,04	0,355	484,86
6422190603	4,691	2,325	0,413	554,38
6422190603	1,731	0,049	0,312	671,05
6422190603	2,49	0,122	0,578	678,84
64664B0002	3,148	0,81	0,362	433,33
64664B0002	3,829	2,302	0,411	554,26
64664B0002	2,354	0,075	0,579	678,9
64664B0002	1,54	0,041	0,325	196,45
64664B0002	2,156	0,037	0,323	250,25
64664B0002	2,702	0,036	0,332	304,48
64664B0002	1,244	0,067	0,341	305,22
64664B0002	1,659	0,049	0,337	391,19
64664B0002	2,021	0,035	0,34	475,84
64664B0002	1,603	0,095	0,295	432,58
64664B0002	1,503	0,06	0,3	552,79
64664B0002	1,729	0,037	0,312	671,06